Development of Indomethacin in Synthetic Liquid Crystal for Topical Dosage Form

Nanchanit Aeinlang

A Thesis Submitted in Partial Fulfillment of the Requirements for the Degree of

Master of Pharmaceutical Sciences in Pharmaceutical Sciences

Prince of Songkla University

2009

Copyright of Prince of Songkla University

Thesis Title Development of Indomethacin in Synthetic Liquid Crystal for Topical Dosage Form

Author Miss Nanchanit Aeinlang

Major Program Pharmaceutical Sciences

Major Advisor

….....
(Assoc. Prof. Dr. Teerapol Srichana)

Co-advisor

….....
(Dr. Sarunyoo Songkro)

Examining Committee

….....Chairperson
(Assist. Prof. Dr. Sirirat Pinsuwan)

….....
(Assoc. Prof. Dr. Teerapol Srichana)

….....
(Dr. Sarunyoo Songkro)

….....
(Assist. Prof. Dr. Chalermkiat Songkram)

….....
(Assoc. Prof. Dr. Pornanong Aramwit)

The Graduate School, Prince of Songkla University, has approved this thesis as partial fulfillment of the requirements for the Master of Pharmacy Degree in Pharmaceutical Sciences

……
(Assoc. Prof. Dr. Krerkchai Thongnoo)
Dean of Graduate School

ชื่อวิทยานิพนธ์ การพัฒนายาอินโดเมธาซินในผลึกเหลวสังเคราะห์เพื่อใช้เป็นรูปแบบยาทาเฉพาะที่

ผู้เขียน นางสาวนันท์ชนิต เอี่ยนเล่ง

สาขาวิชา เภสัชศาสตร์

ปีการศึกษา 2551

บทคัดย่อ

วัตถุประสงค์หลักของงานวิจัยนี้เพื่อพัฒนาสูตรตำรับยาอินโดเมธาซิน (Indomethacin) ในรูปแบบยาทาเฉพาะที่ เพื่อลดอาการข้างเคียงจากการบริหารยาโดยการรับประทาน โดยบรรจุในผลึกเหลวสังเคราะห์ โคเลสเทอริล เซททิล คาร์บอเนต (cholesteryl cetyl carbonate (CCC)) ที่เกิดจากการ condensation ของ cholesteryl chloroformate กับ cetyl alcohol ในอัตราส่วนโมล 1:1 CCC mixture ประกอบไปด้วย cholesterol, cetyl alcohol และ CCC ซึ่ง CCC ถูกทำให้บริสุทธิ์ด้วยวิธี flash column chromatography โดยคุณสมบัติความเป็นผลึกเหลวแบบ thermotropic สามารถพบได้ทั้ง CCC ที่บริสุทธิ์และสารผสม เมื่อนำผลึกเหลวดังกล่าวมาศึกษาสมบัติทางเคมีกายภาพ พบว่าผลึกเหลวสังเคราะห์ที่ได้มีลักษณะเป็นรูปเข็ม เมื่อให้ความร้อนจะเกิดการหลอมเหลวและตกผลึกเป็น spherulite สวยงาม จาก IR สเปกตรัม

พบว่ามีหมู่คาร์บอนิล ที่ความยาวคลื่นประมาณ 1745 cm^{-1} ซึ่งเป็นหมู่ฟังก์ชันหลักของ carbonate ester จาก DSC พบว่าผลึกเหลวมีการดูดความร้อน ที่อุณหภูมิ 72.83°C มีค่า enthalpy ประมาณ 79.63 J/g และเกิดการคายความร้อนที่อุณหภูมิสูงสุด 41.96, 53.96 และ 72.96°C โดยมีค่าพลังงานจากการคายความร้อน 1.77, 1.04 และ 59.18 J/g ตามลำดับ จากข้อมูลข้างต้นจึงนำผลึกเหลวมาเตรียมเป็นสูตรตำรับกับยาอินโดเมธาซิน (Indomethacin) ในรูปแบบยาทาเฉพาะที่ พบว่าสูตรตำรับดังกล่าวสามารถควบคุมการปลดปล่อยยาได้อย่างน้อย 12 ชั่วโมง และเมื่อนำไปศึกษาการซึมผ่านหนังหมูโดยใช้ Franz diffusion cell พบว่าสูตรตำรับดังกล่าวสามารถเพิ่มการกักเก็บอยู่ในชั้นของหนังหมู (5.41%) ได้ดีกว่ายาอินโดเมธาซินเดี่ยว (0.66%) และเมื่อทำ freeze thaw cycle พบว่าลักษณะทางกายภาพของสูตรตำรับไม่มีการเปลี่ยนแปลง แต่ปริมาณยาและความสามารถในการปลดปล่อยยาของสูตรตำรับมีปริมาณลดลง แต่ทั้งนี้สูตรตำรับมีลักษณะไม่เหมาะแก่การใช้ทางผิวหนังเนื่องจากมีลักษณะเป็นผงแห้ง และแข็ง งานวิจัยนี้จึงยังคงต้องพัฒนาการเตรียมสูตรตำรับที่เหมาะสมต่อไป

Thesis Title	Development of indomethacin in synthetic liquid crystal for topical dosage form
Author	Miss Nanchanit Aeinlang
Major Program	PharmaceuticalSciences
Academic Year	2008

The main objective of this research was to develop the topical formulation of indomethacin in synthetic liquid crystal (Cholesteryl cetyl carbonate (CCC)). CCC was synthesized from cetyl alcohol and cholesteryl chloroformate at of mole ratio 1:1. CCC mixture was purified by liquid-liquid extraction and flash column chromatography. Thermotropic liquid crystal was formed in both pure CCC and CCC mixture. CCC mixture composes of cholesterol, cetyl alcohol and CCC (30:20:50, %). FTIR and NMR were employed to confirm the functional groups of CCC. Thermal properties of CCC were determined by DSC and polarized light microscope. The phase transitions from isotropic liquid to nematic appear at 73°C, nematic to smectic appear at 54°C and smectic to crystal appear at 42°C. Indomethacin could be prepared as topical dosage form by incorporation into CCC. Liquid crystalline phase properties of indomethacin-CCC mixture were detected by polarized light microscope. Control release of indomethacin was observed over 12 h. Indomethacin (1% in CCC) was retained in newborn pig skin (5.41%) much greater than that of pure drug (0.66%). After freeze thaw cycle, preformed preparations have a physical stability. The release and the content of indomethacin were decreased that compare with initial.

CONTENTS

CONTENTS (continued)

CONTENTS (continued)

CHAPTER THREE

CONTENTS (continued)

CONTENTS (continued)

CONTENTS (continued)

LIST OF TABLES

LIST OF ILLUSTRATIONS

LIST OF ILLUSTRATIONS (Continued)

LIST OF ILLUSTRATIONS (Continued)

LIST OF ILLUSTRATIONS (Continued)

ABBRIEVIATIONS AND SYMBOLS

%	=	Percentage
% RSD	=	Percentage of relative standard deviation
^{o}C	=	Degree Celcius
µl	=	Microliter
µm	=	Micrometer
ANOVA	=	Analysis of variance
cm	=	Centimeter (s)
cm^2	=	Square centimeter (s)
CCC	=	Cholesteryl cetyl carbonate
CGC	=	Cholesterol-modified glycol chitosan
CMC	=	Critical micelle concentration
CN	=	Cholesteryl nonanoate
COC	=	Cholesteryl oleyl carbonate
DADLE	=	[D-Ala^2, D-Leu^5] enkephalin
DSC	=	Differential scanning calorimetry
DW	=	Distilled water
FTIR	=	Fourier transform infrared
g	=	Gram (s)
GMO	=	Glyceryl monooleate
h	=	Hour

ABBRIEVIATIONS AND SYMBOLS (Continued)

HPLC	=	High performance liquid chromatography
IPB	=	Isotonic phosphate buffer
J/g	=	Joule/gram
LLCs	=	Lyotropic liquid crystals
LOD	=	Limit of detection
LOQ	=	Limit of quantification
M	=	Mole
mA	=	Milliampere
mg	=	Milligram
ml	=	Milliliter
mm	=	Millimeter
mM	=	Millimolar
mmol	=	Millimole
min	=	Minute
MW	=	Molecular weight
nm	=	Nanometer
NMR	=	Nuclear magnetic resonance
NSAIDs	=	Non-steroidal anti-inflammatory drugs
PLM	=	Polarized light microscope
ppm	=	Part per million
r^2	=	Correlation coefficient

ABBRIEVIATIONS AND SYMBOLS (Continued)

rpm	=	Round per minute
RT	=	Room temperature
S	=	Second
SB	=	Stratum basale
SC	=	Stratum corneum
SD	=	Standard deviation
SG	=	Stratum granulosum
SS	=	Stratum spinosum
TLC	=	Thin layer chromatography
UV	=	Ultraviolet
V	=	Volt
v/v	=	Volume/volume
w/w	=	Weight/weight
XRD	=	X-ray diffractometer

CHAPTER 1

INTRODUCTION

1.1. Introduction

Indomethacin (Figure 1.1) is a non-steroidal anti-inflammatory drug (NSAID) that reduces fever, pain and inflammation. It inhibits the cyclooxygenase 1 and 2 that synthesize prostaglandin which causes fever, pain and inflammation. As a result, those symptoms can be reduced (Zhang *et al*., 2007).

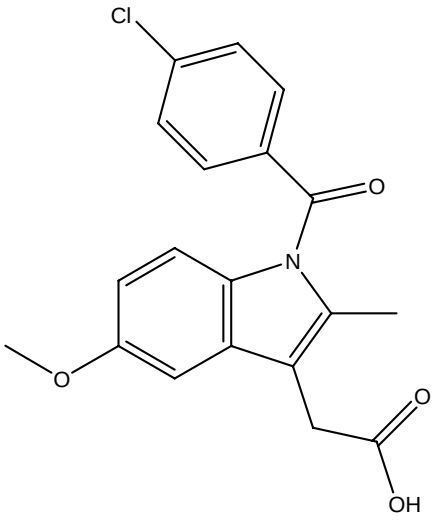

Figure 1.1 The chemical structure of indomethacin

1.2. Side effect of indomethacin

The most common side effects of indomethacin are nausea, vomiting, diarrhea, stomach discomfort, headache, dizziness and drowsiness (Ogbru, 2008).

Indomethacin may cause or worsen stomach or intestinal bleeding or ulcers. It may lead to perforation of the intestine.

Indomethacin also reduces plasma renin activity and aldosterone levels. In addition, indomethacin can increase blood pressure and decrease kidney function. This may lead to edema, hyperkalemia, hypernatremia and hypertension (Ogbru, 2008). The drug may cause renal damage following by elevations of serum creatinine.

1.3. The solubility of indomethacin

Indomethacin is practically insoluble in water and sparingly soluble in alcohol. There have been numerous efforts to improve drug dissolution rate. These include, (1) reducing particle size to increase surface area, (2) solubilization in surfactant systems, (3) formation of water-soluble complex, (Jambhekar *et al*., 2004) (4) use of prodrug and drug derivatization (Jona *et al*., 1995) and (5) manipulation of solid state of drug substance to improve drug dissolution by decreasing crystallinity of drug substance through formation of solid solutions (Spireas and Sadu, 1998).

1.4. Stability of indomethacin

In general, the shelf-life of indomethacin solid dosage forms is five years at room temperature. Exposure to strong direct sunlight induces color intensity of indomethacin; however, degradation is slight. Nevertheless, the precaution of employing light resistant containers should be taken to minimize discoloration (Loukas, *et al.,* 1998).

Indomethacin undergoes alkaline hydrolysis to *p*-chlorobenzoate and 2-methyl-5-methoxy-indole-3-acetate (Figure 1.2). These transformation products are the primary metabolic products of indomethacin.

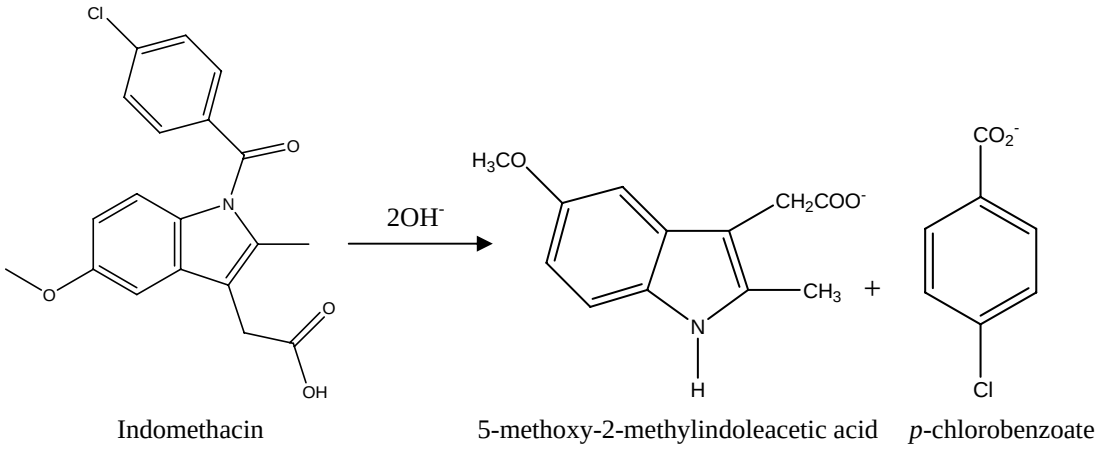

Indomethacin 5-methoxy-2-methylindoleacetic acid *p*-chlorobenzoate

Figure 1.2 Alkaline hydrolysis of indomethacin (Loukas, *et al.*, 1998)

In aqueous solutions, indomethacin is degraded and the therapeutic activity is impaired by the drug instability. It is well known that allergy is, in many cases, due to *p*-chlorobenzoate rather than to the drug itself. Various methods have been used to increase drug stability in aqueous solvent systems to some extent such as adjustments of pH of the aqueous solution, the encapsulation of drugs in liposomal suspensions, the complexation of drugs with various cyclodextrins and the formation of gels or emulsions (Loukas, *et al.*, 1998).

However, there is need to further increase the stability of indomethacin against hydrolysis. For example, (1) the entrapment of cyclodextrin inclusion complexes of indomethacin in multilamellar liposomes greatly increased indomethacin chemical stability (Loukas and Gregoriadis, 1997), (2) the synthesis of ester prodrug prevented

hydrolysis of indomethacin in aqueous solution (Chandrasekaran, *et al.,* 2006) and (3) the spray-drying technique was applied to dry nanocapsule and nanosphere suspension to improve indomethacin stability (Pohlmann *et al.,* 2002).

1.5. Rationale of this study

In a view of several drawbacks, it is important to find strategies to tackle problems. Topical formulation may be a solution for indomethacin. A topical preparation must not only have excellent properties of drug penetration into the painful area, but must also be devoid of a cutaneous reaction due to intolerance and must also be easily applicable. However, the cutaneous absorption of indomethacin is not sufficient due to its limited release of drug from formulation (Fitzpatrick and Colish, 2006), easily hydrolysable and lacks of stability (Loukas and Gregoriadis, 1997).

Several types of indomethacin formulations have been investigated. For instance, indomethacin was incorporated in microemulsion to control drug release (Trotta, 1999). Phosphatidylcholine (Fujii *et al.,* 2001) was used as a permeation enhancer of indomethacin. Furthermore, liquid crystalline gel was used to control release of indomethacin sodium salt (Fitzpatrick and Colish, 2005) with the release of 19%.

There are interests in liquid crystalline phases as delivery systems in the cosmetic and chemical industries (Toshiyuki, *et al.,* 2001) and also in the field of pharmacy (Muller-Goymann, 2004). This is because they are thermodynamically stable, and can be stored for long periods of time without phase separation. Therefore, the development of liquid crystals as drug delivery system is expected to increase the

efficiency of drug by increasing the drug stability and its absorption (Lee and Kellaway, 2000a). Applications of liquid crystals are such as thermoresponsive membrane (Lin *et al.*, 2001) and controlling drug release (Makai *et al.*, 2003).

In this study we synthesized and characterized cholesteryl cetyl carbonate (CCC) as thermotropic liquid crystals. The chemical structure of CCC is composed of cholesterol ring conjugated via carbonate ester linkage with alkyl chain. According to, it chemical properties, CCC is a hydrophobic molecule, thus CCC could improve loading capacity of indomethacin. In addition, thermotropic liquid crystal may protect drug molecule from light by its reflected properties.

Objectives of this thesis are as follows:

- Synthesize and purify cholesteryl cetyl carbonate (CCC)
- Chemical and physical characterization of CCC
- Evaluation of indomethacin-CCC mixture
    - Physical properties of indomethacin-CCC mixture
    - Dissolution test
    - *In vitro* skin permeation study
    - *In vitro* skin retention study
- Stability studies of indomethacin-CCC mixture

CHAPTER 2

LITERATURE REVIEWS

2.1. What are liquid crystals?

Liquid crystals are a phase of matter whose order is intermediate between that of a liquid and a crystal (Figure 2.1). For instance, liquid crystals may flow like a liquid, but have the molecules in the liquid arranged and/or oriented in a crystal-like way. In a crystal, the molecules or atoms have both orientational and three-dimensional positional order over a long range. In an isotropic liquid, the molecules have neither positional nor orientational order, they are distributed randomly. When heated most crystalline substances are transformed directly to isotropic liquid. Some compounds show a different behavior and exhibit different intermediate states in between the crystalline and the liquid state (http://en.wikipedia.org/wiki/Liquid_crys tal). These phases are called liquid crystals or mesophases, and their properties are somewhere between those of liquids and those of crystals. There are various kinds of liquid crystals, with different degrees of order. Some possess only orientational order, others show both orientational order and positional order in one or two dimensions. The number of order also influences the physical properties of the liquid crystal phases, the more order there is, the more viscous the sample will generally be. One thing all liquid crystals have in common is that they are anisotropic. This anisotropy can be achieved in two ways: either the molecules have one molecular axis, which is very different from the other ones, or the molecules possess parts with very different

solubilities. Hence one main distinction can be made between lyotropic and thermotropic liquid crystals (http://en.wikipedia.org/wiki/Liquid_crystal).

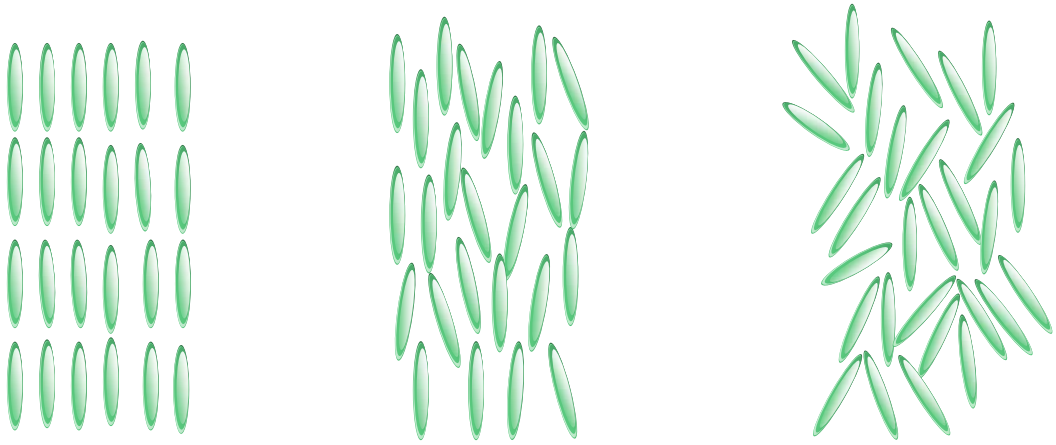

Solid **Liquid crystal** **Liquid**

Figure 2.1 Comparative orientations of solid, liquid crystal and liquid (represents molecule)

2.2. Types of liquid crystal

Liquid crystals come in two basic classifications: thermotropic and lyotropic. The phase transitions of thermotropic liquid crystals depend on temperature, while those of lyotropic liquid crystals depend on both temperature and concentration in liquid medium.

2.2.1. Lyotropic liquid crystals

Lyotropic liquid crystals (LLCs) are formed by amphiphilic molecules. LLCs usually have one part, which is hydrophilic, and another one which is just the opposite, hydrophobic. Due to the fact that the anisotropy is based on the different solubility properties of the different ends of the molecules, a solvent is required in

order to generate LLCs. Typical examples for this kind of molecules are soaps (http://en.wikipedia.org/wiki/Liquid_crystal).

LLCs consist of a polar, hydrophilic head group and an unpolar, hydrophobic tail. Depending on both the temperature and the concentration of the surfactant, different types of liquid crystals can be formed in contact with a solvent, e.g. water. If the concentration of the surfactant is very low, the molecules diffuse randomly. Once a certain concentration, called the critical micelle concentration (CMC), is reached, the amphiphilic molecules arrange themselves to spherical or rod-shaped micelles, assembling the tails together and exposing the polar heads to the water (Figure 2.2). With increasing concentration, the single micelles organize themselves to loose lattices. Spherical micelles preferably form cubic arrangements, whereas rod-shaped micelles usually show a hexagonal arrangement of the cylindrical rods. If the concentration is increased even more, sandwich-shaped bilayers are formed, with the hydrophobic tails pointing to the inside, and the heads to the outside. These bilayers can also be shaped into a three-dimensional tube-like structure, which is then called vesicle. A generic phase diagram for lyotropic liquid crystals is shown in Figure 2.3. The lamellar arrangement is particularly important for phospholipids, which are also amphiphilic, because it is the basis for the biological cell membranes (Friberg, 2003).

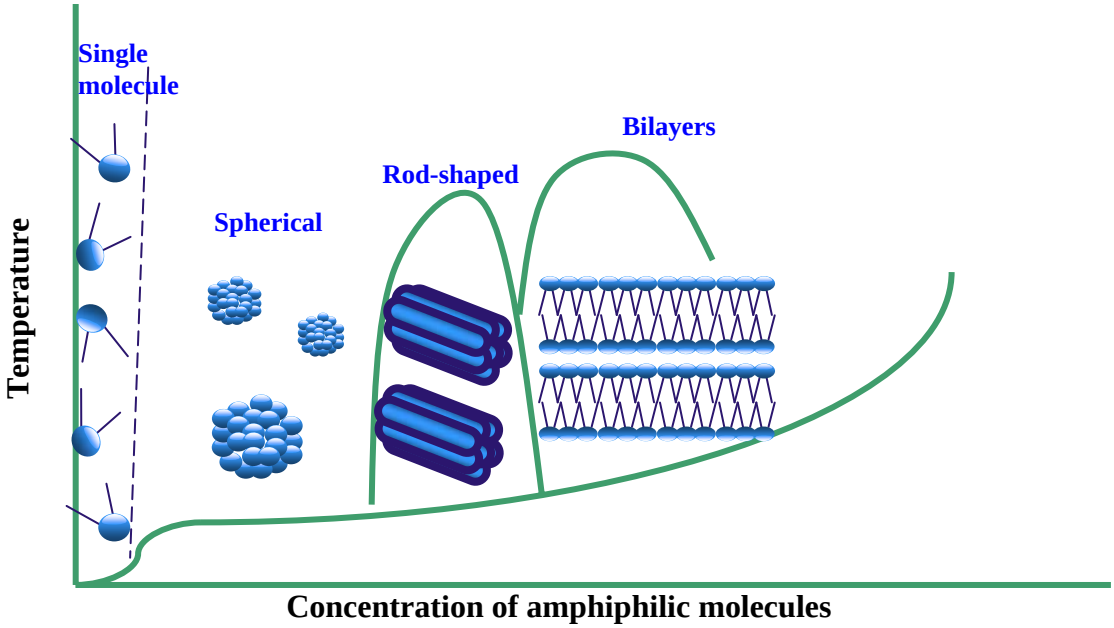

Figure 2.2 Changing of lyotropic liquid crystal formation (adapted from Friberg, 2003

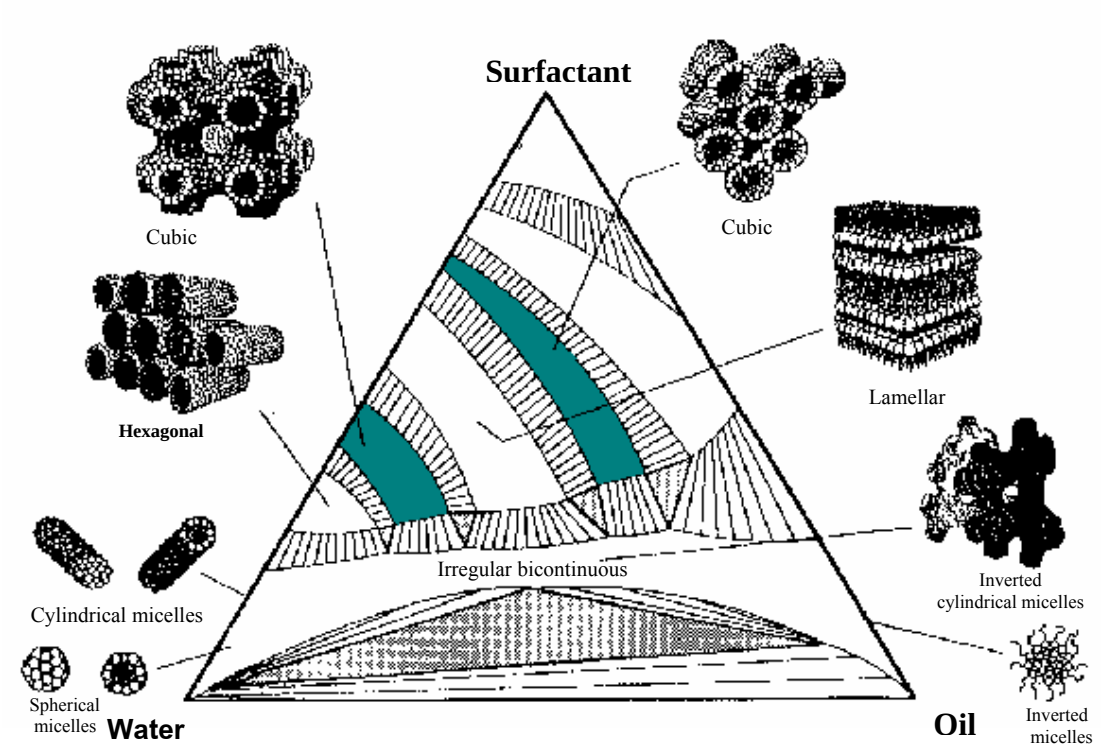

Figure 2.3 The phase diagram of water, oil and surfactant show the arrangement of molecules (Enlow, *et al.,* 2007)

2.2.2. Thermotropic liquid crystals

Thermotropic phases occur in a certain temperature range. If the temperature is raised too high, thermal motion will destroy the delicate cooperative ordering of the liquid crystal phase, pushing the material into a conventional isotropic liquid phase. At low temperature, most liquid crystal materials will form a conventional crystal. Many thermotropic liquid crystals exhibit a variety of phases as temperature changes. For instance, a particular mesogen may exhibit various smectic and nematic (and finally isotropic) phases as temperature increases (http://en.wikipedia.org/wiki/Liquid _crystal) (Figure 2.4).

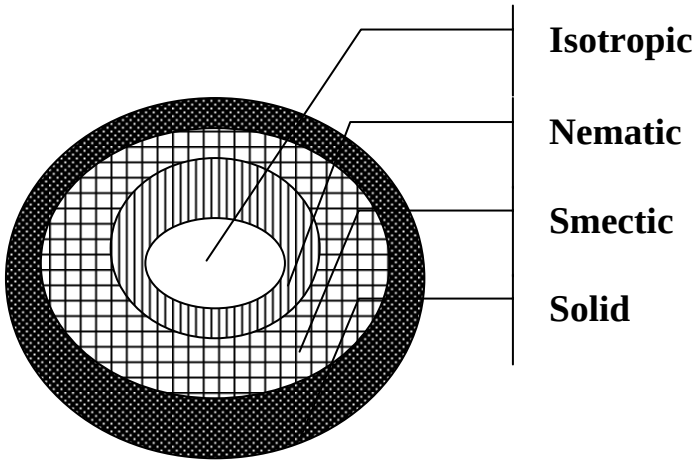

Figure 2.4 The phases of thermotropic liquid crystal

2.2.2.1. Smectic phase

The smectic phase is close to the solid phase. The liquid crystals are ordered in layers. Inside these layers, the liquid crystals normally float around freely, but they cannot move freely between the layers. Still, the molecules tend to arrange themselves

in the same direction (Figure 2.5). The smectic phase is in turn divided into several sub-phases with slightly different properties (Rosenblatt, 2008).

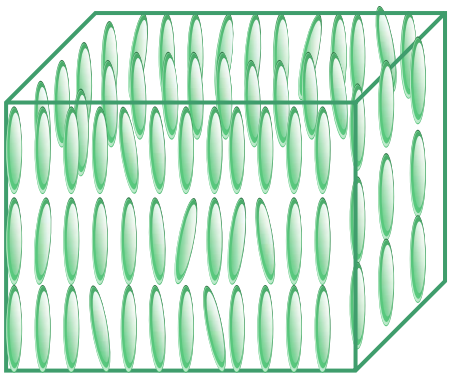

Figure 2.5 The arrangement of smectic phase (represents molecule)

2.2.2.2. Nematic phase

In nematic phase, the molecules have no positional order, but they do have long-range orientational order (Figure 2.6). Thus, the molecules flow and their centre of mass positions are randomly distributed as in a liquid, but they all point in the same direction (within each domain). When the molecules are chiral and in the nematic phase, they arrange themselves into a strongly twisted structure that often reflects visible light in different bright colors which depend on the temperature. They can therefore be used in temperature sensors (thermometers) (Rosenblatt, 2008).

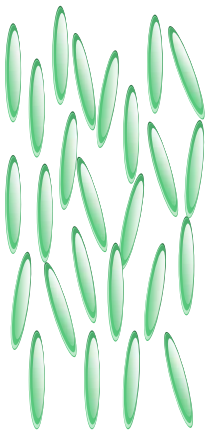

Figure 2.6 The arrangement of nematic phase (represents molecule)

The development of liquid crystals for drug delivery system was able to increase the efficiency of drug. Solubility of drugs can be increased by means of solubilization, which is either insoluble or slightly soluble in water (Muller-Goymann, 2004). Liquid crystals were employed to control drug release (Makai *et al.,* 2003), and enhance drug absorption (Lee and Kellaway, 2000b). There also were applied as thermoresponsive membrane for controlling drug release at needed temperature (Lin *et al.,* 2001).

2.3. How do we know a compound shows a liquid crystal phase?

Liquid crystal exhibits physical properties such as phase transition behavior, the orientation of structure and birefringence. There are several techniques to characterize physical properties of liquid crystal such as differential scanning calorimetry, X-ray diffraction and polarized light microscope.

2.3.1. Differential scanning calorimetry

Differential scanning calorimetry (DSC) is a useful tool which complements optical methods in the study of liquid crystal phase transitions. It utilizes in determining the heat absorption or release during heating or cooling down process.

In Figures 2.7, DSC traces obtained from a sample of octyloxy cyanobiphenyl at a heating rate of 1°C/min. The lower curve displayed liquid crystal properties of materials (Friberg, 2003).

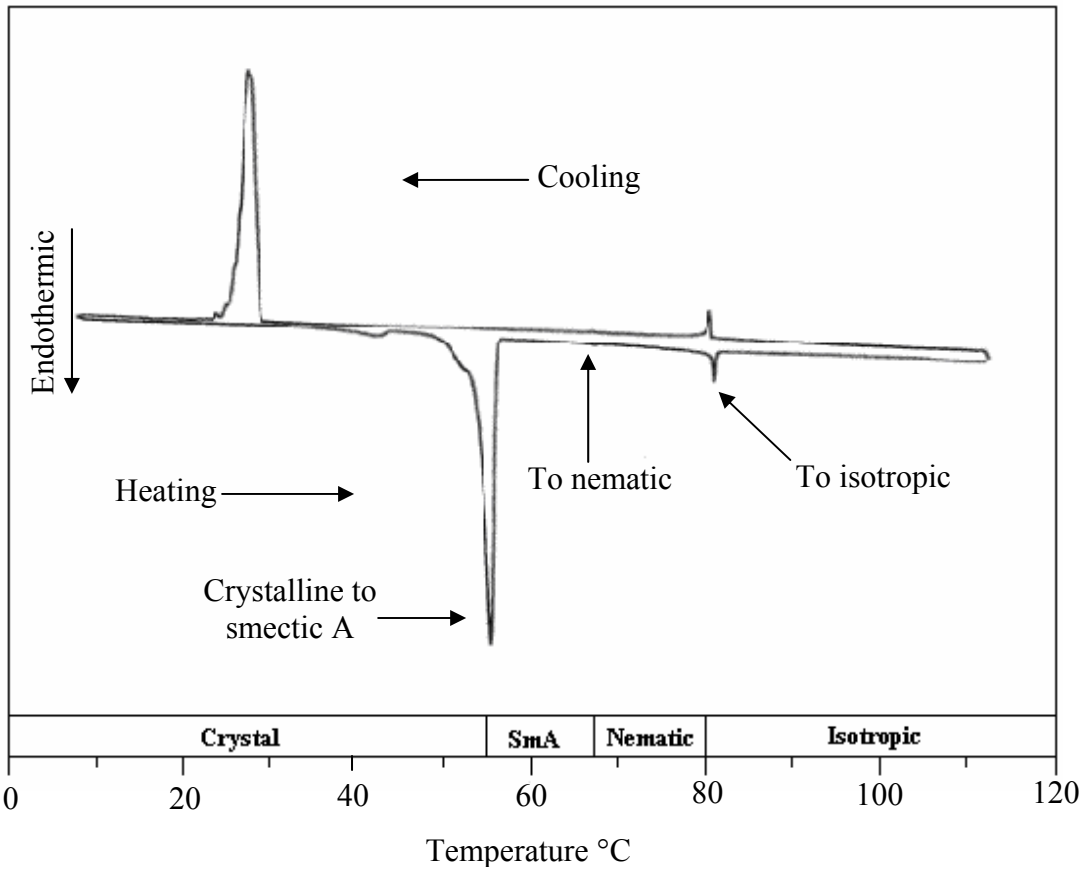

Figure 2.7 The thermogram of octyloxy cyanobiphenyl liquid crystal (Friberg, 2003)

A phase changes during the heating process is placed just above the temperature axis. This includes a crystal to liquid crystal (smectic A) transition at

55°C following by a barely detectable smectic A to nematic transition at 67°C and finally the nematic to isotropic transition near 80°C. The cooling curve shows a slight displacement of the nematic to isotropic transition, partially due to supercooling and partially instrumental hysteresis attributable to the temperature scan rate. The smectic A to crystal transition is depressed strongly due to supercooling of the smectic A phase. Thus, the phase diagram for the cooling process would not be identical to that for heating.

2.3.2. X-ray crystallography

The structure of crystalline compounds and the type of phase can be determined by X-ray crystallography. The structure and the orientation of 7,16-bis(2-hydroxybenzoyl)-5,14-dihydrodibenzo[1,4,8,11]-tetraazacyclotetradecine was established by Grolik *et al.* (2006) (Figure 2.8).

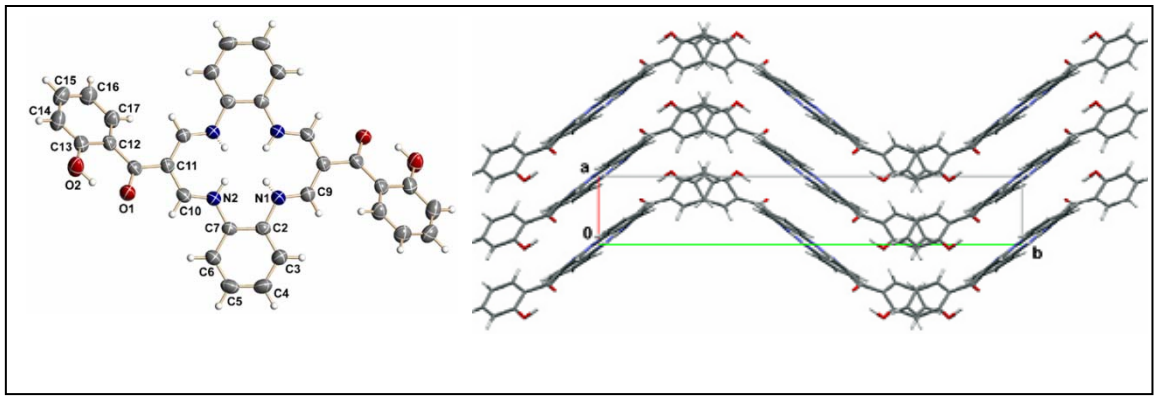

Figure 2.8 3D structure and orientation of 7,16-bis(2-hydroxybenzoyl)-5,14-dihydrodibenzo [1,4,8,11]-tetraazacyclotetradecine (Grolik *et al.,* 2006)

2.3.3. Polarized Light Microscopy

Liquid crystals can be visualized under a polarized light microscope fitted with a heating stage. The thickness of the sample usually has the greatest effect on the

colors that are seen. A liquid crystal phase acts like a single crystal when polarized light is passed through it (Friberg, 2003).

When an organic compound is placed on a microscope slide with a cover slip and the slide is heated and viewed using the high magnification of the microscope, textures characteristic of each type of liquid crystal can be observed. Cooling the liquid can also yield similar textures when liquid crystal phases are present. If the materials have no liquid crystals properties, birefringence cannot be observed. With a great deal of practice and experience, the viewer can develop the skill to determine the type of liquid crystal phases present.

2.4. Topical delivery system

Topical delivery system has been used as a route of medicinal delivery for many years. Advantages include: (1) a reduction in first pass metabolism by the liver (2) non-invasiveness (3) avoidance of the gastric route, reducing the potential for both degradation of the drug and gastric irritation, and (4) patient compliance with drug administration (Magnusson *et al.,* 2001).

2.4.1. Overview of the anatomy and function of the skin

The skin is accounting for more than 10% of body mass and the one that enables the body to interact most intimately with its environment. It consists of the epidermis, the dermis and the subcutaneous tissue which anchors the skin to underlying tissues. Each layer is physically and functionally distinct with appendages, including hair follicles, sweat ducts and sebaceous glands, bridging between the

layers and the skin surface (Figure 2.9). A more detailed account of skin structure and physiology can be found in some excellent reviews (Mills and Cross, 2006).

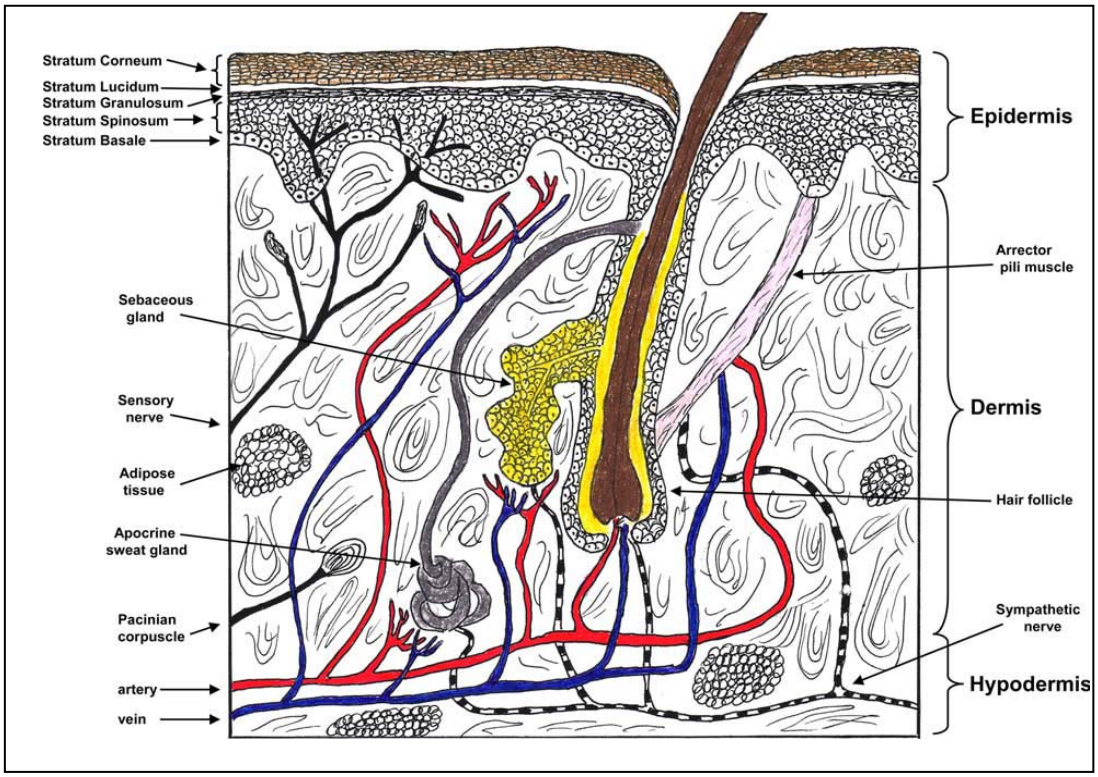

Figure 2.9 The typical structure of mammalian skin (Mills and Cross, 2006)

2.4.1.1. Epidermis

The epidermis is divided into four anatomical layers namely stratum basale (SB), stratum spinosum (SS), stratum granulosum (SG) and stratum corneum (SC). The SC is the heterogeneous outermost layer of the epidermis and is approximately

10 - 20 μm thick. It is non-viable epidermis and consists of 15 - 25 flattened, stacked, hexagonal and cornified cells embedded in a mortar of intercellular lipid. Each cell is approximately 40 μm in diameter and 0.5 μm thick (Buck, 2004). The thickness varies and may be a magnitude of order larger in areas such as the palms of the hands and soles of the feet. These are areas of the body associated with frequent direct and substantial physical interaction with the physical environment. Not surprisingly, absorption is slower through these regions than through the skin of other parts of the body. The cells of the SC, keratinocytes, originate in the viable epidermis and undergo many morphological changes before desquamation. The keratinocytes are metabolically active and capable of mitotic division (Buck, 2004) and therefore the epidermis consists of several cell strata at varying levels of differentiation (Figure 2.10).

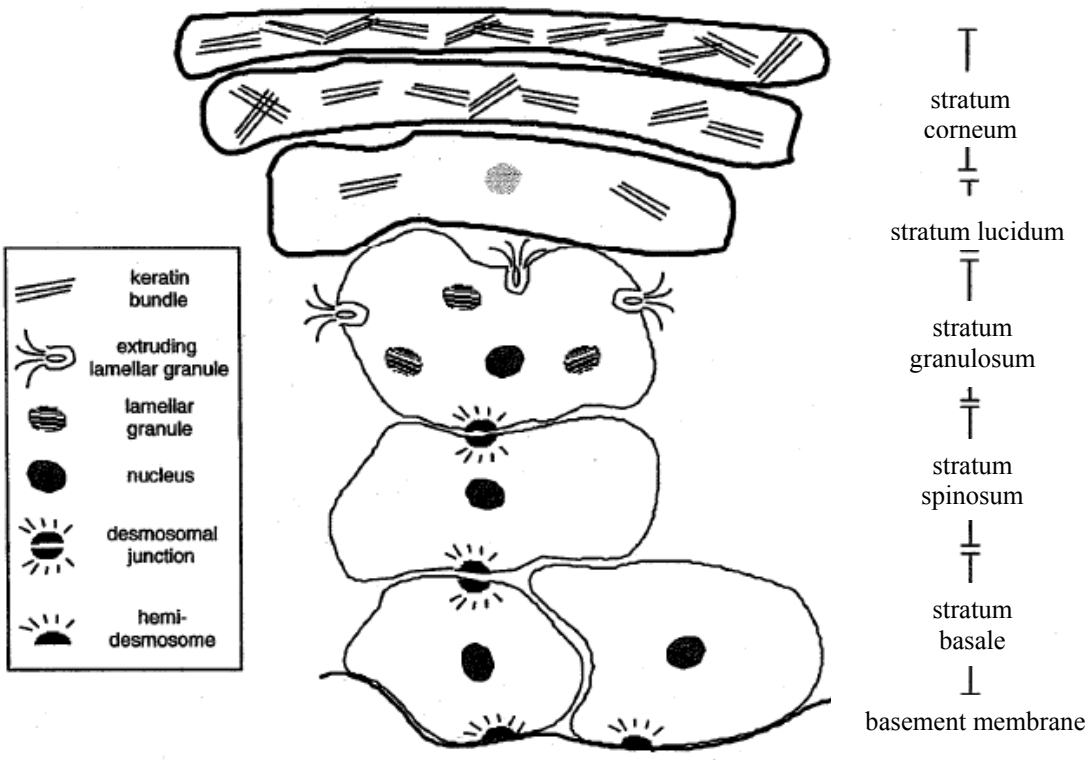

Figure 2.10 Epidermal differentiation: major events include extrusion of lamellar bodies, loss of nucleus and increasing amount of keratin in the stratum corneum (adapted from Walters and Roberts, 2002)

The origins of the cells of the epidermis lie in the basal lamina between the dermis and viable epidermis (Walters and Roberts, 2002). In the basal layer of the epidermis there is continuous renewal of cells. These cells are subsequently transported to the upper layers of the epidermis. The composition of lipids changes markedly during apical migration through successive epidermal layers. When the differentiation process is accomplished (*i.e.,* in the SC), lipid composition changes markedly, phospholipids are degraded enzymatically into glycerol and free fatty acids and glucosylceramides into ceramides. The main constituents of the SC lipids are cholesterol, free fatty acids and ceramides. At physiological temperature, which is below the gel-to-liquid crystalline phase transition temperature, the lipids are highly ordered. The SC is a composite of corneocytes (terminally differentiated keratinocytes) and secreted contents of the lamellar bodies (elaborated by the keratinocytes), that give it a 'bricks-and-mortar' structure (Menon, 2002). This arrangement creates a tortuous path through which substances have to traverse in order to cross the SC. The classic 'bricks-and-mortar' structure is still the most simplistic organizational description. The protein-enriched corneocytes (bricks) impart a high degree of tortuosity to the path of water or any other molecule that traverses the SC, while the hydrophobic lipids, organised into tight lamellar structures (mortar) provide a water-tight barrier property to the already tortuous route of permeation in the interfollicular domains (Menon, 2002).

Because of its highly organized structure, the SC is the major permeability barrier to external materials, and is regarded as the rate-limiting factor in the penetration of therapeutic agents through the skin. The ability of various agents to interact with the intercellular lipid therefore dictates the degree to which absorption is enhanced (Foldvari, 2000).

2.4.1.2. Dermis

The dermis is much wider than the overlying epidermis which it supports and thus makes up the bulk of the skin. The dermis, which provides the elasticity of the skin, contains immune cells and has the vascular network that supplies the epidermis with nutrients that can carry absorbed substances into the body. The dermis consists of a matrix of connective tissue woven from fibrous proteins (collagen 75%, elastin 4% and reticulin 0.4%) which is embedded in mucopolysaccharide providing about 2% of the mass. Blood vessels, nerves and lymphatic vessels cross this matrix and skin appendages (endocrine sweat glands, apocrine glands and pilosebaceous units). In human, the dermis divides into a superficial, thin image of the ridged lower surface of the epidermis and a thick underlying reticular layer made of wide collagen fibres. It also plays a role in temperature, pressure and pain regulation (Walters and Roberts, 2002).

2.4.1.3. Subcutis

The subcutis or hypodermis is mostly composed of adipocytes with fewer fibroblasts, endothelial cells and macrophages. It connects to the dermis via collagen

and elastin, while anchoring the skin to underlying muscle. Its major role is to carry the vessels and nerves that supply the skin (Mills and Cross, 2006).

2.4.1.4. Skin appendages

The SC is interrupted at regular intervals by appendages penetrating through from the dermis, particularly hair follicles (with associated sebaceous glands) and sweat glands (apocrine and eccrine). The number and type of appendages vary with species and body region. Hair follicles function to protect the epidermis, while lubrication is provided by the sebum. Eccrine glands are important to body cooling, while the apocrine glands release a lipid secretion and may function as a vestigial secondary sex gland. While the fractional area of hair follicles represents approximately 0.1% of the skin surface in man, it may be considerably greater in some domestic species (Mills and Cross, 2006).

2.4.2. Routes of drug permeation across the skin

The permeation of drug through the skin includes the diffusion through the intact epidermis and through the skin appendages occupy only 0.1% of the total human skin surface and the contribution of this pathway is usually considered to be small. As stated above, drug permeation through the skin is usually limited by the SC. The pathways through the intact barrier may be identified: the intercellular lipid route between the corneocytes and the transcellular route crossing the corneocytes and the intervening lipids (Figure 2.11). Both cases the permeant must diffuse at some point through the intercellular lipid matrix, which is now recognized as the major determinant of percutaneous transport rate (Moser *et al.,* 2001).

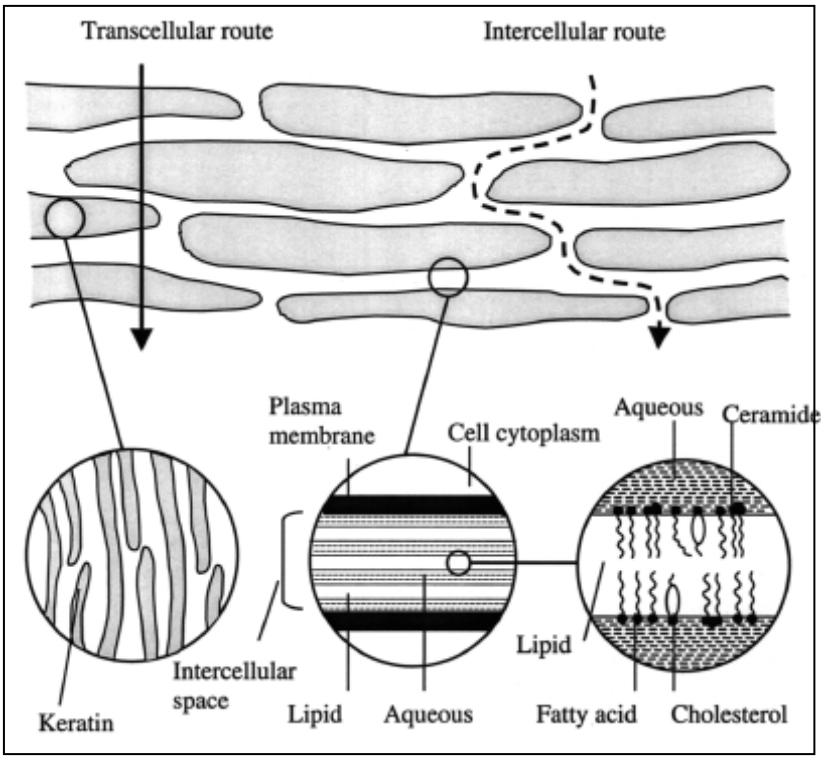

Figure 2.11 Permeation route through the SC (Moser *et al.*, 2001)

2.4.3. Percutaneous drug absorption

Percutaneous drug absorption is described by Fick's first law of diffusion as in equation 2.1:

$$\frac{dQ}{dt} = Jss = \frac{Ks \times D}{h} \times \Delta Cv \times A \qquad \text{(Eq. 2.1)}$$

where *dQ/dt* is the amount of drug diffused per unit time (i.e. drug flux), *Jss* is the drug flux. *Ks* is the partition coefficient. *D* is the diffusion coefficient. *h* is the diffusional path length (thickness of SC). ΔCv is the concentration gradient of drug and *A* is the skin surface area treated.

Attempts can be made to manipulate any of these parameters (*Ks*, *D* or ΔCv) in order to influence drug delivery through the skin. Earlier efforts concentrated on

the chemical modification of drug molecules in order to increase drug flux through the production of derivatives with optimum lipid solubilities. This concept is also applicable in the prodrug approach, in which inactive but highly absorbable prodrug molecules are subsequently activated within the skin. This approach, however, is rarely possible with proteins and DNA. The remaining and most feasible option might therefore involve manipulation of the skin barrier (Foldvari, 2000).

2.4.3.1. Chemical enhancement

(A) Drug modification

With respect to the drug molecule itself, its lipophilicity can be modified by derivatization. This derivatization strategy is the basis of the prodrug approach in which the therapeutic entity is chemically modified to facilitate its permeation. Such a prodrug approach has been successfully exploited in the topical steroidal anti-inflammatory field where the intrinsic pharmacological potency of these molecules is often not matched by their topical efficacy (Naik *et al.,* 2000).

(B) Colloidal system

Colloidal drug carrier systems such as micellar solutions, vesicle and liquid crystal dispersions, as well as nanoparticle dispersions consist of small particles of 10–400 nm diameters.

-Reverse micelles

Amphiphilic molecules such as surfactants associate to form micelles beyond the CMC of the compound in an aqueous solution. Micellar solutions not only exist in aqueous systems but also form in oily systems. In this case reverse micelles are formed with the lipophilic part of the surfactant molecule facing the oily medium and the hydrophilic part representing the inner core of the associate. A widely used excipient in drug development is lecithin, which is able to form reverse micelles in oily media. Normal micelles of lecithin do not exist, instead liposomes are formed when phospholipids are dispersed in aqueous media. Solubilization of drug molecules is possible both in normal micelles and in reverse micelles (Muller-Goymann, 2004).

-Liquid crystals

A requirement for the formation of liquid crystalline phases is an anisometric molecular shape, which is generally associated with a marked anisotropy of the polarizability. Even drug compounds themselves, e.g. the salts of organic acids or bases with anisometric molecular shape, may fulfill the requirements for the liquid crystal formation. Starting with the crystalline state, the mesophase is reached either by increasing the temperature or by adding a solvent (Muller-Goymann, 2004).

-Vesicles

With some molecules, a high concentration results in a lamellar phase but no additional mesophases are formed if the concentration is reduced. The lamellar phase is dispersed as concentric layered particles in an excess of solvent (water or aqueous solution). This results in a vesicular dispersion. If the mesogenic material consists of

phospholipids, the vesicular dispersion is called a liposomal dispersion (Muller-Goymann, 2004).

Liposomes consist either of many, a few or just one phospholipid bilayer. Therefore multilamellar vesicle, oligolamellar vesicles, small unilamellar and large unilamellar vesicles have to be distinguished. Furthermore multivesicular liposomes may be formed. The polar character of the liposomal core enables polar drug molecules to be encapsulated. Amphiphilic and lipophilic molecules are solubilized within the phospholipid bilayer according to their affinity towards the phospholipids (Muller-Goymann, 2004).

(C) Chemical penetration enhancer

Chemical penetration enhancers are substances that can partition into, and interact with skin constituents (mainly the intercellular lipid fraction) and induce a temporary and reversible decrease in skin barrier properties. Similar to hydration, penetration enhancers possibly interact with some components of the skin to increase fluidity in the intercellular lipids, possibly induce swelling of keratinocytes and/or leaching out of structural components, thereby reducing the barrier function of the SC (Mills and Cross, 2006).

Example of enhancers are water, hydrocarbons, sulphoxides and their analogues, pyrrolidones, fatty acids, esters, alcohols, Azone and its derivatives, surfactants (anionic, cationic and nonionic), amides, essential oils, terpenes and oxazolidines (Barry, 2001).

2.4.3.2. Physical penetration enhancement

There are several techniques where electrically generated currents or energy fields can assist in transdermal drug penetration.

(A) Phonophoresis

Phonophoresis (or sonophoresis) uses ultrasound energy in order to enhance the skin penetration of active substances. Ultrasound assists transdermal drug penetration because low frequency energy waves disturb the SC layers by cavitation. Early attempts relied on physiotherapy wave frequency settings which focuses on deeper muscle structures, while lower frequency ultrasound (~20 kHz) can enhance drug penetration by up to 1000-fold (Mills and Cross, 2006).

(B) Iontophoresis

Iontophoresis uses a small electrical current (0.5 mA/cm^2) applied between two electrodes in contact with the skin to drive a charged molecule (although neutral molecules can also be enhanced through electroosmosis) through the barrier. The efficiency of iontophoresis depends on the polarity, valency and mobility of the drug molecule, plus the electrical cycle and formulation containing the drug (Mills and Cross, 2006).

(C) Electroporation

Electroporation involves the application of short electrical pulses (100–1000 V/cm) to the skin. This creates transient aqueous pores through the SC, which permits drugs to penetrate more readily. Electroporation has been used to enhance the transport of liposomes and microspheres (Mills and Cross, 2006).

2.5. Research and development of topical indomethacin

The transdermal route is frequently utilized for delivery of potent therapeutic agents with low molecular weight, and offers several advantages over conventional dosage forms such as tablets and injections. These advantages include avoidance of first-pass metabolism, minimization of pain, and possible sustained release of drugs. For example, the administration of NSAIDs via the dermal route has been adopted to bypass the disadvantages of the oral route, such as irritation and ulceration of the gastrointestine. Although, the utility of transdermal delivery is limited due to the low drug penetration across the SC of the skin (Fitzpatrick and Corish, 2005).

Several strategies have been employed to enhance the skin penetration of indomethacin. These include the use of chemical enhancer, nanoparticle and prodrug. 3-*l*-Menthoxypropane-1,2-diol as chemical enhancer has been demonstrated to enhance the permeation of indomethacin though *in vitro* animal skin.

Phospholipids in liquid paraffin was found to improve the permeation of indomethacin across animal skin. This enhancing effect was due to the solubilization of indomethacin in the vehicle. Permeation rates were proportional to skin drug concentration and the enhancement of permeation was dependent upon high partition of indomethacin (Fujii *et al.*, 2001).

Cholesterol-modified glycol chitosan (CGC) conjugate was synthesized and characterized. The physicochemical properties of the self-aggregated nanoparticles were studied using dynamic light scattering, transmission electron microscopy and fluorescence spectroscopy. Indomethacin was physically entrapped into the CGC nanoparticles. CGC nanoparticles had a potential as a drug delivery carrier because of

the initial rapid release in 2 h and slower release for up to 12 h was observed (Jing-Mou *et al.,* 2008).

Indomethacin terpenoid esters were synthesized and assessed both *in vitro* and *in vivo* as indomethacin dermal prodrug. The indomethacin terpenoid esters were assessed in their chemical and enzymatic stability, solubility, lipophilicity and flux through excised human skin. The indomethacin dermal prodrug slightly increased the cumulative uptake of indomethacin through excised human skin compared with the parent drug. In addition, *in vivo* results showed an interesting delayed and sustained activity of ester compared with the parent drugs in human volunteers (Palagiano *et al.,* 1997).

2.6. Liquid crystals as drug delivery system

Liquid crystals have a considerable solubilizing capability for both oil and water soluble compounds. They have been found to be a part of the microstructure of a variety of preparations suitable for topical use. The total therapeutic effect of percutaneous preparations depends not only on the action of the drug itself, but also on other factors related to the structure of the vehicle (Nesseem, 2001).

Lamellar liquid crystals have been proposed as semisolid vehicles for topical administration of drugs (Nesseem, 2001). Liquid crystals incorporated in microcapsules made of gelatin which rupture on topical application are available. Lyotropic liquid crystals are also incorporated in special dermatological formulations that exhibit hydrating properties. Most of all, liquid crystals are used as excipients to protect sensitive substances (e.g. vitamins, antioxidants and oils). They may enhance the stability of creams while creating a rheological barrier resulting in an increase in

the viscosity and a decrease in coalescence by modification of Van der Waals forces (Benita, 1996).

2.6.1. Control release of drug

Makai and co-workers (2003) formulated multicomponent lamellar liquid crystal systems with relatively low surfactant content. This research revealed that poly-oxyethylene-10-oleyl ether (Brij 96) is a proper surfactant suitable for the formation of lamellar liquid crystals with water. The samples contained Brij96/glycerol/liquid petrolatum/distilled water formed stable well-tolerable lyotropic lamellar liquid crystals (Table 2.1). A prolonged drug release was observed in the case of very water-soluble ephedrine hydrochloride and the same phenomena were observed in the case of tenoxicam, which is practically insoluble in water (Makai *et al.,* 2003).

Table 2.1 Compositions of four-component samples investigated (Makai *et al.,* 2003)

Sample	Brij 96/water (%w/w)	Brij 96 (%w/w)	Glycerol (%w/w)	Liquid petrolatum (%w/w)	DW (%w/w)
1	2:1	60	-	10	30
2	3:2	45	15	10	30
3	4:3	42.5	17.5	10	30
4	4:3	40	20	10	30
5	1:1	30	30	10	30

DW = Distilled water

The release of ephedrine hydrochloride showed a first-order kinetic. A fast release was observed followed by a slow release in case of samples 2–4 (Figure 2.12) containing glycerol 15–20% (w/w). Zero order release kinetic was found in case of sample 5. Higher glycerol content caused a softer consistency of semisolid dosage form.

The release of tenoxicam followed zero order release kinetic. The highest amount of released tenoxicam was measured in sample 5 (Figure 2.13) with the highest diffusion coefficient. The other glycerol-containing sample showed slower drug release when lamellar liquid crystalline structures were present.

This phenomenon was explained as follows: the water present in the lamellar liquid crystal systems was sufficient for dissolving the very soluble ephedrine hydrocloride. Tenoxicam as a practically insoluble drug was completely solubilized in the selected systems. An increase in the interlamellar distance was detected in case of both incorporated model drugs, meaning that the drugs were partly built between the lamellar space, and partly located at a given polarity part of the amphiphilic surfactant molecules.

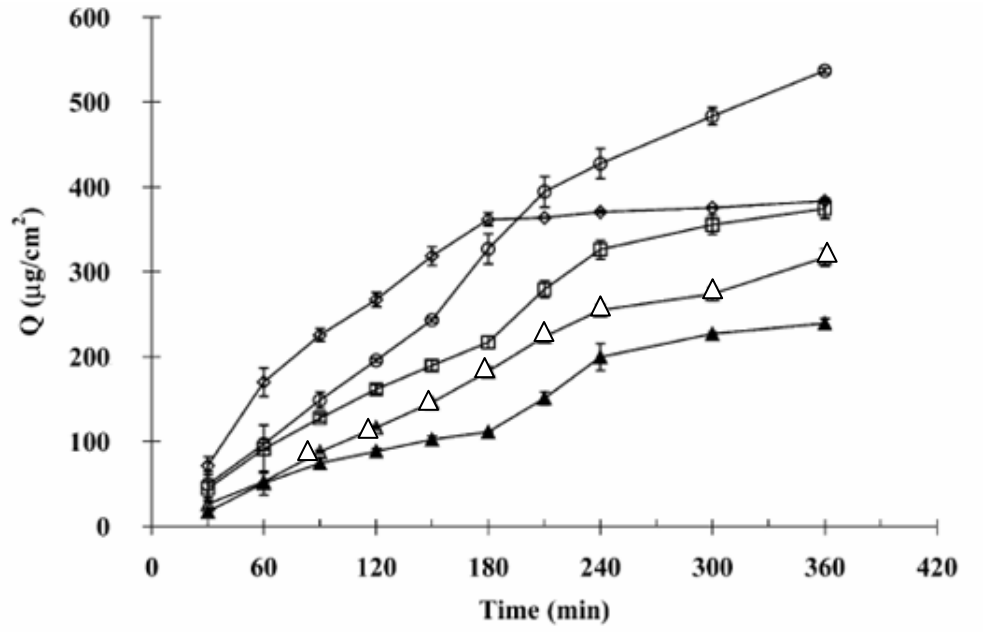

Figure 2.12 Ephedrine hydrochloride release from samples 1 (▲), sample 2 (Δ), sample 3 (□), sample 4 (◊) and sample 5 (○) (mean ± SD, n=3) (Makai *et al.,* 2003)

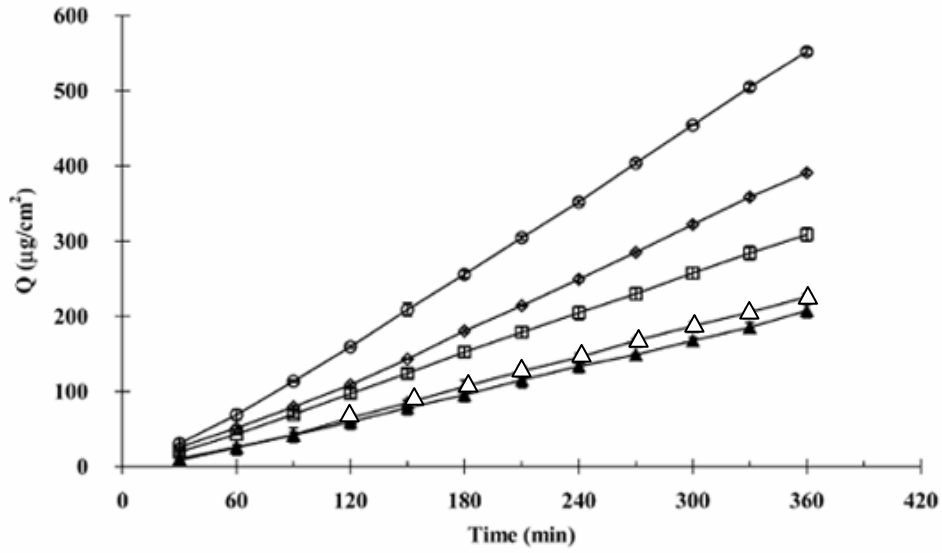

Figure 2.13 Tenoxicam hydrochloride release from samples 1 (▲), sample 2 (Δ), sample 3 (□), sample 4 (◊) and sample 5 (○) (mean ± SD, n=3) (Makai *et al.,* 2003)

2.6.2. Enhanced drug permeation

Buccal permeability of a [D-Ala^2, D-Leu^5] enkephalin (DADLE) from the cubic and lamellar liquid crystalline phases of glyceryl monooleate (GMO) was examined across excised porcine buccal mucosa mounted in a Franz cell. GMO was released from the liquid crystalline phases indicating the erosion of the liquid crystal matrices. GMO released from the liquid crystalline matrices and permeated the porcine buccal mucosa with fluxes of 0.10 ± 0.03 and 0.07 ± 0.02% cm^2/h for the cubic and lamellar phases, respectively. The flux of DADLE (1.21 ± 0.32 and 1.15 ± 0.11% cm^2/h for the cubic and lamellar phases, respectively) from the liquid crystalline phases was significantly enhanced by the GMO compared with PBS solution (0.43 ± 0.08% cm^2/h) during the initial permeation phase (Figure 2.14). The results suggest that the cubic and lamellar liquid crystalline phases are promising

buccal drug carriers for peptide drugs as well as acting as permeation enhancers (Lee and Kellaway, 2000a).

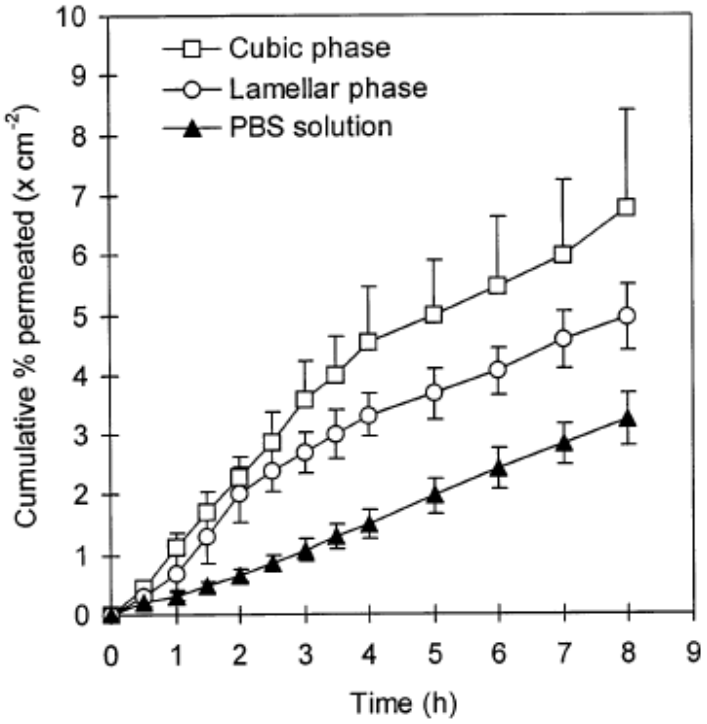

Figure 2.14 Permeation of **[**^{3}H**]** DADLE to the receiver compartment across porcine buccal mucosa (Lee and Kellaway, 2000a)

2.6.3. Thermoresponsive membrane

A thermo-responsive membrane was developed by embedding with the binary mixture of 36% cholesteryl oleyl carbonate (COC) and 64% cholesteryl nonanoate (CN) to achieve a rate and time-controlled drug release in response to the skin temperature (i.e., 32°C). The temperature-sensitive on–off pulsatile function of drug penetration through this thermo-responsive membrane was investigated. The switching mechanism of this thermo-responsive membrane was proposed. The results reveal that this binary mixture has a good temperature response in precision,

sensitivity, obedience and reproducibility. The results strongly indicate that the binary COC–CN mixture-embedded membrane can be used to deliver the drug in a pulsatile fashion with respect to skin temperature (Lin *et al.*, 2001).

CHAPTER 3

MATERIALS AND METHODS

3.1. Synthesis and characterization of cholesteryl cetyl carbonate

3.1.1. Synthesis of cholesteryl cetyl carbonate

The synthetic route of cholesteryl cetyl carbonate (CCC) was given in scheme 3.1 (adapted from Elser *et al.,* 1973). Cholesteryl chloroformate (Sigma-Aldrich, Steinheim, Germay) (2.50 g, 5.57 mM) was dissolved in dichloromethane (J.T. Baker, NJ, USA) (15.0 ml) in a clean and dry round bottom flask until a clear solution was obtained. Cetyl alcohol (Sigma-Aldrich, Steinheim, Germay) (1.35g, 5.57 mM) was dissolved in 10.0 ml of dichloromethane, transferred to a dropping funnel and the solution was slowly added to the round bottom flask, at a rate of 1 drop/s and the mixture was stirred at room temperature for 30 min. Pyridine (1.0 ml) was added into the solution and reflux overnight. The end product from the reaction was well washed with water. The organic phase containing CCC was collected and any residual water was removed by adding 2 g of anhydrous sodium sulfate (Fisher Scientific, Leicestershire, UK) and filtered though filter paper (Whatman, 0.45µm). The solvent was removed using a rotary evaporator to afford CCC.

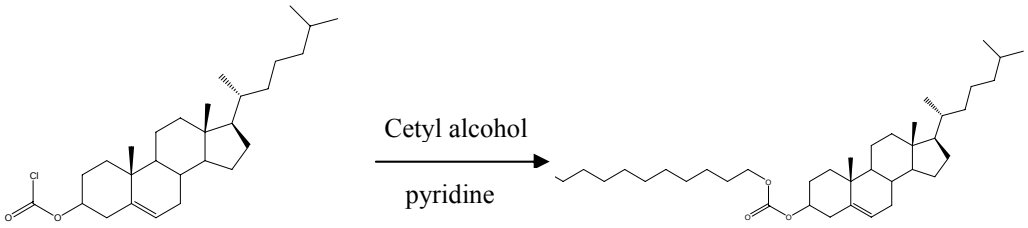

Cholesteryl chloroformate

Cholesteryl cetyl carbonate

Scheme 3.1 Synthesis of cholesteryl cetyl carbonate

3.1.2. Component determination

The purity of CCC was checked in two thin layer chromatographic (TLC) systems, which one hexane-diethyl ether (J.T. Baker, NJ, USA) 80:20 (v/v) and the other hexane-chloroform (J.T. Baker, NJ, USA) 80:20 (v/v) (Chuealee *et al.*, 2007).

The eluting solvent (10 ml) was placed in a 100 ml TLC tank covered with a lid, to ensure that the tank was saturated with solvent vapor. The samples (5 µl) were applied on TLC plate (silica gel 60 F254) using capillary column. The resolved spots were detected by two spraying reagents; first, compounds were detected by iodine vapor, the separated components appeared as yellow-colored spots. For second system, 0.1% phosphotungstic acid in ethyl alcohol followed by heating at 100°C for 15 minutes (Dean, 1995). The red spots were appeared, Rf values were recorded.

3.1.3. Purification

Flash column chromatography was employed to purify CCC. CCC mixture was dissolved with eluent (hexane-chloroform 80:20 (v/v)) and then carefully poured into stationary phase (silica gel 60) with eluent flow rate of 2 ml/5 min. Thirty

fractions was kept (5 ml of each fraction) after 30 min. The pure CCC was separated in fraction 5-15 and the eluent was removed by rotary evaporator.

3.1.4. Physical characterization

3.1.4.1. Polarized optical microscopy (PLM)

Thermal phase transitions and texture changes of CCC were observed with an Olympus BH-2 polarizing optical microscope (Tokyo, Japan) equipped with a hot stage (RT-200°C) (Westler, Germany). The sample (5 mg) was placed on a glass slide and covered with a glass cover slip (Bagheri and Rad, 2008).

3.1.4.2. Differential scanning calorimetry

The thermal behavior of CCC was studied with Perkin-Elmer DSC-7 (Massachusetts, USA). The samples were examined at a scanning rate of 10°C/min by applying heat following by cooling cycle between 0 and 200°C. Transition temperatures were determined as an onset of the transition peaks at which the tangential line of the inflection point of the rising part of the peak cross over the extrapolated baseline. The thermogram of the buffer solvent used was subtracted from the thermogram obtained and then corrected for the thermal delay of the calorimeter. The decomposition of the thermogram was obtained by further processing the data using the software spectra (Fischer *et al.,* 2007).

3.1.5. Structure elucidation

3.1.5.1. Fourier Transform Infrared Spectrophotometer (FTIR)

The functional group of liquid crystal was characterized by FTIR (Spectrum one, Perkin Elmer, USA) in the region 4000-400 cm^{-1}. FTIR spectrum were obtained at 4 cm^{-1} resolution under a dry air purge, accumulation of 8 scans. A small amount of sample was sealed into KBr pellet by hydraulic press prior to measurement at ambient temperature.

3.1.5.2. Nuclear Magnetic Resonance Spectroscopy (NMR)

The chemical structure of CCC was confirmed by ^{13}C-NMR and ^{1}H-NMR (Unity inova 500, Varian California, USA). CCC (30 mg) was dissolved in deuterated chloroform in NMR tube. All the NMR spectra were run at 25ºC. Chemical shifts were referenced to internal standard TMS.

3.1.6. Chemical characterization

3.1.6.1. TLC densitometry

The stability of CCC could be measured by TLC densitometry. CCC was applied as small spots at the base line as previously described in section 3.1.2. The Camag TLC scanner II (Muttenz, Switzerland) equipped with a deuterium lamp set at 358 nm in the reflection mode used for scanning the plates. The peak heights and areas of chromatograms were determined using Camag version 3.11 software (Muttenz, Switzerland).

3.2. Properties of indomethacin

3.2.1. UV spectra study

In order to choose a suitable solvent for preparation of indomethacin-CCC mixture, UV spectra studies of indomethacin was performed in different organic solvents (ethanol, ethyl acetate and chloroform).

3.2.2. Solubility study of indomethacin in isotonic phosphate buffer pH 7.4

3.2.2.1. Preparation of isotonic phosphate buffer (IPB) pH 7.4

IPB pH 7.4 was prepared by mixing two stock solutions, 200 ml of a stock solution containing 8.0 g of monobasic sodium phosphate (NaH_2PO_4) (Ajax Finechem, Auckland, New Zealand) and 800 ml of a stock solution containing 9.5 g of dibasic sodium phosphate (Na_2HPO_4) (Ajax Finechem, Auckland, New Zealand), the weights being on an anhydrous basis. Then the obtained solution was adjusted with respect to tonicity by adding 4.4 g of sodium chloride (Ansel *et al.,* 1995). The obtained IPB was filtered through a 0.45 μm cellulose acetate membrane (Sartorius AG, Goettingen, Germany).

3.2.2.2. Solubility study

An excess amount of indomethacin (10 mg) was added to IPB pH 7.4 (10 ml) maintained at 37°C with shaking water bath (American Heto Lab, Maryland, USA). Solution was taken (2 ml) from separated test tube at 24, 48 and 72 h. The solution was centrifuged at 10000 rpm for 10 min. Supernatant (1 ml) from centrifugation was diluted with IPB pH 7.4 to an appropriate concentration. The concentration of

indomethacin was determined by HPLC. Solubility studies were performed in triplicate.

3.3. Validation of HPLC method for determination of indomethacin

3.3.1. Equipment and chromatographic condition

The HPLC apparatus (Thermoelectron Corporation, Massachusetts, USA.) consists of pump spectra system (T 200) dual auto sampler spectra system (AS 300), empower station (SCM 1000) and UV-VIS detector. Chromatographic separation was performed on a 10 µm size, 4.6 mm x 250 mm Phenomenax® RP18 stainless steel analytical column (California, USA) fitted with a Phenomenax® security guard (USA), 4 mm x 2.0 mm C18. The mobile phase contained 0.2 mM acetate buffer and acetonitrile with a volume ratio of 65:35 v/v. The flow rate was 1.0 ml/min with an injection volume of 20 µl. The detection wavelength of indomethacin was 254 nm.

3.3.2. Method validation of indomethacin

A stock solution was prepared by the following method. Twelve mg of indomethacin was weighed, dissolved in IPB pH 7.4 and completed to 100 ml volumetric flask. The stock solution of indomethacin was diluted stepwise with IPB pH 7.4 to obtain concentrations of 1.2, 2.4, 4.8, 7.2 and 9.6 µg/ml.

The intra-day precision was determined by performing five repeated analyses of a preparation on the same day. The inter-day precision was determined by analyzing freshly prepared samples for three days over a period of 1 week. The

precision was determined by the relative standard deviation (%RSD) of peak area. This was calculated using the following equation:

$$\%RSD = \frac{S.D. \times 100}{\overline{X}} \qquad \text{(Eq.3.1)}$$

where S.D. is standard deviation and $\overline{X}$ is a mean of peak area. The method was acceptable when %RSD was less than 2, in both intra-day and inter-day (Swartz and Krull, 1998).

The accuracy of an analysis was determined by the systemic error involved. It was determined by calculating the recovery of the analyte by a standard addition method at concentration between 1.2-9.8 µg/ml. The accuracy of assay should be more than 90% (Xu, 2003).

The linearity response for indomethacin was determined by analyzing the corresponding reference standards three times for each concentration in the range of 1.2-9.8 µg/ml. The linearity was determined by calculating the correlation coefficient value (r^2), generated by plotting the analyte peak area versus the concentration of the drug. Linearity was confirmed if the %RSD values of the slope and the intercept were less than 3%.

The limit of detection is the lowest concentration that can be detected but necessarily quantified; the quantification limit is the lowest concentration that can be quantified with acceptable precision. The limit of quantification is the lowest level of analyte that can be reported.

The limit of detection (LOD) may be calculated as:

$$LOD = \frac{3\sigma}{S} \qquad \text{(Eq.3.2)}$$

The limit of quantitation (LOQ) may be calculated as:

$$LOQ = \frac{10\sigma}{S} \qquad \text{(Eq.3.3)}$$

where σ = the standard deviation of the response

S = the slope of the calibration curve

The slope S may be estimated from the calibration curve of the analyte. The estimate of σ may be a measurement of the magnitude of analytical background by analyzing an approximate number of samples and calculating the standard deviation of these responses (ICH, 1996).

3.4. Preparation of indomethacin-CCC mixture

3.4.1. Melting method

CCC was heated at 70°C for 10 min and cooled to 37°C. Indomethacin was added into CCC and mixed together until the mixture was cooled to room temperature. Three formulations containing 1, 2 and 5 % w/w indomethacin in CCC were prepared.

3.4.2. Solvent evaporation method

3.4.2.1. Solvent screening for indomethacin-CCC mixture

Indomethacin-CCC mixtures 0.5 g (20:80 %w/w) were prepared by dissolving in various solvents (ethyl acetate, chloroform and ethanol) (10 ml). The solvent was evaporated by rotary evaporator. Dried indomethacin-CCC mixtures were kept in dessicator (25ºC, 46% relative humidity) before subjecting to thermal analysis.

3.4.2.2. Loading capacity of indomethacin into CCC

A mixture of indomethacin and CCC 0.5 g (1:99, 2:98, 5:95, 10:90, 20:80, 30:70 and 40:60 %w/w) was prepared by dissolving in chloroform (10 ml). When the mixture was completely dissolved, the solvent was removed by a rotary evaporator. Dried samples of indomethacin-CCC were analyzed by FTIR and DSC to study the interaction between indomethacin and CCC.

Indomethacin-CCC mixtures (1:99, 2:98, 5:95 %w/w) were used to investigate their texture by PLM, release kinetics and permeation across excised newborn pig skin.

3.5. Evaluation of indomethacin-CCC mixture

3.5.1. Content uniformity of indomethacin

Each formulation was examined by sampling a mixture (10 mg) from each formulation (n=3). The sampling mixture was dissolved, adjusted to the volume with methanol and sonicated for 10 min to obtain clear solution. Indomethacin content was analyzed by HPLC technique as described in section 3.3.

3.5.2. Differential scanning calorimetry

DSC (Perkin Elmer DSC 7, USA.) was used to investigate the thermal properties of the indomethacin-CCC mixture. The sample (5 mg) was placed in an aluminium pan, sealed hermetically, and then assessed by DSC in the heating mode from 20°C to 200°C and cooling from 200°C to 20°C at a rate of 10°C/min. All samples were analyzed in triplicate. The DSC thermograms were analyzed using the Universal analysis 2000 program version 3.4c (TA instruments, Newcastle, USA).

3.5.3. Polarized light microscopy

Indomethacin-CCC mixture was examined under polarized light microscope (Olympus BH-2, Japan) with hot stage, in order to study the texture of anisotropic phases. A small quantity of the sample was placed on a clean glass slide. The existence of birefringence was verified by observation under crossed polarizer at magnification of 400X. Photographs of these samples were taken at RT before heating to 200°C and after cooling down to RT.

3.5.4. Dissolution test

Dissolution studies were conducted using an automated dissolution apparatus. IPB pH 7.4 (150 ml) was used as dissolution medium and maintained at 37°C. The volume of dissolution medium was justified from LOD of analytical method. The dissolution study was performed for indomethacin, indomethacin-CCC mixtures and indomethacin-cholesterol mixture. Indomethacin-CCC mixtures (100 mg) were added to the dissolution apparatus II. At appropriate time intervals, 2 ml of the dissolution medium was withdrawn and immediately replaced with fresh medium. The dissolved indomethacin was analyzed using a HPLC assay as described in section 3.3.

3.5.5. *In vitro* permeation experiments

In vitro skin permeation studies were performed using vertical diffusion Franz cells (Hanson Research Corporation, California, USA) (Siewert *et al.,* 2003) with an effective diffusion area of 1.77 cm^2 (Figure 3.1). The experiments were carried out using a newborn pig skin. The skin, previously frozen at -20°C, was pre-equilibrated in IPB pH 7.4 at 25°C overnight before the experiments (Songkro *et al.,* 2003). A circular piece of this skin was sandwiched securely between the two halves of the cells with the stratum corneum side facing the donor compartment. The receiver compartment was filled with 12 ml of IPB pH 7.4 (Fujii *et al.,* 1996) which was continuously stirred (400 rpm) and thermostated at 37°C (Michniak *et al.,* 1993) throughout the experiments. Approximately 100 mg of indomethacin-CCC mixture was applied to a new born pig skin. At appropriate time intervals (0.5, 1, 2, 3, 4, 6, 8, 10, 12, 24 h), samples (1 ml) were withdrawn from the receptor compartment and an equal volume of fresh receptor solution was immediately replaced. Samples were analyzed using HPLC system as described in section 3.3.

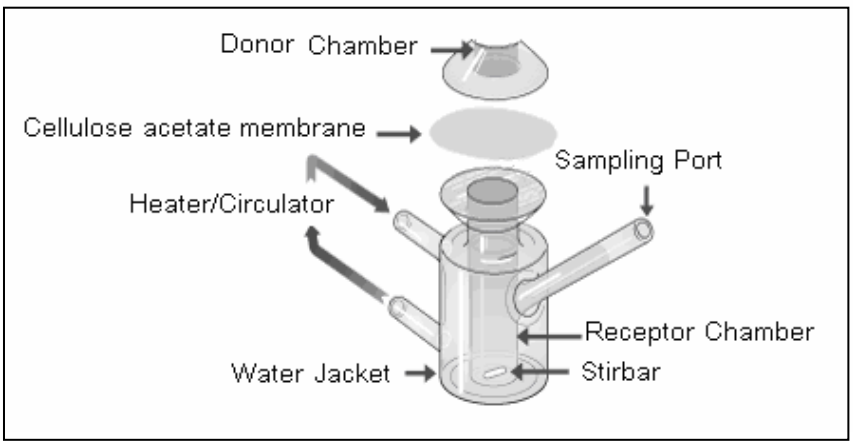

Figure 3.1. Modified Franz diffusion cell (www.permegear.com/franz.htm accessed : January, 2008)

3.5.6. *In vitro* skin retention study

Following the skin permeation studies, after 24 h the diffusion cells were dismantled, the effective diffusion area was cut off and washed briefly in methanol. The skin was then homogenized (Ystral X10/25, Ballrechtar-Dottingen, Germany) in 5 ml of methanol under ice bath for 10 min using homogenizer. The skin homogenate was centrifuged using a centrifuge (Hettich Universal Zentrifuger 16R Tuttlingen, Germany) at 10000 g for 10 min. The clear supernatant was obtained by filtering the skin homogenate with cellulose acetate membrane. The amount of indomethacin was then determined by HPLC analysis as described in section 3.3 for indomethacin retention in the skin (Yoo *et al.,* 2008).

3.5.7. Amount of indomethacin remained in donor compartment after permeation study

After permeation study, indomethacin-CCC mixture remained in the donor compartment was dissolved in methanol and adjusted to 25 ml in volumetric flask. The mixture was sonicated until clear solution was obtained and filtered with cellulose acetate membrane (0.22 μm). Then the amount of indomethacin was analyzed by HPLC.

3.6. Stability testing of indomethacin-CCC mixture

The short term freeze thaw stability of the samples was obtained over six freeze-thaw cycles, by thawing at 45°C for 48 h and freezing at 4°C for 48 h for each cycle, respectively (Shafiq-un-Nabi *et al.,* 2007). Sufficient samples (100 mg) were weighed and stored in the freezer for freezing. The content of indomethacin from each storage period was compared with the initial concentration of freshly prepared samples. The samples were evaluated for drug content**,** dissolution test, functional group (FTIR), phase transition (DSC), break down product of indomethacin-CCC mixture during the experiment by TLC and the texture of indomethacin-CCC mixture was observed under PLM as previously described in section 3.1.4.1.

3.7. Analysis of data

The cumulative amount of indomethacin released or permeated through the skin was calculated from dissolution data and *in vitro* permeation data, respectively using the following equation:

$$Q_t = V_r C_t + \sum_{i-0}^{t-1} V_s C_i \qquad \text{(Eq.3.4)}$$

where C_t is the drug concentration of the receptor fluid at each sampling time, C_i is the drug concentration of the i^{th} sample, and V_r and V_s are the volumes of the receptor fluid and the sampling volume, respectively.

Indomethacin release kinetics were analyzed by zero order, first order and Higuchi's model (Table 3.1), which were applied considering the amounts of drug released from 30 min to 24 h.

Table 3.1 Kinetics of drug release

Model	Equation
Zero order	$Q_t = Q_0 + K_0 t$
First order	$\ln Q_t = \ln Q_0 + K_f t$
Higuchi	$Q_t = K_H t^{1/2}$

Q_t, is the cumulative amounts of drug release in time t; Q_0 is initial amounts of drug in the preformed preparations; k_0, k_f, k_H are release rate constants of zero order, first order and Higuchi, respectively.

In the permeation study, data were expressed as the cumulative drug permeation per unit of skin surface area, Qt/S (S = 1.77 cm^2) (Songkro *et al.*, 2003).

The steady-state fluxes (J_{SS} (0 – 24 h)) were calculated by linear regression interpolation of the experimental data at steady state (between 0 and 24 h, ΔT) as shown in equation:

$$Jss = \Delta Qt / (\Delta T.S) \qquad \text{(Eq. 3.5)}$$

The characterization data were expressed as the means of three experiments ± SD. The skin permeation data were expressed as the means of at least four experiments ± SD. One-way analysis of variance (ANOVA) and Tukey's multiple comparison tests were used to compare the fluxes of indomethacin from different preformed preparations. Paired *t*-test was used to compare the percentage of drug released before and after freeze thaw cycles (Janyaprasert *et al.*, 2007). P value of less than 0.05 was considered to be statistically significant.

CHAPTER 4

RESULTS AND DISCUSSION

4.1. Synthesis and characterization of CCC

CCC was synthesized by condensation of cholesteryl chloroformate and cetyl alcohol with a yield of 50 %. The pure CCC is a white and odorless powder at room temperature (25ºC). Its chemical structure is illustrated in Figure 4.1. The chemical structure of the compound was confirmed by using FTIR and NMR.

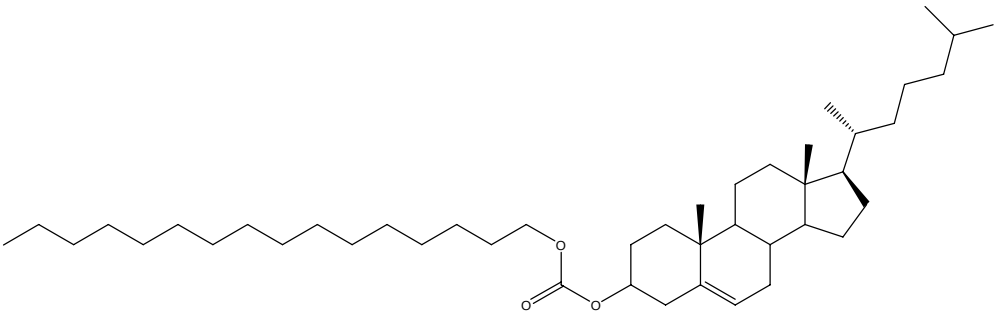

$C_{44}H_{78}O_3$ MW = 654

Figure 4.1 Chemical structure of cholesteryl cetyl carbonate

CCC mixture was subjected to silica gel 60 TLC with 2 systems. In the first system (hexane:diethyl ether (4:1 v/v)), cholesterol and cetyl alcohol were separated and occurred as yellow-colored spots. In the second system (hexane:chloroform (4:1 v/v)) CCC was appeared as red spots. From TLC (Figure 4.2), lane 1 shows a spot of cetyl alcohol which appeared at Rf 0.2 and lane 2 reveals a spot of cholesterol with Rf 0.4. Furthermore, a spot at Rf 0.7 of CCC was found on lane 3. The reaction mixture was purified by liquid extraction and flash column chromatography. After

purification, the CCC was appeared as one spot on TLC system. This was confirmed on both TLC systems and spraying reagents. This can be confident that the CCC is pure enough to analyze with NMR.

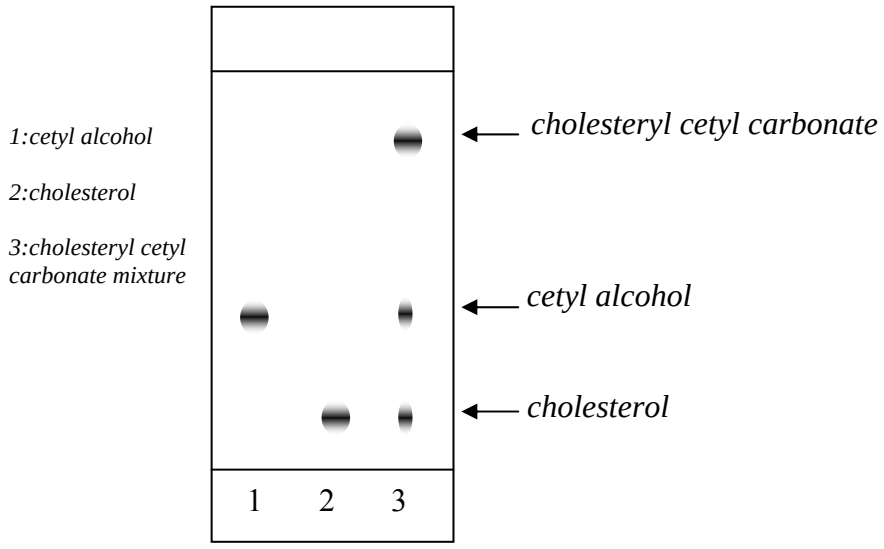

Figure 4.2 TLC of starting materials: cetyl alcohol (1), cholesterol (2) and CCC mixture (3)

4.1.1. Chemical characterization

4.1.1.1. FTIR spectrum analysis

The FTIR spectrum from 4000 to 400 cm^{-1} for CCC is shown in Figure 4.3. There are 3 main peaks of methylene, carbonate ester and carbonyl group. The methylene group shows 2 distinct bands of C-H stretching locating at 2918 and 2850 cm^{-1}. A carbonate ester of CCC appears at 1468 and 1289 cm^{-1} corresponding to the O–C–O stretching mode. Carbonyl carbonate (C=O) stretching was at 1743 cm^{-1} (Chuealee *et al.,* 2007).

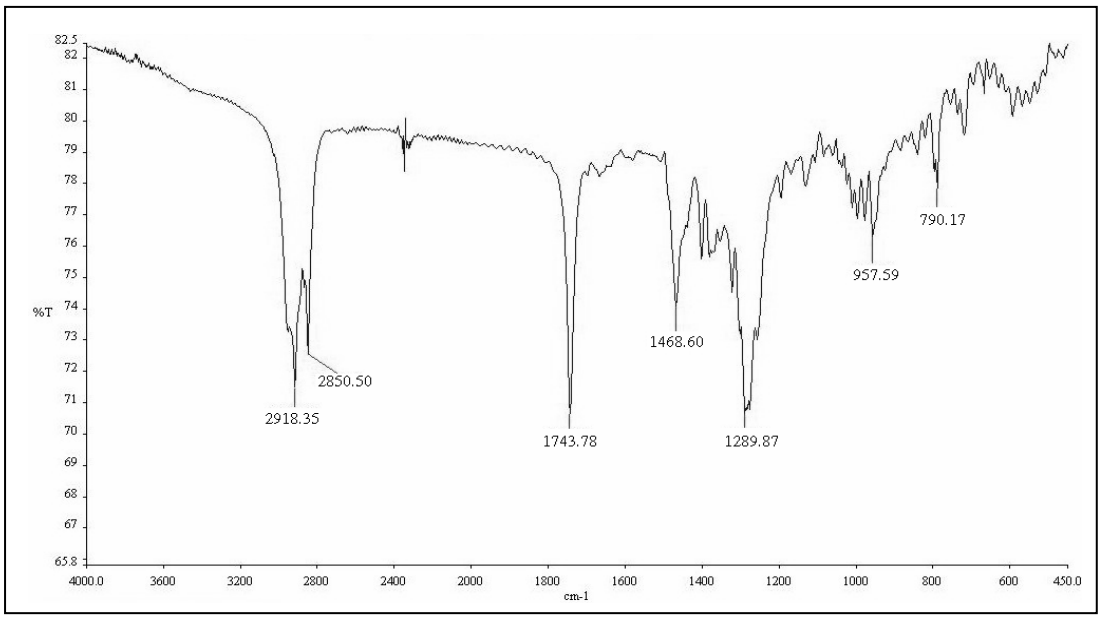

Figure 4.3 FTIR spectrum of CCC

4.1.1.2. NMR spectrum analysis

Table 4.1 gives assignments and chemical shift for all carbons of CCC. ^{13}C-NMR showed that the chemical shift for the carbonyl of carbonate resonance appeared at 154.7 ppm, which 20 ppm upfield from the carbonyl ester, and the acyl carbon linked to oxygen which appeared at 68.0 ppm. In addition, the chemical shift of the C_3 steroid ring carbon of carbonate was at 77.5 ppm (Figure 4.4).

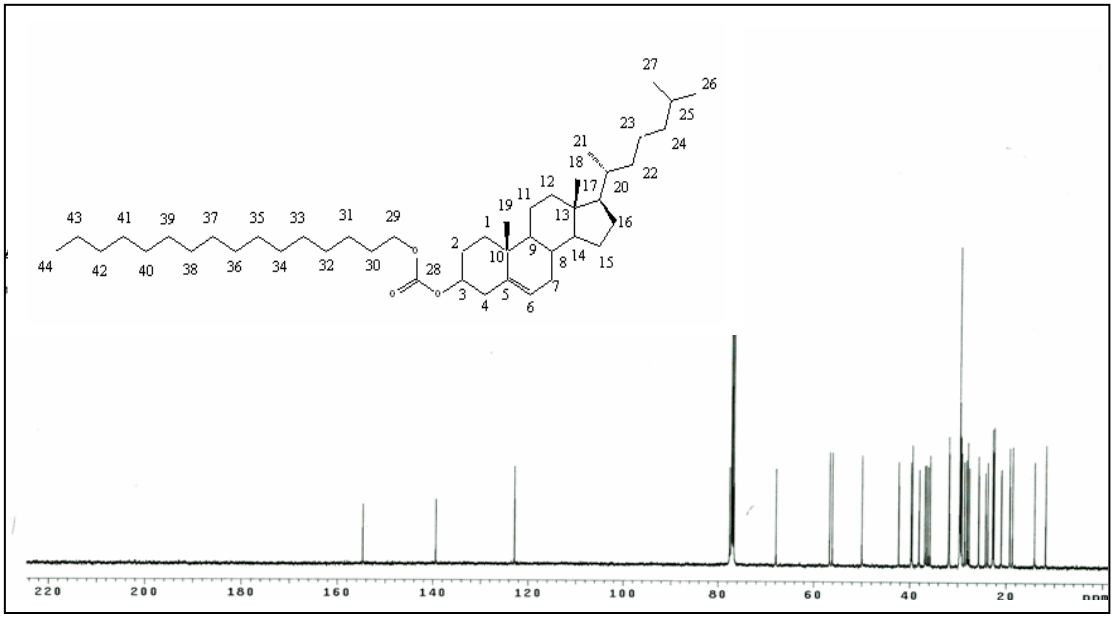

Figure 4.4 ^{13}C-NMR spectrum of cholesteryl cetyl carbonate

^{1}H-NMR is illustrated in Figure 4.5, the chemical shift for the proton of cyclohexene (C-6) appeared at 5.37 ppm, methylene (C-29) at 4.45ppm, methine (C-3) at 4.08 ppm and methylene of alkyl chain appeared at 1.23, respectively (see appendix).

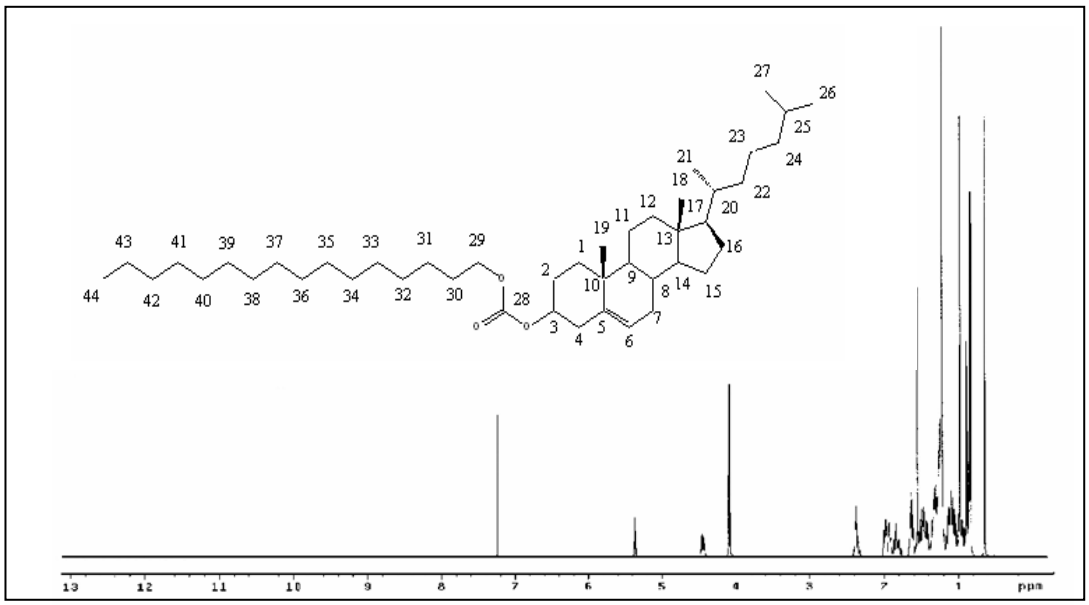

Figure 4.5 ^{1}H-NMR spectrum of cholesteryl cetyl carbonate

Table 4.1 ^{13}C and ^{1}H resonance assignment of CCC

Position	Type	Carbon (ppm)	Proton (ppm)
1	CH_2	36.9	2.4 (t, 2H)
2	CH_2	28.7	1.7 (t, 2H)
3	CH	38.0	4.5 (m, 1H)
4	CH_2	39.7	2.1 (m, 2H)
5	C	139.4	-
6	CH	77.6	5.4 (t, 1H)
7	CH_2	31.9	2.0 (m, 2H)
8	CH	32.0	1.4 (t, 1H)
9	CH	50.0	0.9 (t, 1H)
10	C	36.5	-
11	CH_2	21.0	1.4 (m, 2H)
12	CH_2	39.5	1.2 (t, 2H)
13	C	42.3	-
14	CH	56.7	1.1 (t, 1H)
15	CH_2	23.8	1.6 (t, 2H)
16	CH_2	28.2	1.9 (t, 2H)
17	CH	56.1	1.0 (t, 1H)
18	CH_3	11.8	0.7 (m, 3H)
19	CH_3	19.3	0.9 (m, 3H)
20	CH	35.8	1.6 (t, 1H)
21	CH_3	18.7	0.9 (t, 3H)
22	CH_2	36.2	1.8 (m, 2H)
23	CH_2	24.3	1.3 (m, 2H)
24	CH_2	38.0	2.0 (m, 2H)
25	CH	28.0	1.9 (m, 1H)
26	CH_3	22.8	1.1 (t, 3H)
27	CH_3	22.6	1.4 (t, 3H)
28	C	154.7	-
29	CH_2	67.9	4.1 (t, 2H)
30	CH_2	29.4	1.6 (m, 2H)
31	CH_2	29.2	1.2 (m, 2H)
32	CH_2	29.2	1.2 (m, 2H)
33	CH_2	29.2	1.2 (m, 2H)
34	CH_2	29.2	1.2 (m, 2H)
35	CH_2	29.2	1.2 (m, 2H)
36	CH_2	29.2	1.2 (m, 2H)
37	CH_2	29.2	1.2 (m, 2H)
38	CH_2	29.2	1.2 (m, 2H)
39	CH_2	29.2	1.2 (m, 2H)
40	CH_2	29.2	1.2 (m, 2H)
41	CH_2	27.7	1.2 (m, 2H)
42	CH_2	25.7	1.2 (m, 2H)
43	CH_2	22.7	1.3 (m, 2H)
44	CH_3	14.1	1.0 (m, 2H)

4.1.1.3. TLC densitometry

CCC may be hydrolyzed by indomethacin and decomposed to cholesterol and cetyl alcohol. The TLC densitometry results obtained from indomethacin-CCC are shown in Figure 4.6. It was found that only two peaks of indomethacin-CCC mixtures after 1 month storage (25ºC) appeared at Rf 0.5 (indomethacin) and 0.7 (CCC). This result indicates that CCC is stable and CCC is likely to be compatible with indomethacin at least 1 month. Although, longer period of time may be required to monitor stability of indomethacin-CCC mixture.

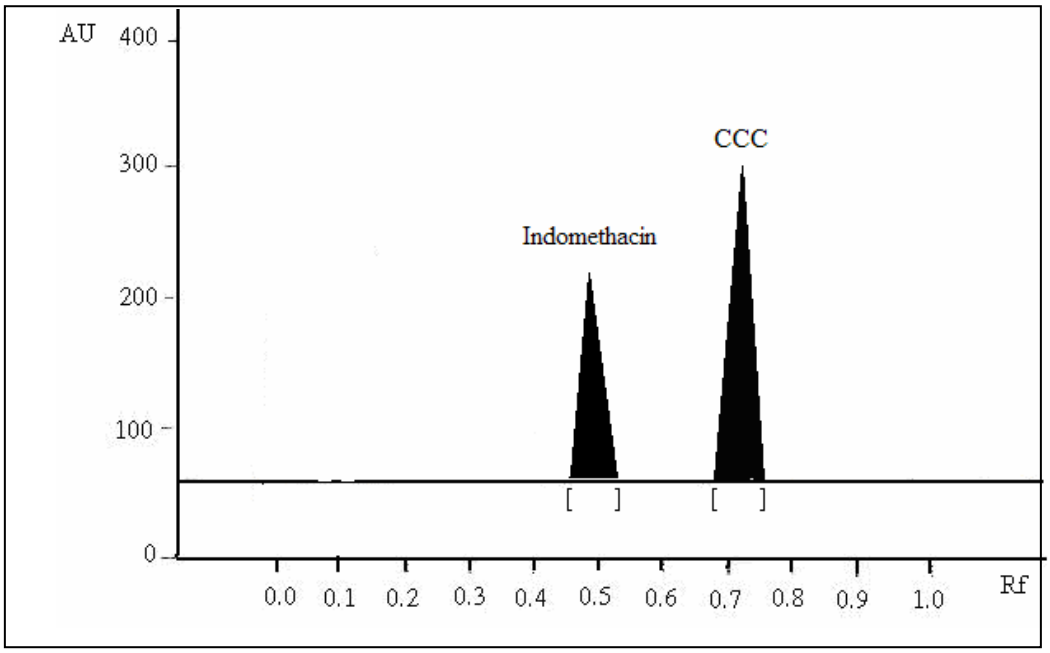

Figure 4.6 TLC densitometry of indomethacin-CCC mixture after preparation and storage for 1 month at 25ºC

4.1.2. Physical characterization

4.1.2.1. PLM

Birefringence of CCC was observed from macroscopic structure of the liquid crystalline phases. The results from PLM exhibited that the texture of CCC was not rearranged to spherulite. It rather shows the maltese cross of CCC at 25°C before heated (Figure 4.7A). Figure 4.7B shows spherulite with different sizes of CCC at 32°C. Upon heating, the crystals melted at 72°C. After cooling down to 25°C, CCC rearranged itself to orderly spherulite (Figure 4.7C). In this case the spherulites are more uniform in size than those observed at 32ºC. During heating, the texture of

CCC showed the phase transition from solid crystal (maltese cross) to isotropic liquid and isotropic liquid back to solid crystal (spherulite).

The result in this study indicates that the molecule arrangement of CCC is time and temperature dependent. It is postulated that indomethacin could be released from CCC at 32°C greater than that of 25°C. This is contributed from a temperature difference of 7 degrees causing less order of liquid crystal.

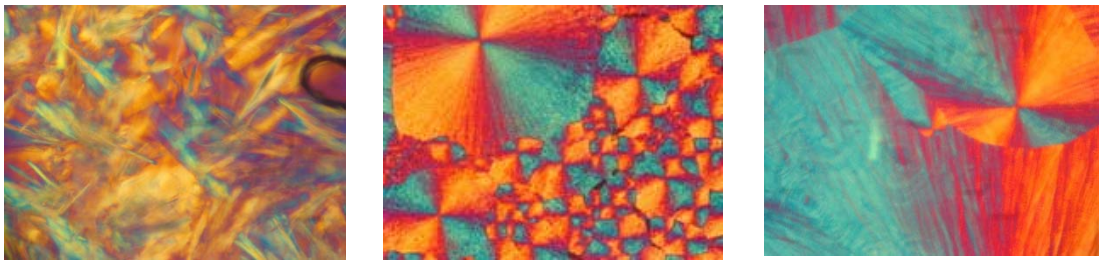

(A) (B) (C)

Figure 4.7 Cholesteryl cetyl carbonate from PLM at 25ºC (A), and after recrystallization from molten state at 32 ºC (B) and at 25ºC (C) (400X)

4.1.2.2. DSC analysis

DSC is a useful tool to study thermal property of compound. CCC exhibits as monotropic liquid crystal behavior which exhibits the liquid crystalline state only when the temperature changes in one direction. The pure CCC had one endothermic peak at 73°C corresponding to solid crystal – isotropic liquid transition on the heating run. Upon cooling from its isotropic phase, CCC had three exothermic peaks at 73, 54 and 42°C corresponding to isotropic liquid - nematic, nematic - smectic and smectic - solid crystal transition, respectively (Figure 4.8). It should be mentioned that the

transition from the CCC to amorphous phase required a high energy input (△S = 47.6 cal/mole-K). This is in contrast to transition from amorphous to liquid crystalline which consumed low amounts of energy (△S were only 0.7 and 0.4 cal/mole-K). It can be postulated that the phase transition from solid crystal-isotropic liquid required much higher energy to change structure of CCC than those energy release from recrystallization.

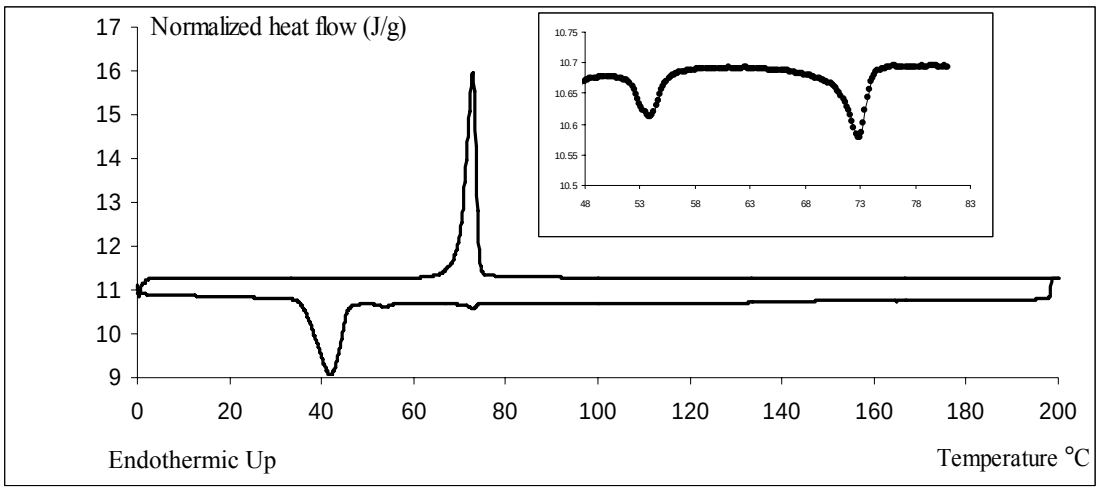

Figure 4.8 Thermogram of cholesteryl cetyl carbonate by heating up at a scanning rate of 10°C/min from 0°C to 200°C following by cooling down to 0°C (inset, expansion scale)

4.2. Solubility indomethacin in isotonic phosphate buffer pH 7.4 at 37°C

Solubility measurements of indomethacin are presented in Table 4.2. The solubility of indomethacin in 24 and 48 h was not at equilibrium. The solubility of indomethacin (pKa = 4.5) in IPB pH 7.4 at 37°C was found to be 920.78 ± 11.77 μg/ml and this value was not further increased after 72 h. From our study, the solubility of indomethacin was slightly higher than the reported value (800μg/ml in

phosphate buffer pH 7.0 at 25ºC) (Florey, 1984). This value was used to justify the sink condition in the dissolution test of indomethacin-CCC mixture.

Table 4.2 Solubility of indomethacin in IPB pH 7.4 at 37°C (mean ± SD, n=3)

Time (h)	Solubility (µg/ml)
24	703.38 ± 19.33
48	785.73 ± 9.64
72	920.78 ± 11.77

4.3. Validation of HPLC method for determination of indomethacin

This method validation follows the guidance for industry: validation of analytical procedure (ICH, 1996). Standard curve of indomethacin in IPB pH 7.4, methanol and spiked in to newborn pig skin homogenate are shown in Figure 4.9. In IPB pH 7.4, the correlation coefficients are above 0.999 over the range of 1.2-9.6 µg/ml. The standard curves of indomethacin in methanol and spiked into newborn pig skin show correlation coefficients only 0.996 over the range of 1-8 µg/ml.

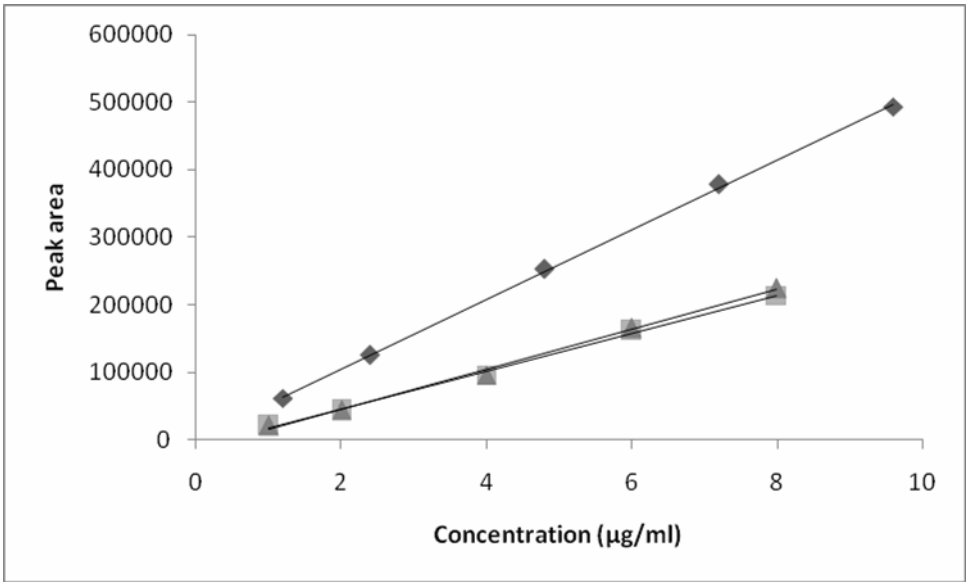

Figure 4.9 Standard curve of indomethacin in IPB pH 7.4 (♦), methanol (■) and spiked into supernatant from pig skin homogenate ( )▲

Table 4.3 shows good linearity of indomethacin determination, with a high correlation coefficient (r^2 > 0.995). Therefore, the concentration ranges of 1.2-9.6 µg/ml for IPB pH 7.4 (y = 51638x + 1649.6) and 1-8 µg/ml for methanol (y = 29584x -14420) and supernatant from skin homogenate with methanol (y = 28091x – 11134) were acceptable for indomethacin analysis from this analytical method. The peak from pig skin did not interfere with the peak of indomethacin. Furthermore, there was no interference from CCC during HPLC analysis.

Table 4.3 Linearity of indomethacin standard curve determination by HPLC

Indomethacin in	No.	Intercept	Slope	r^2
IPB pH 7.4[1]	1	-4309	52441	0.9998
	2	1649	51638	0.9996
	3	-1550	53041	0.9996
Methanol[2]	1	-14420	29584	0.9964
	2	-9283	28367	0.9955
	3	-11371	29716	0.9952
Supernatant from	1	-11134	28091	0.9976
pig skin	2	-13443	28723	0.9952
homogenate[3]	3	-10642	27203	0.9955

1) For determination the amount of indomethacin in the receptor fluid and indomethacin release from indomrthacin-CCC mixture.

2) For determination the amount of indomethacin remaining in the donor compartment at 24 h.

3) For determination the amount of indomethacin retained in pig skin at 24 h.

Table 4.4 shows the intra-day and inter-day precision of indomethacin analysis. The %RSD of indomethacin in IPB pH 7.4 are not over 2% in all concentrations. The analysis of indomethacin was more precise when the same sample was analyzed in the same day than the different day. However, both inter-day and intra-day are acceptable. Therefore, this study analyzed indomethacin in the same day and different day upon the instrument availability.

The precisions of indomethacin analysis in methanol and supernatant from pig skin homogenate were less than that in IPB pH 7.4 (%RSD within 4). This may be caused by the volatility of methanol. This analytical method may be improved by employing the internal standard in the system.

Table 4.4 Inter-day and intra-day precision of indomethacin in IPB pH 7.4, methanol and supernatant from pig skin homogenate (n=3)

Indomethacin concentration (µg/ml)	Intra-day (%RSD)	Inter-day (%RSD)
IPB pH 7.4		
1.2	0.96	1.00
2.4	1.13	1.41
4.8	1.73	1.88
7.2	0.75	1.79
9.6	0.82	1.03
Methanol		
1.0	1.37	2.61
2.0	3.24	3.91
4.0	0.50	4.09
6.0	0.73	1.43
8.0	1.20	1.93
Supernatant from pig skin homogenate		
1.0	1.17	0.95
2.0	0.55	3.13
4.0	2.79	2.50
6.0	1.90	0.66
8.0	2.17	2.55

RSD = Relative standard deviation

Table 4.5 shows high accuracy of indomethacin analytical method. The recovery of indomethacin was 96-101% (IPB pH 7.4), 93-118% (methanol) and 94-115% (supernatant from pig skin homogenate). The results suggest that the analytical method of indomethacin is accurate if the concentration is 2 µg/ml or higher. It is important to note that at the lowest concentration (1 µg/ml), the results indicate the least accurate as compared to other concentrations. Therefore, it has to adjust the final concentration of indomethacin to be higher than 1 µg/ml to obtain more accurate results.

Table 4.5 Accuracy of indomethacin standard determined by HPLC

	Theoretical Concentration (µg/ml)	**Measured Concentration (µg/ml)**	**%Recovery**
IPB pH 7.4	1.2	1.15	96.06
	2.4	2.39	99.60
	4.8	4.85	101.12
	7.2	7.29	101.20
	9.6	9.52	99.13
Methanol	1	1.18	118.13
	2	1.94	97.04
	4	3.73	93.30
	6	6.08	101.31
	8	8.07	100.84
Supernatant	1	1.14	113.88
from pig	2	1.93	96.51
skin	4	3.80	94.99
homogenate	6	6.12	102.09
	8	8.00	100.08

The LOD of indomethacin in IPB pH 7.4, methanol and supernatant from skin homogenate were found to be 0.25, 0.52 and 0.3µg/ml, respectively. From calculation, the respective order of LOQ values were 0.83, 1.73 and 1.00 µg/ml. It is worth to note that the LOD is not a very stable parameter because of its susceptibility to minor changes in the conditions of the analytical method like temperature, purity of reagents, sample matrices and instrumental system changes (Rosing *et al.,* 2000). Therefore, the LOQ are taken as the minimal values of analytical samples.

Table 4.6 The LOD and LOQ values in IPB pH 7.4, methanol and supernatant from skin homogenate

	LOD (μg/ml)	**LOQ** (μg/ml)
IPB pH 7.4	0.25	0.83
Methanol	0.52	1.73
Supernatant from skin homogenate	0.30	1.00

4.4. Preparation of indomethacin-CCC mixture

Indomethacin-CCC mixture could be prepared with melting and solvent evaporation method. For melting method, CCC and indomethacin could not mix homogeneously because the melting point of CCC was 72°C. While indomethacin melted at 160°C so the melting method required higher temperature to prepare indomethacin-CCC mixture. However, in this study we cannot use the high temperature because it could change liquid crystalline property of CCC and also the stability of indomethacin. Finally, we used solvent evaporation method to prepare indomethacin-CCC mixture.

According to the results of UV-Vis spectrum, there was no interaction between indomethacin and CCC shown in various solvents (ethyl acetate, chloroform and ethanol) (data not shown). Further, the thermal behaviors of indomethacin-CCC mixture were recorded to monitor its crytallinity and perhaps an interaction.

DSC thermograms of dried indomethacin-CCC mixture prepared with various solvents (ethyl acetate, chloroform and ethanol) are shown in Figure 4.10. Indomethacin-CCC mixture prepared with ethyl acetate and ethanol showed the endothermic peak of CCC and indomethacin at 68 and 160°C, respectively. While the

preparation with chloroform, endothermic peak appeared at 72 and 140°C. It is expected that there is an interaction between indomethacin-CCC mixture prepared with chloroform. Whereas indomethacin incorporated into CCC using either ethyl acetate or ethanol as a solvent does not change peak characteristics of the drug and CCC. Additionally, the endothermic peak of indomethacin in case of ethanol and ethyl acetate was larger than that observed in the mixture prepared by chloroform. Henceforth, the preparation of indomethacin-CCC mixture in chloroform gave the best drug-CCC interaction and chloroform was chosen as a solvent for further study.

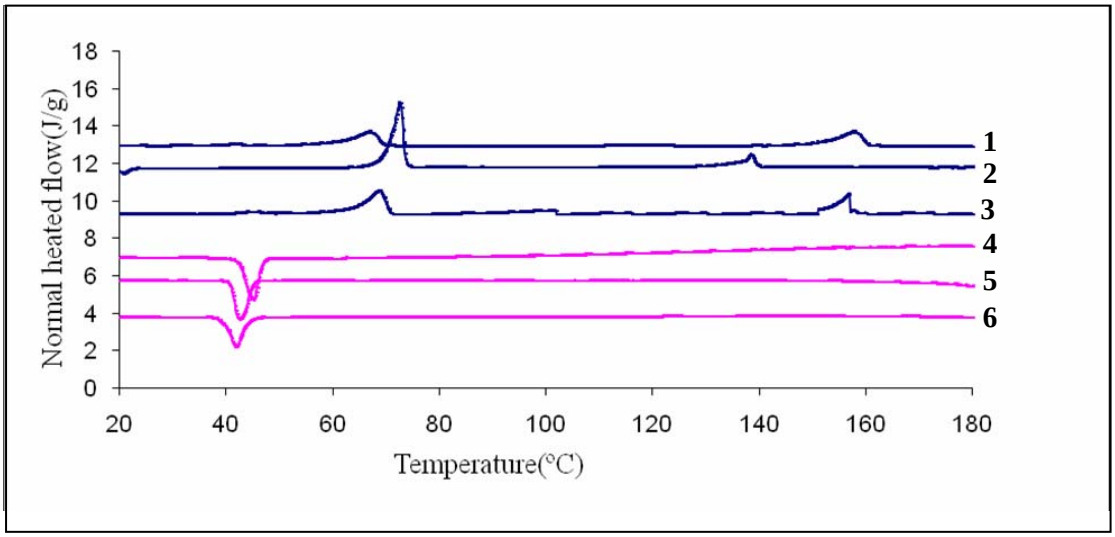

Figure 4.10 DSC thermograms of indomethacin-CCC mixture (20:80 %w/w) prepared with various solvents (ethyl acetate (1), chloroform (2) and ethanol (3) during heating at rate of 10ºC/min and cooling down of similar mixtures at respective order of 4, 5 and 6)

4.5. Content uniformity of indomethacin in CCC

The content uniformity of all indomethacin-CCC mixtures are summarized in Table 4.7. The assay values are between 95.4-97.7 % w/w. This means that the solvent evaporation method is able to provide a uniformity of indomethacin-CCC mixture.

Table 4.7 Content uniformity of indomethacin in CCC (mean ± SD, n=3)

Preformed preparations	% Drug content (w/w)	%RSD
1% indomethacin	95.4 ± 0.02	1.7
2% indomethacin	95.9 ± 0.02	1.2
5% indomethacin	97.7 ± 0.05	1.2

4.6. Evaluation of indomethacin-CCC mixture

4.6.1. FTIR analysis of indomethacin-CCC mixture

The FTIR spectra of CCC, pure indomethacin and indomethacin-CCC mixture with different drug contents (1, 2, 5, 10, 20, 30, 40 % indomethacin) are shown in Figure 4.11. Some band assignments for the solid state infrared absorption are given in Table 4.8. The higher content of indomethacin in indomethacin-CCC mixture, the sharper peak of C=O stretching at 1699 and 1675 cm^{-1} were obtained. Pure indomethacin shows the carbonyl group at 1716 and 1692 cm^{-1}. These results suggest that there are some interaction between indomethacin and CCC. Because of the wavelength of the carbonyl group was shifted 17 cm^{-1}, whereas no changes of finger print region in the FTIR spectra was observed. However, the interaction of indomethacin-CCC mixture will be further confirmed by DSC analysis.

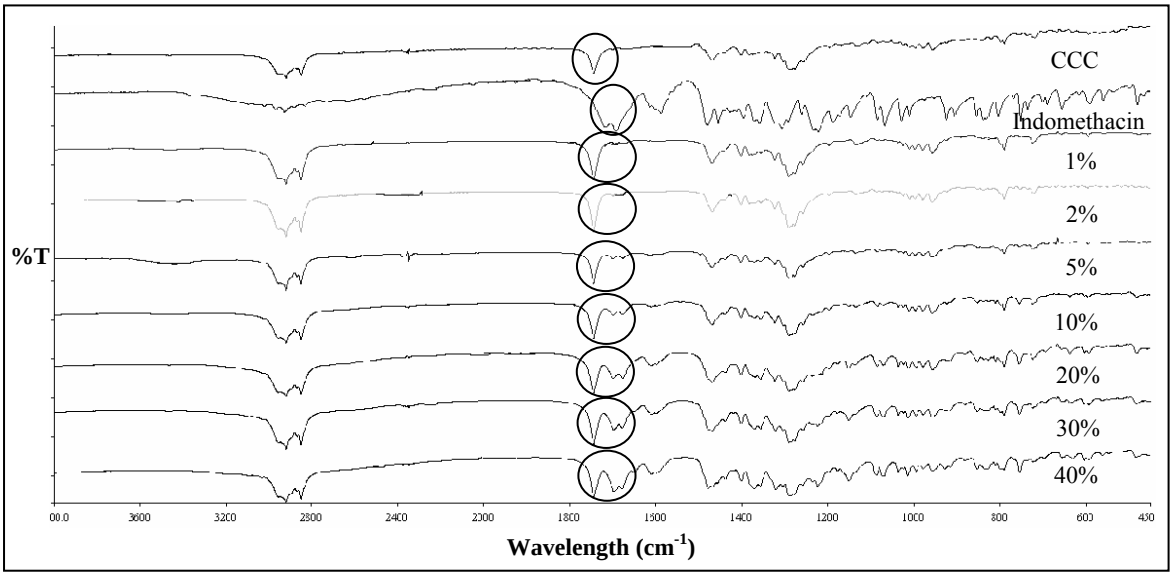

Figure 4.11 FTIR spectra of CCC, pure indomethacin and indomethacin-CCC mixtures at various concentrations of indomethacin from 1 to 40%

Table 4.8 The FTIR assignment of indomethacin, CCC and indomethacin-CCC mixture

Wavelength (cm^{-1})	**Functional group**
Indomethacin	
3000	Aromatic C-H stretching
2500	Carboxylic acid O-H stretching
1716, 1692	C=O stretching
1588	Aromatic C=C stretching
1479	O-CH_3 deformation

CCC	
2918, 2850	CH_2, CH_3 stretching
1743	C=O stretching
1468, 1289	O-C-O stretching
indomethacin-CCC mixture	
2918, 2850	CH_2, CH_3 stretching
1743	C=O stretching of CCC
1699, 1675	C=O stretching of indomethacin
1468, 1289	O-C-O stretching

4.6.2. DSC analysis of indomethacin-CCC mixture

Indomethacin at concentrations of 1, 2 and 5 % w/w could be completely incorporated into CCC. However, indomethacin-CCC at higher ratios could not form homogeneously mixture as can be seen in Figure 4.12. In the case of pure indomethacin or CCC, the endothermic peaks were observed at 160 and 73 ºC, respectively. Despite the endothermic peak of indomethacin in the mixture at higher concentrations (> 5% w/w) were shifted to lower temperature (from 160ºC to 140ºC). The results suggest that there are physical interactions between indomethacin and CCC occurred.

As the concentration of 1, 2 and 5 % w/w, the mixtures showed only one endothermic peak of CCC at 73°C. This result indicates that the indomethacin can be completely incorporated in CCC. Thus, the suitable content of indomethacin used to prepare the indomethacin-CCC mixtures is up to 5%.

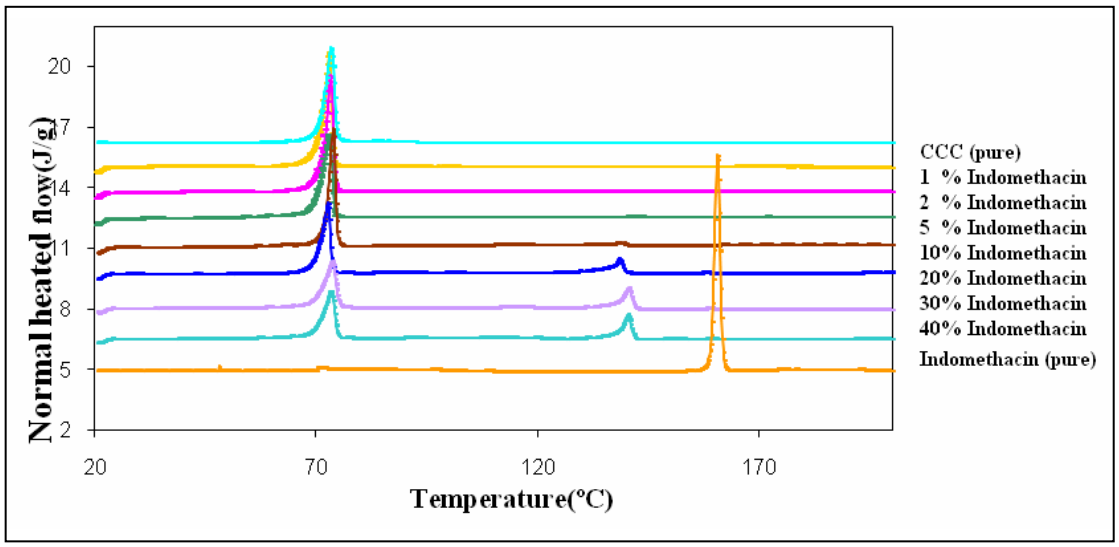

Figure 4.12 Thermogram of CCC, pure indomethacin and indomethacin-CCC mixture at various concentrations with a scanning rate of 10°C/min from 0 to 200°C

When indomethacin in synthetic liquid crystal is developed as topical application, it is necessary to consider the transition temperature of formulation to be close to skin temperature (32°C). At skin temperature, indomethacin should be released from liquid crystalline of indomethacin-CCC mixture. However, the thermogram of indomethacin-CCC mixture showed that endothermic peak at 73°C was far from 32°C. Therefore, it is important to lower the phase transition temperature by adding other components (e.g. cetyl alcohol, cholesterol and propylene glycol) into the liquid crystalline system to bring down the phase transition temperature in a complete topical formulation. However, it is not the aim in this study, we want to investigate only the effect of CCC liquid crystal on drug release and skin permeation. The conclusion from this study would lead to future development of topical indomethacin in liquid crystal.

4.6.3. PLM of indomethacin-CCC mixture

From PLM results, poor birefringence of indomethacin-CCC mixture was obtained during heating process and the liquefied was observed at temperature over 73°C. Upon cooling down process, the nematic phase of indomethacin-CCC mixtures were occurred at temperature between 71 to 55°C. Whereas, nematic-smectic phase transition temperature was 54°C and smectic-solid phase transition temperature was occurred at 54-42°C. The results revealed that the incorporation of indomethacin into CCC remained having three phase transition temperatures during cooling down process. The birefringence of indomethacin-CCC remained unchanged as detected by PLM as compared to that of pure CCC. It is important to note that no spherulite in indomethacin-CCC mixture was observed before heating (Figure 4.13A), whereas the spherulite texture was observed after cooling down the mixture to 25°C (Figure 4.13B). This is also contributed from indomethacin-CCC mixtures rearrangement to more ordered crystals.

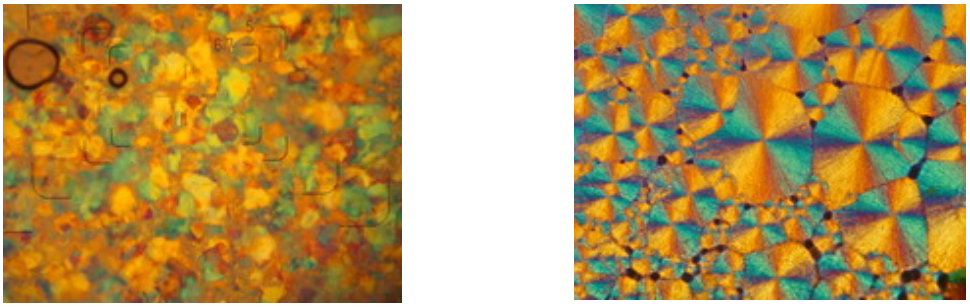

(A) (B)

Figure 4.13 Texture of 5% indomethacin-CCC mixture from polarized light microscope (400X) at 25°C (A) and after recrystallization from molten state (B)

All indomethacin-CCC mixtures at 32°C exhibited the spherulite textures (Figure 4.14) as similar to those observed at 25ºC. However, the higher temperature resulted in less ordering of the molecules as compared with the lower temperature. Thus, the birefringence of indomethacin-CCC mixture at 32ºC was slightly different from that of 25ºC. Moreover, there was no difference between different concentrations of indomethacin (1, 2 and 5%) containing in CCC.

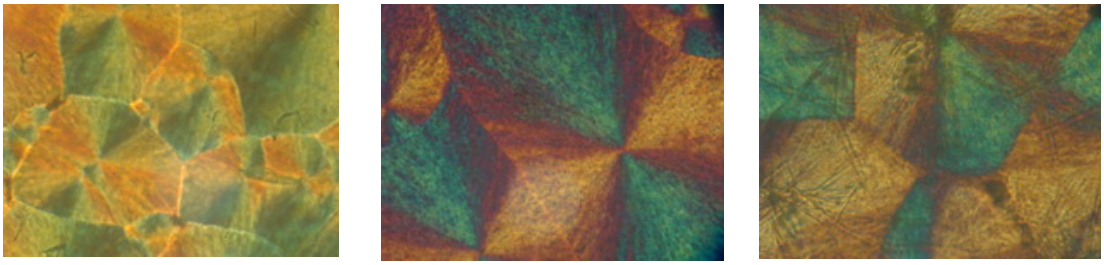

1% indomethacin 2% indomethacin 5% indomethacin

Figure 4.14 Texture of indomethacin-CCC mixtures from polarized light microscope at 32°C (400X)

4.6.4. Dissolution test of indomethacin-CCC mixture

The dissolution profiles of indomethacin-CCC mixtures are illustrated in Figure 4.15. All indomethacin-CCC mixtures, the drug was gradually released with time over 24 h. It was found that indomethacin-CCC mixtures could control the release of indomethacin. While in the case of 1% indomethacin in cholesterol and pure indomethacin, the drug was immediately released within 30 min. The release of pure drug or drug incorporated in cholesterol was found to reach the maximum within 3 h, whereas the release of indomethacin from indomethacin-CCC mixture was delayed up to at least 24 h. These results suggest that CCC can control the release of

indomethacin better than cholesterol. The cholesterol was used as a control release matrix in this case.

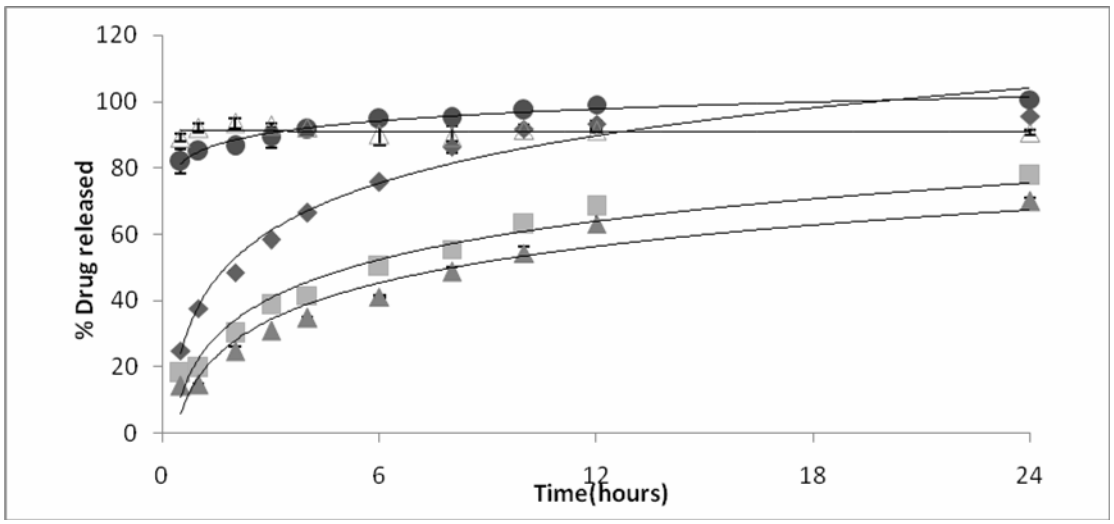

Figure 4.15 The dissolution profiles of indomethacin-CCC mixtures at 1% indomethacin (▲), 2% indomethacin (■) and 5% indomethacin (♦), 1%indomethacin in cholesterol (●) and pure indomethacin (Δ) (mean ± SD, n=3)

The data obtained from release studies were evaluated kinetically, and fitted to three different kinetic models; zero order, first order, and Higuchi. The release rate constants of each model are summarized in Table 4.9.

The correlation coefficient of linear regression was greater than 0.93 in all models. In all ratios, the Higuchi model fitted the best of indomethacin release from indomethacin-CCC mixture, followed by first order and zero order. It was found that the release of indomethacin from indomethacin-CCC mixtures complied with the Higuchi kinetic model based on those 3 concentrations. From Higuchi model, the release rate constants of 1, 2 and 5% indomethacin-CCC mixtures were 166.6, 346.0

and 1387.3 μg ml^{-1} $h^{-1/2}$, respectively. CCC may work as a matrix in the mixture (Boyd *et al.,* 2007). It can be seen that as the concentrations of indomethacin increased from 1 to 5%, the release rate constants were significantly increased ($p < 0.05$, ANOVA). This indicates that the controlled system loss its controlled release properties easily at 37ºC where drug concentration in idomethacin-CCC mixtures was at 5%.

Table 4.9 Kinetic Parameters of indomethacin release from preformed preparations (mean ± SD, n=3)

Kinetic Model		**1% indomethacin**	**2% indomethacin**	**5% indomethacin**
Zero order	R^2	0.997	0.984	0.936
	k_0 (μg/ml·h)	33.98 ± 1.75	69.94 ± 3.43	199.03 ± 2.66
First order	R^2	0.978	0.981	0.996
	k_1 (h^{-1})	0.06 ± 0.00	0.07 ± 0.00	0.22 ± 0.01
Higuchi	R^2	0.994	0.997	0.993
	k(μg/ml ·$h^{1/2}$)	166.61 ± 7.6	346.04 ± 16.68	1387.33± 45.65

k_0, k_1 and k are release rate constant of zero order, first order and Higuchi model, respectively.

4.6.5. *In vitro* skin permeation study

The *in vitro* skin permeation of various indomethacin-CCC mixtures were evaluated using modified Franz diffusion cell. The amount of indomethacin that penetrated through skin into the receptor fluid could not be measured. Though, we observed indomethacin peak in the chromatogram but it was unable to quantitate (<0.83 μg/ml).

4.6.6. *In vitro* skin retention study

The skin retention of indomethacin at 24 h in the presence of 1, 2, 5% indomethacin, pure indomethacin and 1% indomethacin-cholesterol mixture were 5.17, 2.61, 1.05, 0.65 and 2.40%, respectively (Figure 4.16A). Cumulative amount of indomethacin in same preformed-preparations were 26.39, 28.40, 27.27, 36.46 and 12.68 μg/ml/cm^2, respectively (Figure 4.16B). In particular, 1% indomethacin exhibited the highest percentage of indomethacin retained in newborn pig skin than the others. These results suggest that CCC influenced the enhancing effect of indomethacin. The enhancement properties also involved with drug loading in liquid crystal system. The amount of indomethacin-CCC mixtures retained in the pig skin was significantly higher when lower concentration of indomethacin was incorporated in the mixture ($p < 0.05$). This can be said that it is a direct contribution from the addition of CCC in the preparation. Also, CCC can enhance the indomethacin retention in the pig skin better than cholesterol ($p < 0.05$).

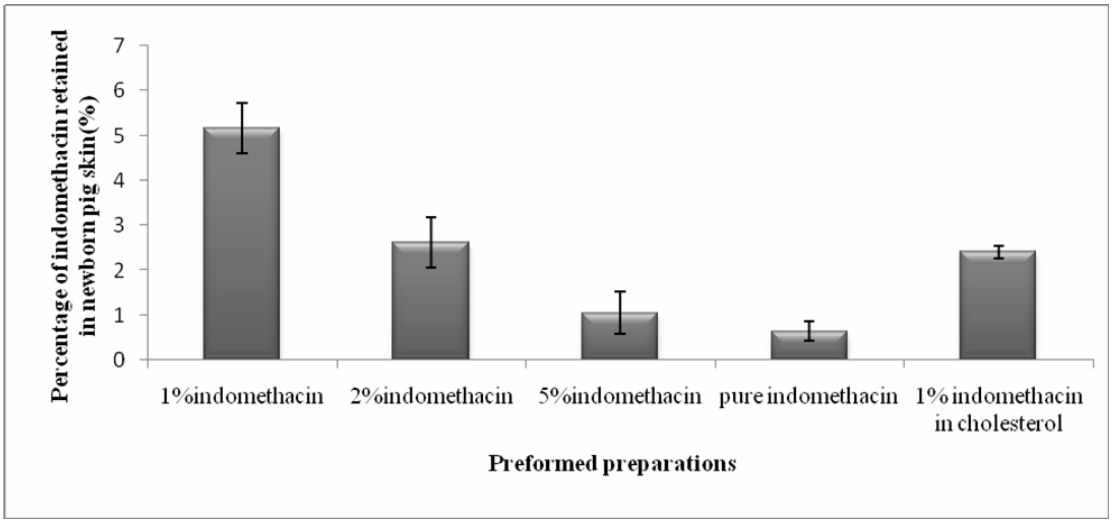

(A)

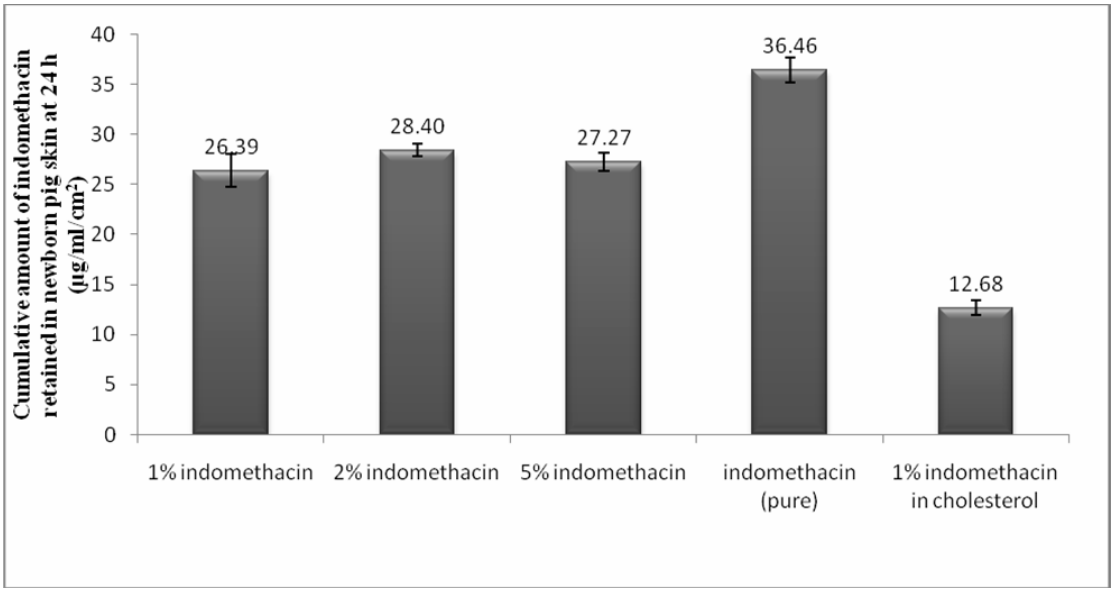

(B)

Figure 4.16 Percentage (A) and cumulative amount (B) of indomethacin retained in newborn pig skin at 24 h (mean ± SD, n=4)

Figure 4.17 shows the percentage of indomethacin retained in newborn pig skin and remained in the donor compartment. The amount of drug remained in the donor compartment for 1, 2, 5%, indomethacin and indomethacin-cholesterol mixture were found to be 88.27 ± 1.3, 95.97 ± 2.0, 97.85 ± 2.1, 94.91 ± 1.0 and 95.98 ± 1.6%, respectively. In such case, the amount of indomethacin in the donor phase may act as a drug reservoir to release and permeate across stratum corneum if the system is not at equilibrium.

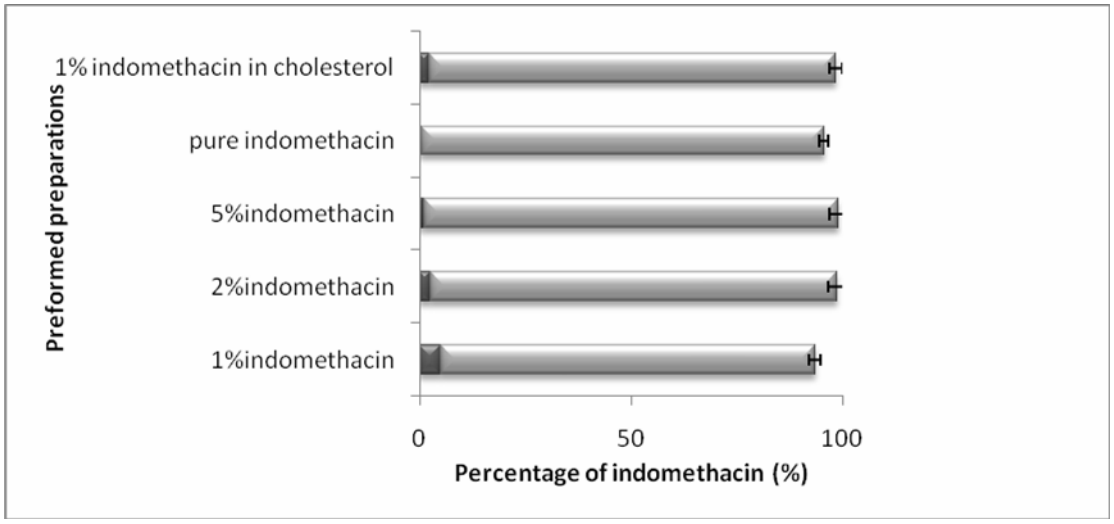

Figure 4.17 Percentage of indomethacin retained in newborn pig skin (■) in comparison with percentage of indomethacin remained in the donor chamber (□) at 24 h after application of 1, 2, 5% indomethacin in CCC, pure indomethacin and 1% indomethacin in cholesterol (mean ± SD, n=4)

Following the skin permeation studies, the newborn pig skin was extracted by $CDCl_3$ and monitored the CCC content by ^{13}C-NMR. ^{13}C-NMR showed all chemical shifts of CCC. Especially, the chemical shift at 154.68 ppm of carbonyl carbonate ester was clearly shown in the spectrum. It indicated that CCC penetrated into skin and retained within the skin. This may be envisaged that CCC may transport together with indomethacin.

4.7. Stability testing of indomethacin-CCC mixture

4.7.1. Content uniformity of indomethacin-CCC mixture

The drug content uniformity of initial preformed indomethacin-CCC preparations and after freeze thaw cycle is shown in Figure 4.18. All of preformed preparations showed insignificant decrease in drug content after freeze thaw cycle from at initial (paired *t*-test, $p>0.05$). The drug content was slightly decreased, the preformed preparation is likely to be chemically stable at room temperature. There are no differences among the three preformed preparations.

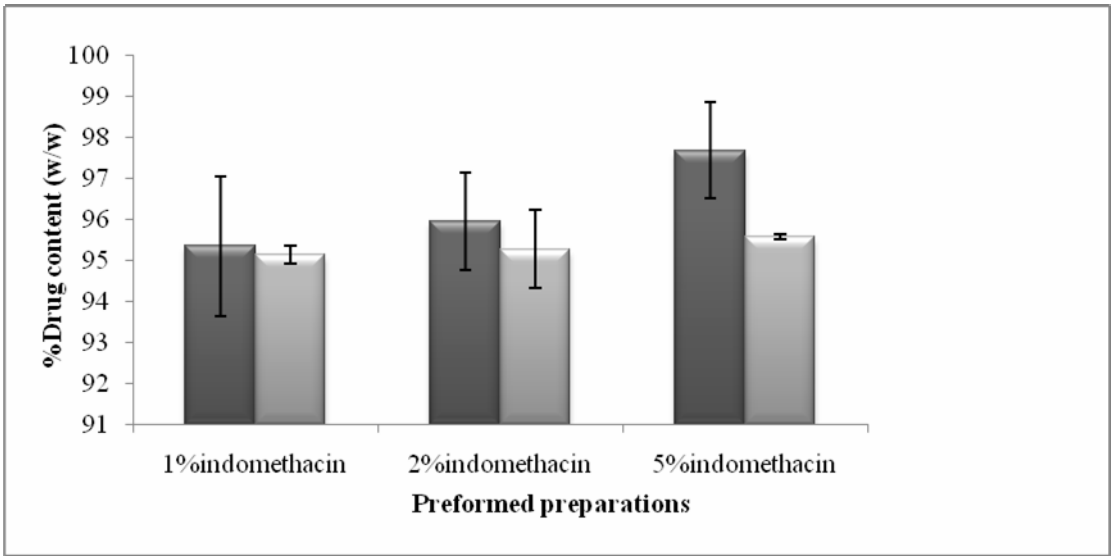

Figure 4.18 The drug content in CCC at initial preformed preparations (■) and after freeze thaw cycle (■) (mean ± SD, n=3)

4.7.2. FTIR analysis of indomethacin-CCC mixture after freeze thaw cycle

The FTIR spectrum of indomethacin-CCC mixtures after freeze thaw cycle is shown in Figure 4.19. All preformed preparations showed spectrum that was not different from its initial. The higher percentage of indomethacin, the shaper peak of C=O stretching of indomethacin at 1716 and 1692 cm^{-1} was obtained. Based on these results, it can be observed that the chemical properties of indomethacin-CCC mixtures were not changed after freeze thaw cycle. At higher concentration of indomethacin (5%) in the mixture, the peak characteristic of indomethacin was clearly observed.

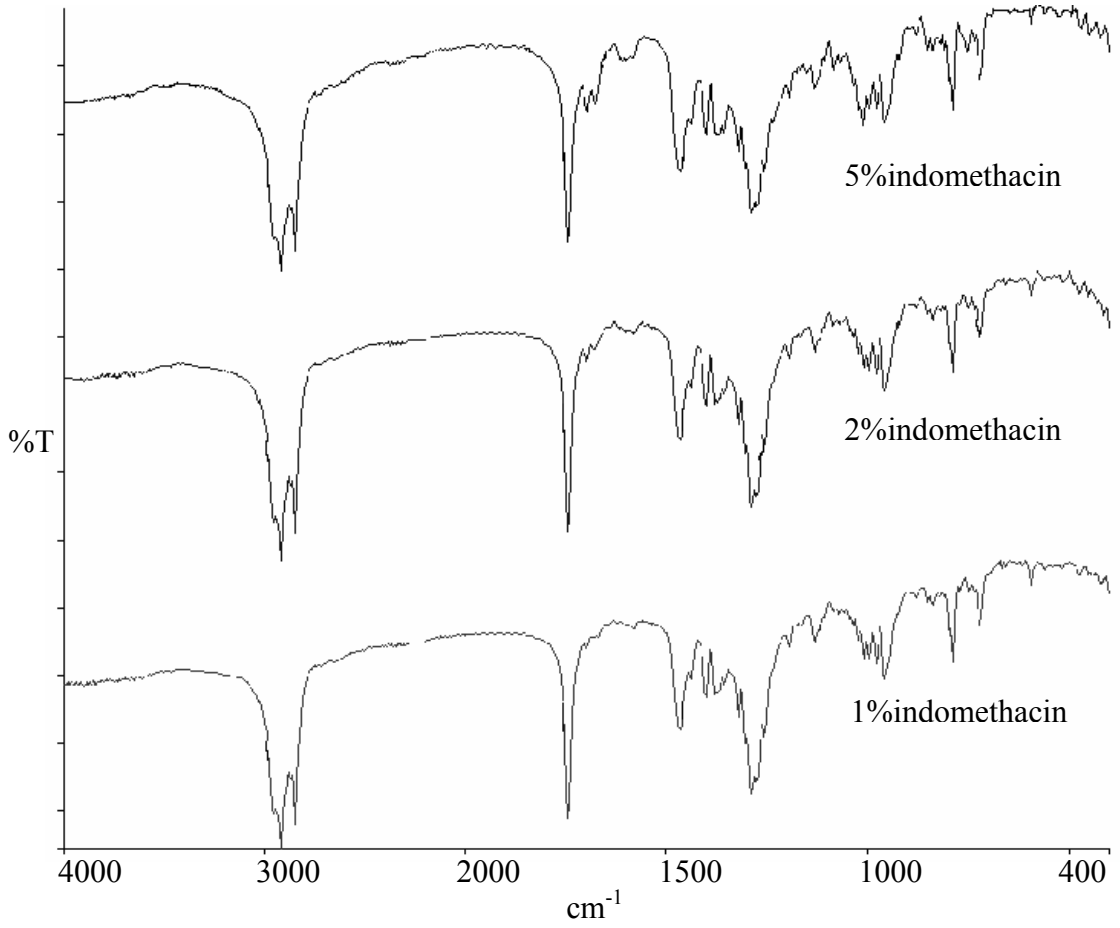

Figure 4.19 FTIR spectrum of indomethacin-CCC mixtures after freeze thaw cycle (6 cycles)

4.7.3. DSC analysis of indomethacin-CCC mixture after freeze thaw cycle

DSC thermograms of indomethacin-CCC mixture are shown in Figure 4.20. All of indomethacin-CCC mixture after freeze thaw showed endothermic peak at 73°C on the heating run. Upon cooling from its isotropic liquid phase, indomethacin-CCC mixture had three exothermic peaks at 65, 47 and 40°C which were shifted to lower temperature than that observed with indomethacin-CCC mixtures before freeze thaw cycle about 2-8 degrees. It should be mentioned that indomethacin incorporated

into CCC may affect the arrangement of CCC resulting in lower phase transition temperature.

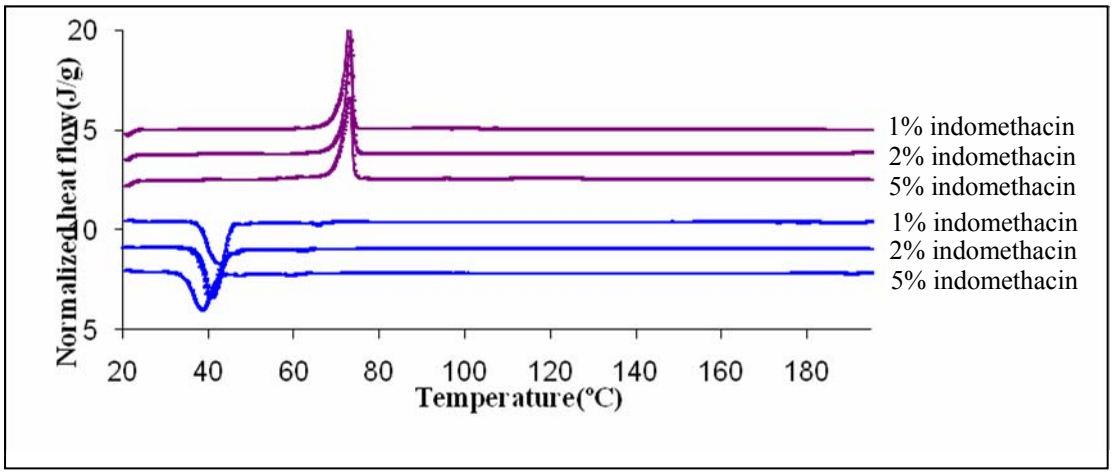

Figure 4.20 DSC thermogram of indomethacin-CCC mixtures after freeze thaw cycle (6 cycles)

4.7.4. PLM of indomethacin-CCC mixtures after freeze thaw cycle

Birefringence of indomethacin-CCC mixtures was observed after freeze thaw cycle. Figure 4.21 (A, C and E) shows the spherulite of indomethacin-CCC mixtures before heating at 25°C. Upon heating, the crystals melted at 72°C. After cooling down to 25°C, CCC rearranged itself to orderly spherulite (Figure 4.21B, D and F). Birefringence of indomethacin-CCC mixtures was transformed to more orderly after being cooled down as compared to that of initial preformed preparations. It is expected that indomethacin-CCC molecules rearrange themselves to perfect and uniform spherulite. However, the interaction between indomethacin and CCC molecules need more advance technique such as single crystal X-ray crystallography.

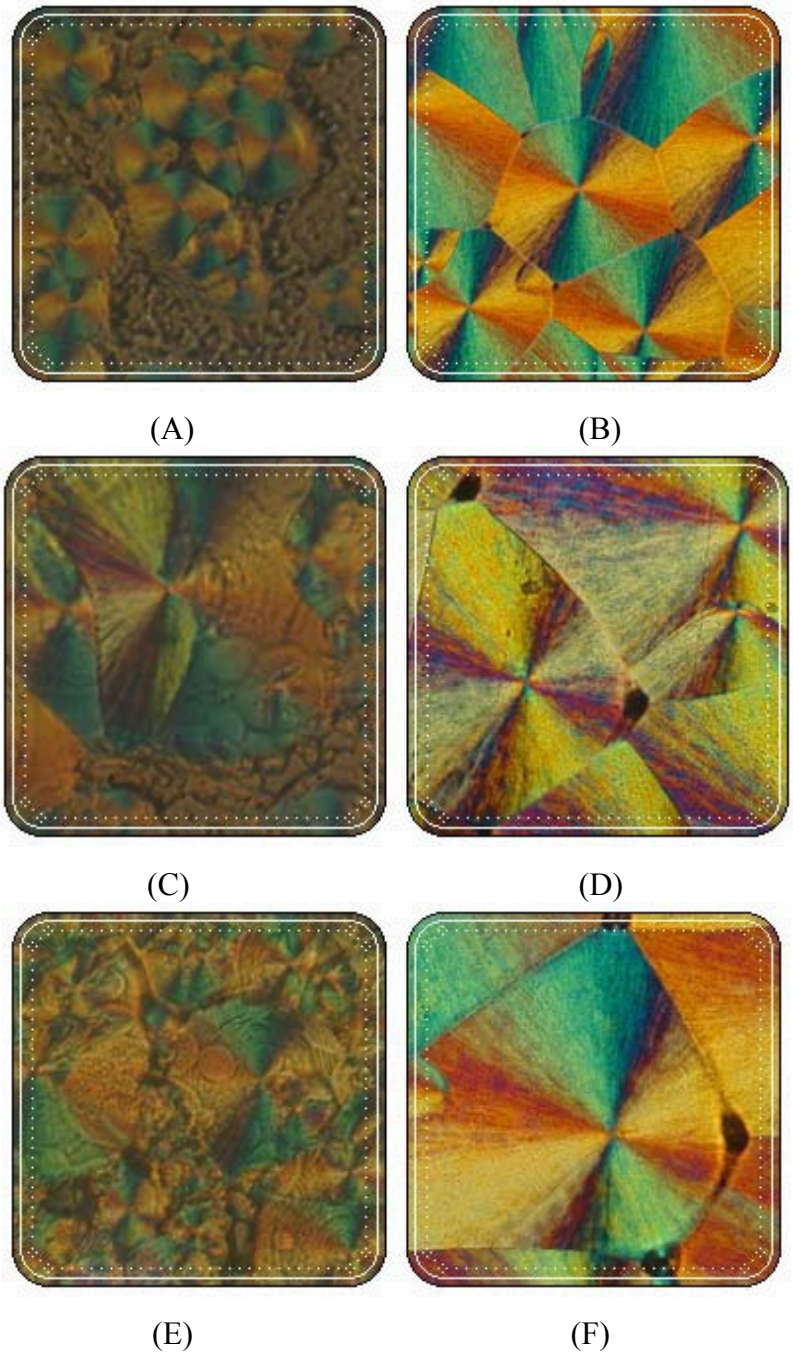

Figure 4.21 Texture of Indomethacin 1% (A), 2% (C) and 5% (E) in CCC from polarized light microscope at 25°C (left) and after recrystallization from molten state (B, D, F) of the same preformed in respective order (400X)

4.7.5. Dissolution test of indomethacin-CCC mixtures after freeze thaw cycle

The dissolution profiles of indomethacin-CCC mixtures are illustrated in Figure 4.22. It was found that the % release of indomethacin in all preformed preparations was apparently changed from at initial. Especially, 5% indomethacin, the release was significantly decreased. The release profiles of 1 and 2% indomethacin were overlapped to one another. The 2% indomethacin was dropped nearly similar to that of 1% indomethacin.

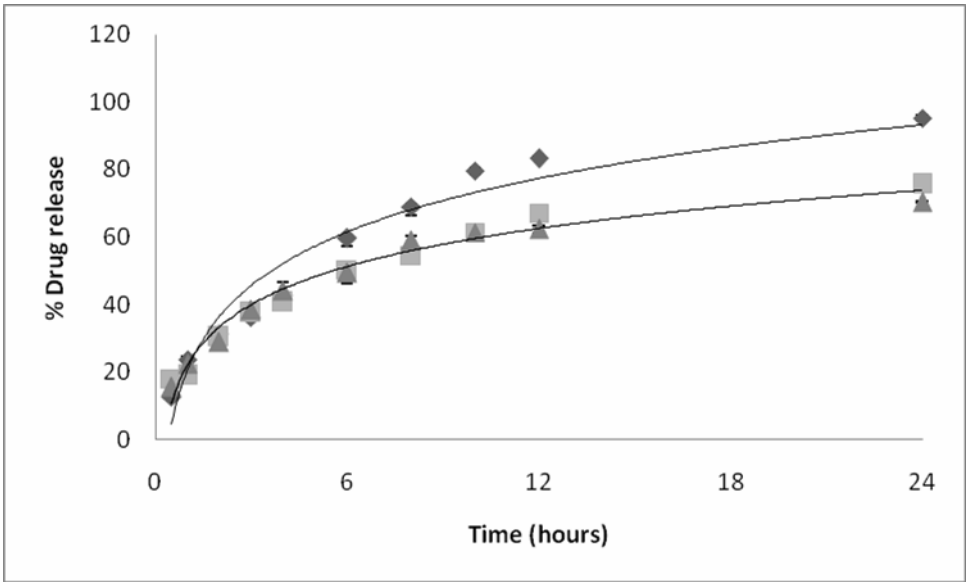

Figure 4.22 The dissolution profiles of indomethacin-CCC mixtures of 1% indomethacin (▲), 2% indomethacin (■), 5% indomethacin (♦) (mean ± SD, n=3)

Table 4.10summaries the kinetic data obtained from the Higuchi plots of each dissolution profile after freeze thaw cycle of preformed preparations compared with at initial. The linear regression correlation coefficient obtained was greater than 0.97. The amount of indomethacin released from preformed preparations was significantly different from that of an initial. The release rate constants of indomethacin-CCC mixtures before and after freeze thaw cycles were also significantly different ($P < 0.05$). All three preformed indomethacin-CCC mixtures (1, 2 and 5% indomethacin), the release rate constants decreased from the initial. The difference was pronounced in case of 5% indomethacin. This may be contributed from the recrystallization of CCC during freeze thaw cycle. The crystal structure of CCC may affect the release of indomethacin. However, this evidence has to be proved in a long term stability of indomethacin-CCC.

Table 4.10 Higuchi released rate constant of indomethacin-CCC mixtures after freeze thaw cycle compare with initial preformed preparations (mean ± SD, n=3)

Preformed Preparations	Initial		After freeze thaw cycle	
	Release rate constant ($\mu g/ml \cdot h^{1/2}$)	R^2	Release rate constant ($\mu g/ml \cdot h^{1/2}$)	R^2
1%indomethacin	166.61 ± 7.6	0.994	152.33 ± 1.94	0.970
2%indomethacin	346.04 ± 16.68	0.997	334.50 ± 5.60	0.995
5%indomethacin	1387.33 ±45.65	0.993	1106.00 ± 34.04	0.972

From this study it can be seen that the indomethacin can be incorporated into CCC at low concentration (low loading capacity). The indomethacin-CCC system can release the drug in a controlled manner and temperature may also affect the release properties. This system works as a reservoir in topical semi-solid dosage form and is able to permeate across the barrier of the skin. At this stage, this system is not suitable for systemic administration due to very low drug found (< 0.83 μg/ml) in the receiving phase.

CHAPTER 5

CONCLUSIONS

In this study, indomethacin was developed as a topical dosage form by incorporation into synthetic liquid crystal (CCC).

Indomethacin was incorporated into CCC by solvent evaporation method. The indomethacin-CCC mixtures exhibited liquid crystalline phase. The FTIR spectrum and DSC thermogram indicate that 1, 2 and 5% of indomethacin are suitable concentration to prepare preformed preparations in this study. The dissolution test and permeation study of indomethacin-CCC mixture were evaluated in comparison with pure indomethacin and indomethacin-cholesterol preformed preparations. Indomethacin-CCC mixtures could prolong release of indomethacin in a controlled manner. The skin retention study indicates that the preformed preparations were capable of localizing indomethacin in the skin layers much higher than the pure indomethacin and indomethacin-cholesterol. CCC seems to be a promising carrier system for topical drug delivery. It is suggested that the preformed preparation would be formulated into dermatological dosage forms such as lamellar gel phase, cream or ointment. It is expected that the addition of other ingredients would decrease transition temperature closer to skin temperature and expected that the release would be enhanced and also the skin retention would be improved to satisfied level. Other issues that can be carried out in the future is that the interaction between indomethacin and CCC at a molecular level by single crystal X-ray crystallography.

This would require the crystallization of pure indomethacin, pure CCC and co-crystallization of indomethacin-CCC mixture. After that those single crystals will be subjected to X-ray crystallography to help in understanding orientation of the molecules.

BIBLIOGRAPHY

Ansel, H.C., Popovich, N.G. and Allen, L.V. Jr. 1995. *Pharmaceutical dosage forms and drug delivery systems*, 6th ed, Williams and Wilkins, 357-372.

Bagheri, M. and Rad, R.Z. 2008. Synthesis and characterization of thermotropic liquid crystalline polyesters with biphenyl unit in the main chain. *React. Funct. Polym.* 68, 613–622.

Barry, B.W. 2001. Novel mechanisms and devices to enable successful transdermal drug delivery. *Eur. J. Pharm. Sci.* 14, 101-114.

Benita, S. 1996. Microencapsulation: methods and industrial applications, Marcel Dekker Inc., New York.

Boyd, B. J., Khoo, S.M., Whittaker, D.V., Davey, G. and Porter, C.J.H. 2007. A lipid-based liquid crystalline matrix that provides sustained release and enhanced oral bioavailability for a model poorly water soluble drug in rats. Int. J. Pharm. 340, 52-60.

Buck, P. 2004. Skin barrier function: effect or age, race and inflammatory disease. *Int. J. Aromatherapy*. 14, 70 - 76.

Chandrasekaran, S., Al-Ghananeem, A.M., Riggs, R.M. and Crooks, P.A. 2006. Synthesis and stability of two indomethacin prodrugs. *Bioorg. Med. Chem. Lett.* 16, 1874-1879.

Chuealee, R., Aramwit, P. and Srichana, T. 2007. Characteristics of cholesteryl cetyl carbonate liquid crystals as drug delivery systems. *Proc 2nd IEEE International Conference on Nano/Micro Enginerred and Molecular System.* 1098-1103

Dean, J.A. 1995, Analytical Chemistry Handbook, McGraw-Hill, INC, New York.

Elser, W., Pohlmann, J. and Boyd, P. 1973, Cholesteryl n-alkyl carbonate. *Mol. Cryst. Liq. Cryst.* 20, 77-86.

Enlow, J.D., McGrath, K.M., Enlow, R.L. and Tate, M.W. 2007. Computational modelling of surfactant liquid crystal structures. Auckland seminar.

Fischer, P., Eugster, A., Windhab, E.J. and Schuleit, M. 2007. Predictive stress tests to study the influence of processing procedures on long term stability of supersaturated pharmaceutical o/w creams. *Int. J. Pharm*. 339, 189-196.

Fitzpatrick, D. and Corish, J. 2005. Release characteristics of anionic drug compounds from liquid crystalline gels I: Passive release across non-rate-limiting membranes. *Int. J. Pharm.* 301, 226–236.

Foldvari, M. 2000. Non-invasive administration of drugs through the skin: challenges in delivery system design. *Pharm. Sci. Tech. Today*. 3, 417-425.

Friberg, S. 2003. Phase of liquid crystal. (http//plc.cwru.edu/tutorial/enhanced/files/lc/phase/phase.htm) (accessed: January 2008).

Fujii, M., Shiozawa, K., Watanabe, Y. and Matsumoto, M. 2001. Effect of phosphatidylcholine on skin permeation of indomethacin from gel prepared with liquid paraffin and hydrogenated phospholipid. *Int. J. Pharm*. 222, 57-64.

Grolik, J., Sieron, L. and Eilmesa, J. 2006. A new liquid crystalline derivative of dibenzotetraaza[14]annulene: synthesis, characterization and the preliminary evaluation of mesomorphic properties. *Tetra. Lett.* 47, 8209–8213.

ICH. 1996. Guidance for industry Q2B validation of analytical procedures : methodology. Center for Drug Evaluation and Research (CDER), Rockville, MD, USA.

Jambhekar, S., Casella, R. and Mahera, T. 2004. The physicochemical characteristics and bioavailability of indomethacin from β-cyclodextrin, hydroxyethyl-β-cyclodextrin and hydroxypropyl-β-cyclodextrin complexes. *Int. J. Pharm*. 270, 149–166.

Jona, A. J., Lewis, W. D., Peter, A. C., Susan, M. M. and Anwar, A. H. 1995. Design of novel prodrugs for the enhancement of the transdermal penetration of indomethacin. *Int. J. Pharm*. 123, 127-136.

Jing-Mou, Y., Yong-Jie, L., Li-Yan, Q. and Yi, J. 2008. Self-aggregated nanoparticles of cholesterol-modified glycol chitosan conjugate: Preparation, characterization, and preliminary assessment as a new drug delivery carrier. *Eur. Polym. J.* 44, 555-565.

Junyaprasert, V., Boonme, P., Songkro, S., Krauel, K. and Rades, T. 2007. Transdermal delivery of hydrophobic and hydrophilic local anesthetics from o/w and w/o Brij 97-based microemulsions. *J. Pharm. Pharmaceut. Sci.* 3, 288-298.

Lee, J. and Kellaway, I.W. 2000a. *In vitro* peptide release from liquid crystalline buccal delivery systems. *Int. J. Pharm*. 195, 29-33.

Lee, J. and Kellaway, I.W. 2000b. Buccal permeation of [D-Ala^2, D-Leu^5] enkephalin from liquid crystalline phases of glyceryl monooleate. *Int. J. Pharm*. 195, 35–38.

Lin, S.Y., Ho, C.J. and Li, M.J. 2001. Precision and reproducibility of temperature response of a thermo-responsive membrane embedded by binary liquid crystals for drug delivery. *J. Control. Release*. 73, 293-301.

Liquid crystal. 2008. (http://en.wikipedia.org/wiki/Liquid_crystal).

Loukas,Y.L., Vraka1, V. and Gregoriadis, G. 1998. Drugs, in cyclodextrins, in liposomes: a novel approach to the chemical stability of drugs sensitive to hydrolysis. *Int. J. Pharm*. 162, 137–142.

Loukas, Y.L. and Gregoriadis, G. 1997. Drugs in cyclodextrins, in liposomes: a novel approach for the reduction of drug leakage from liposomes. *Proceedings of the twenty fourth international symposium on controlled release of bioactive materials. Stockholm, Sweden,* 15–19.

Magnusson, B. M., Walters, K. A. and Roberts, M. S. 2001. Veterinary drug delivery: potential for skin penetration enhancement. *Adv. Drug Deliv. Rev.* 50, 205-227.

Makai, M., Csányi, E., Németh, Zs., Pálinkás, J. and Er´os, I. 2003. Structure and drug release of lamellar liquid crystals containing glycerol. *Int. J. Pharm.* 256, 95–107.

Menon, G.K. 2002. New insights into skin structure: scratching the surface. *Adv. Drug. Deliv. Rev.* Supplementary 1, S3-S17.

Michniak, B.B., Player, M.R., Chapman, J.M. and Sowell, J.W. 1993. *In vitro* evaluation of a series of azone analogs as dermal penetration enhancers. *Int. J. Pharm.* 91, 85-93.

Mills, P.C. and Cross, S.E. 2006. Transdermal drug delivery: Basic principles for the veterinarian. *Vet. J.* 172, 218-233.

Moser, K., Kriwet, K., Naik, A., Kalia, Y. N. and Guy, R. H. 2001. Passive skin penetration enhancement and its quantification *in vitro*. *Eur. J. Pharm. Biopharm.* 52, 103-112.

Muchtar, S., Abdulrazik, M., Frucht-Pery, J. and Benita, S. 1997. *Ex-vivo* permeation study of indomethacin from a submicron emulsion through albino rabbit cornea. *J. Control. Release.* 44, 55-64.

Muller-Goymann, C.C. 2004. Physicochemical characterization of colloidal drug delivery systems such as reverse micelles, vesicles, liquid crystals and nanoparticles for topical administration. *Eur. J. Pharm. Biopharm*. 58, 343–356.

Naik, A., Kalia, Y. N. and Guy, R. H. 2000. Transdermal drug delivery: overcoming the skin's barrier function. *Pharm. Sci. Tech. Today.* 3, 318-326.

Nesseem, D. I. 2001. Formulation and evaluation of itraconazole via liquid crystal for topical delivery system. *J. Pharm. Biomed. Anal*. 26, 387–399.

Nováková, L., Matysová, L., Havlíková, L. and Solich, P. 2005. Development and validation of HPLC method for determination of indomethacin and its two degradation products in topical gel. *J. Pharm. Biomed. Anal.* 37, 899-905.

Palagiano, F., Arenare, L., Barbato, F., La Rotonda, M. I., Quaglia, F. Bonina, F. P. Montenegro, L. and Caprarüs, P. 1997. *In vitro* and *in vivo* evaluation of terpenoid esters of indomethacin as dermal prodrugs. *Int. J. Pharm.* 149, 171-182.

Perme Gear Franz Cells. 2008. (http://www.permegear.com/franz.htm).

Pohlmann, A. R., Weiss, V., Mertins, O., Pesce da Silveira, N. and Guterres, S. S. 2002. Spray-dried indomethacin-loaded polyester nanocapsules and nanospheres: development, stability evaluation and nanostructure models. *Eur. J. Pharm. Sci.*16, 305-312.

Rosenblatt, C. 2008. Case liquid crystal and complex fluids group (http://liq-xtal.cwru.edu/).

Rosing, H., Man, W. Y., Doyle, E., Bult, A. and Beijnen, J. H. 2000. Bioanalytical liquid chromatographic method validation. A review of current practises and procedures. *J. Liq. Chrom. Relat. Tech.* 23, 329 - 354.

Shafiq-un-Nabi, S., Shakeel F., Talegaonkar S., Ali, J., Baboota, S., Ahuja, A. Khar, R.K. and Ali, M. 2007. Formulation development and optimization using nanoemulsion technique: a technical note. *AAPS Pharm. Sci. Tech.* 8, E1-E6.

Siewert, M., Dressman, J., Brown, C.K. and Shah, V.P. 2003. FIP/AAPS guidelines to dissolution/*in vitro* release testing of novel/special dosage form. *AAPS Pharm. Sci. Tech.* 6-15.

Songkro, S., Purwo, Y., Becket, G. and Rades, T. 2003. Investigation of newborn pig skin as an *in vitro* animal model for transdermal drug delivery. *S.T.P. Pharm. Sci.* 13, 133-139.

Songkro, S., Rades, T. and Becket, G. 2003. The effects of p-methane monoterpenes and related compounds on the percutaneous absorption of propanolol hydrochloride across newborn pig skin I. *In vitro* permeation and retention studies. *S.T.P. Pharm. Sci.* 13, 349-357.

Spireas, S. and Sadu, S. 1998. Enhancement of prednisolone dissolution properties using liquid solid compacts. *Int. J. Pharm.* 166, 177-188.

Swartz, M.E. and Krull, I.S. 1998. Validation of chomatographic methods. *Pharm.Technol*. 22, 20-104.

Toshiyuki, S., Keiko, Y., Hidetaka, I., Keiichi, F. and Hajime, H. 2001. Multiphase emulsions by liquid crystal emulsification and their application. *Stud. Surf. Sci. Catal.* 132, 1025-1030.

Trotta, M. 1999. Influence of phase transformation on indomethacin release from Microemulsions. *J. Control. Release.* 60, 399–405.

Walters, K.A. and Roberts, M.S. 2002. The structure and function of skin. In dermatological and transdermal formulations. New York, Mercel Dekker, USA. 1 - 39.

Xu, Q.A. 2003. Stablity-indicating HPLC methods for drug analysis, 2nd ed, Pharmaceutical Press, London. 373-376.

Yoo, J., Shanmugam, S., Song, C.K., Kim, D.D., Choi, H.G., Yong, C.S., Woo, J.S. and Yoo, B. K. 2008. Skin penetration and retention of L-ascorbic acid 2-phosphate using multilamellar vesicles. *Arch. Pharm. Res.* 31, 1652-1658.

Zhang, Y., Zhang, Z., Qi, G., Sun, Y., Wei, Y. and Ma, H. 2007. Detection of indomethacin by high-performance liquid chromatography with in situ electrogenerated Mn(III) chemiluminescence detection. *Anal. Chim. Acta.* 582, 229–234.

APPENDIX

CHEMICAL COMPOUNDS

INDOMETHACIN

Chemical name: 2-{1-[(4-chlorophenyl)carbonyl]-5-methoxy-2-methyl-1*H*-indol-3-yl}acetic acid

Molecular formula: $C_{19}H_{16}ClNO_4$

Molecular weight: 357.79

Chemical structure:

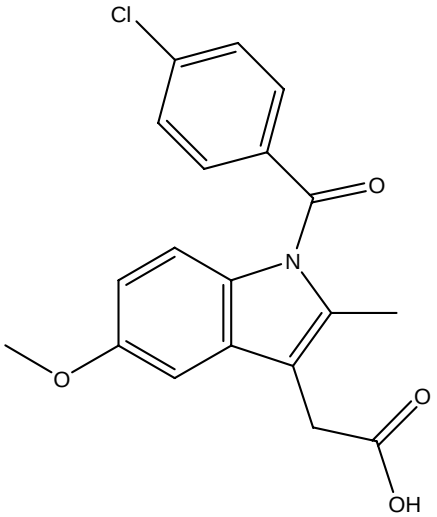

Description: Indomethacin is defined as the Form I crystalline, non-solvated free acid moiety of the compound unless otherwise noted. Indomethacin can exist as several crystalline forms but has been used in pharmaceutical preparations principally as Form I and less frequently as the crystalline sodium trihydrate.

Solubility: Indomethacin is practically insoluble in water. It is soluble in ethanol, ether, acetone and castor oil. Indomethacin as a free base is soluble 1 g/50 mL ethanol, 1 g/30 mL chloroform and 1 g/40-45 mL diethyl ether. However, it should be noted that indomethacin is not stable in alkaline solutions. Indomethacin solutions below pH 7.4 were stable. Solutions at pH 7.4 showed no changes up to 24 hours, but decomposition was rapid in alkaline solutions.

Stability: In general, the integrity of indomethacin power and formulation product exists for at least 5 years at room temperature. Exposure to strong direct sunlight induces an increase in the color of indomethacin; however, degradation is slight, but the precaution of employing light resistant containers should be taken to minimize discoloration of solid. Indomethacin undergoes alkaline hydrolysis to p-chlorobenzoate and 2-methyl-5-methoxy-indole-3-acetate. These transformation products are also primary metabolic products. The half-life at room temperature is about 200 h in pH 8.0 buffer and about 90 min in pH 10.0 solutions.

CETYL ALCOHOL

Chemical name: Palmityl alcohol, 1-Hexadecanol, Hexadecan-1-ol, Hexadecyl alcohol

Molecular formula: $CH_3(CH_2)_{15}OH$

Molecular weight: 242.44

Chemical structure:

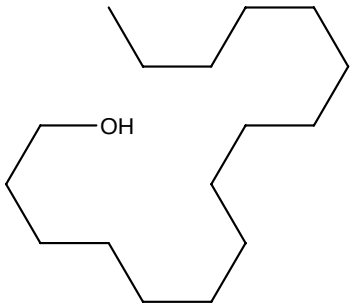

Description: Fatty alcohols, derived from natural fats and oils, are high molecular straight chain primary alcohols. They include lauryl (C12), myristyl (C14), cetyl (or palmityl: C16), stearyl (C18), oleyl (C18, unsaturated), and linoleyl (C18, polyunsaturated) alcohols. There are synthetic fatty alcohols equivalent physically and chemically to natural alcohols obtained from oleochemical sources such as coconut and palm kernel oil.

Application: Fatty alcohols are emulsifiers and emollients to make skin smoother and prevent moisture loss. Identical fatty esters are used to improve rub-out of formulas and to control viscosity and dispersion characteristics in cosmetics, personal care products and pharmaceutical ingredients. As chemical intermediates, the primary use of fatty alcohols are as raw material for the production of fatty sulfate salts and alcohol ethoxylates for foaming and cleaning purposes in the field of detergent industry. Chemical reactions of primary alcohols

include esterifications, ethoxylation, sulfation, oxidation and many other reactions.

CHOLESTERYL CHLOROFORMATE

Chemical name: Cholest-5-ene-3-beta-yl chloroformate

Molecular formula: $C_{28}H_{45}ClO_2$

Molecular weight: 449.12

Chemical structure:

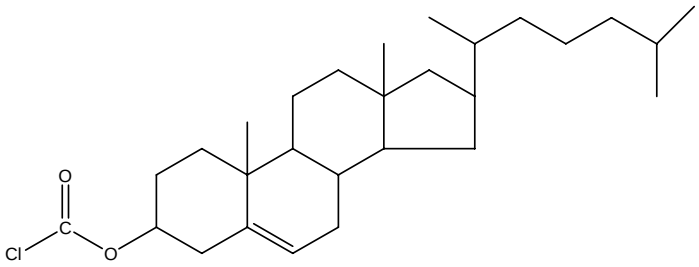

Description:

Application: Cholesteryl chloroformate can be used to isolate small amounts of amines from aqueous solutions as N-substituted cholesteryl carbarnates. These derivatives are easily isolated and identified. Their possible use for identification of amines obtained in degradative studies.

PYRIDINE

Chemical name: Azabenzene, Azine

Molecular formula: C_5H_5N

Molecular weight: 79.10

Chemical structure:

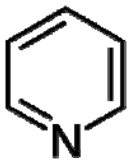

Description: The nitrogen atom on pyridine features a basic lone pair of electrons. Because this lone pair is not delocalized into the aromatic pi-system, pyridine is basic with chemical properties similar to tertiary amines. The pKa of the conjugate acid is 5.21. Pyridine is protonated by reaction with acids and forms a positively charged aromatic polyatomic ion called pyridinium. The bond lengths and bond angles in pyridine and the pyridinium ion are almost identical.

Application: As a base

In organic reactions pyridine behaves both as a tertiary amine, undergoing protonation, alkylation, acylation, and N-oxidation

at nitrogen, and as an aromatic compound, undergoing Nucleophilic substitutions.

As an *N*-nucleophile

Pyridine is a good nucleophile with a donor number of 33.1. It is easily attacked by alkylating agents to give *N*-alkylpyridinium salts. One example is cetylpyridinium chloride, a cationic surfactant that is a widely used disinfection and antiseptic agent. Pyridinium salts can be obtained in the Zincke reaction. Useful adducts of pyridine include Pyridine-borane, $C_5H_5NBH_3$ (m.p. 10–11 °C), a mild reducing agent with improved stability relative to $NaBH_4$ in protic solvents and improved solubility in aprotic organic solvents. Pyridine-sulfur trioxide, $C_5H_5NSO_3$ (mp 175 °C) is a sulfonation agent used to convert alcohols to sulfonates, which in turn undergo C-O bond scission upon reduction with hydride agents.

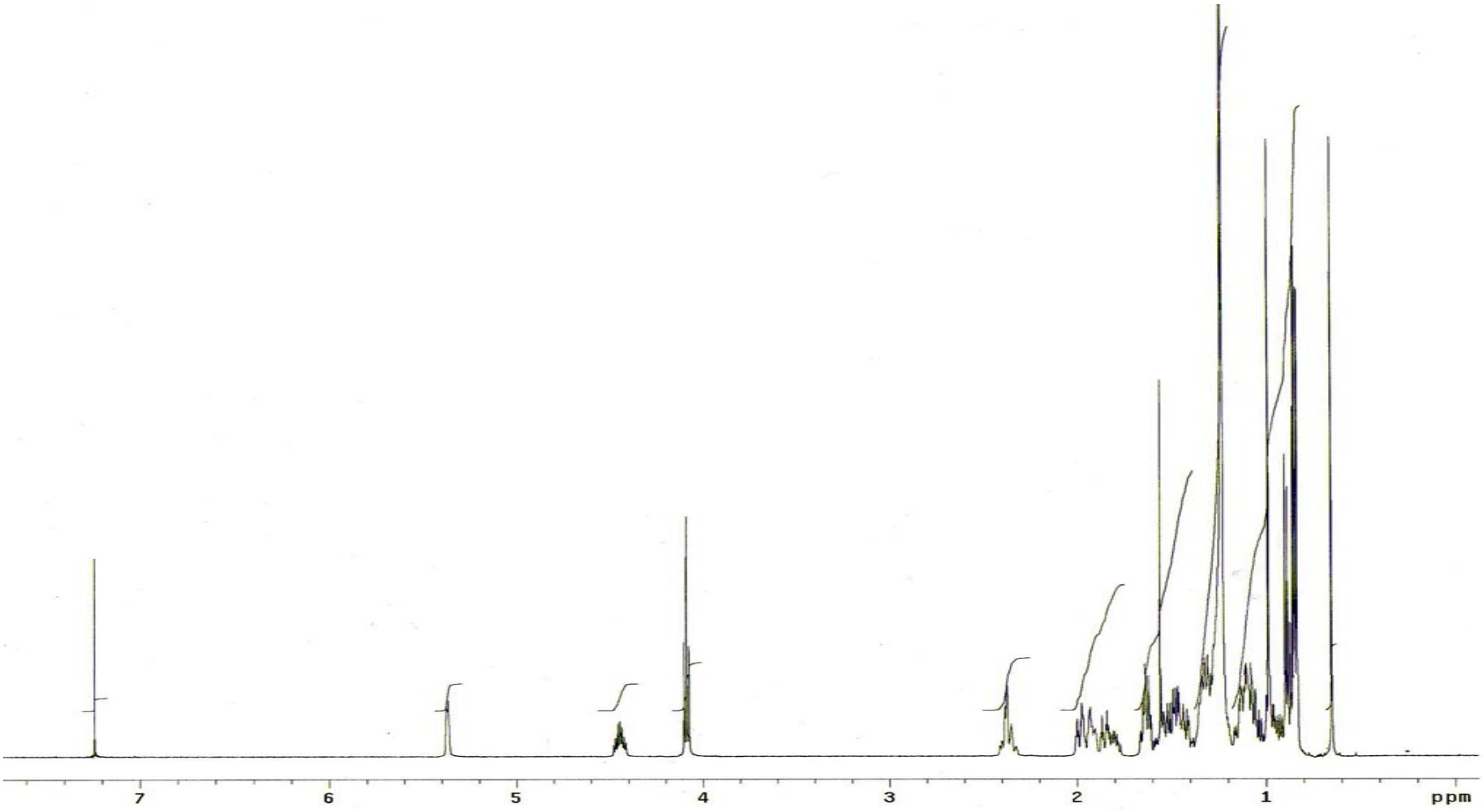

^{1}H-NMR spectra of cholesteryl cetyl carbonate (CCC)

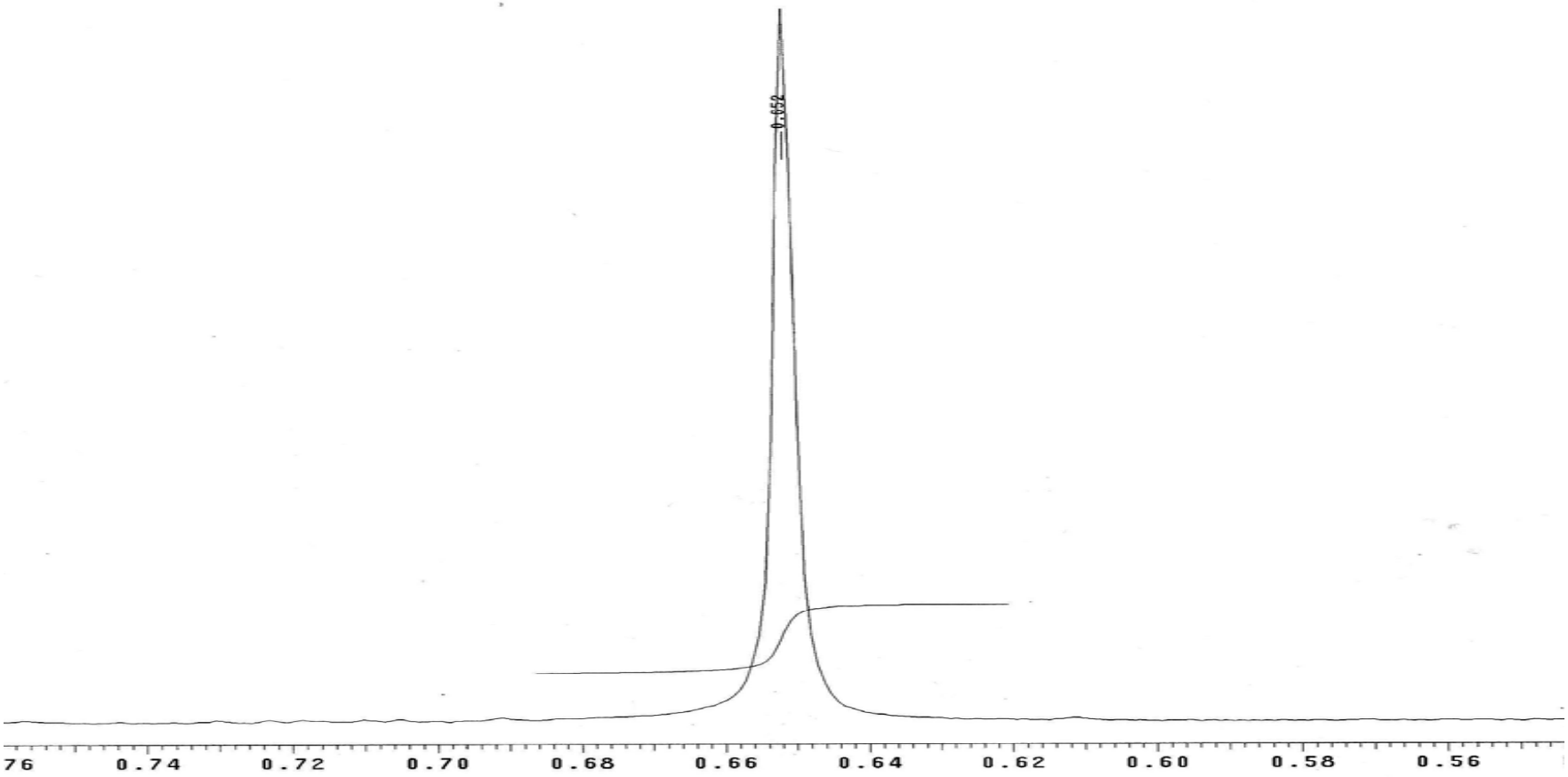

^{1}H-NMR spectra of cholesteryl cetyl carbonate (CCC)

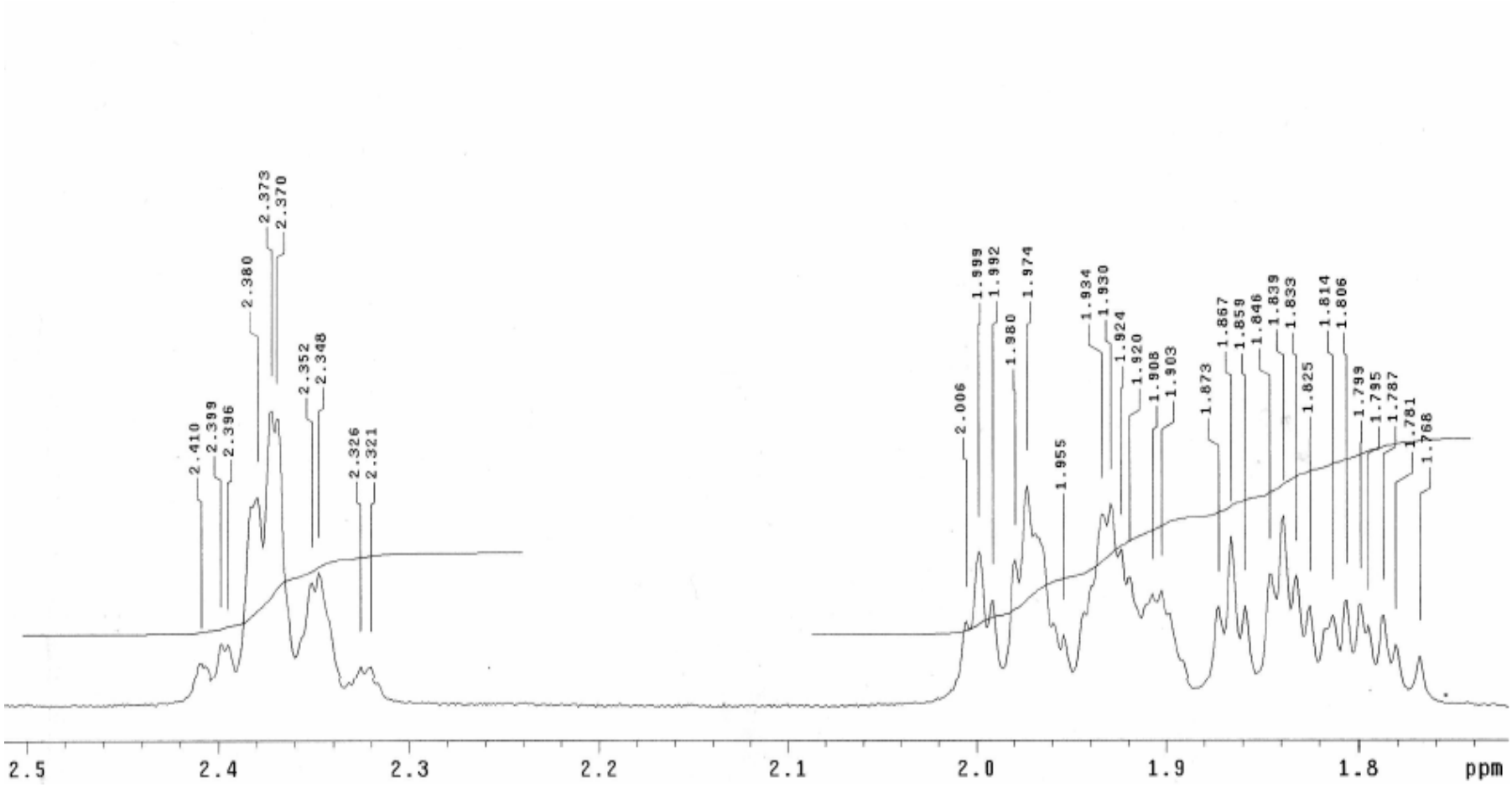

^{1}H-NMR spectra of cholesteryl cetyl carbonate (CCC)

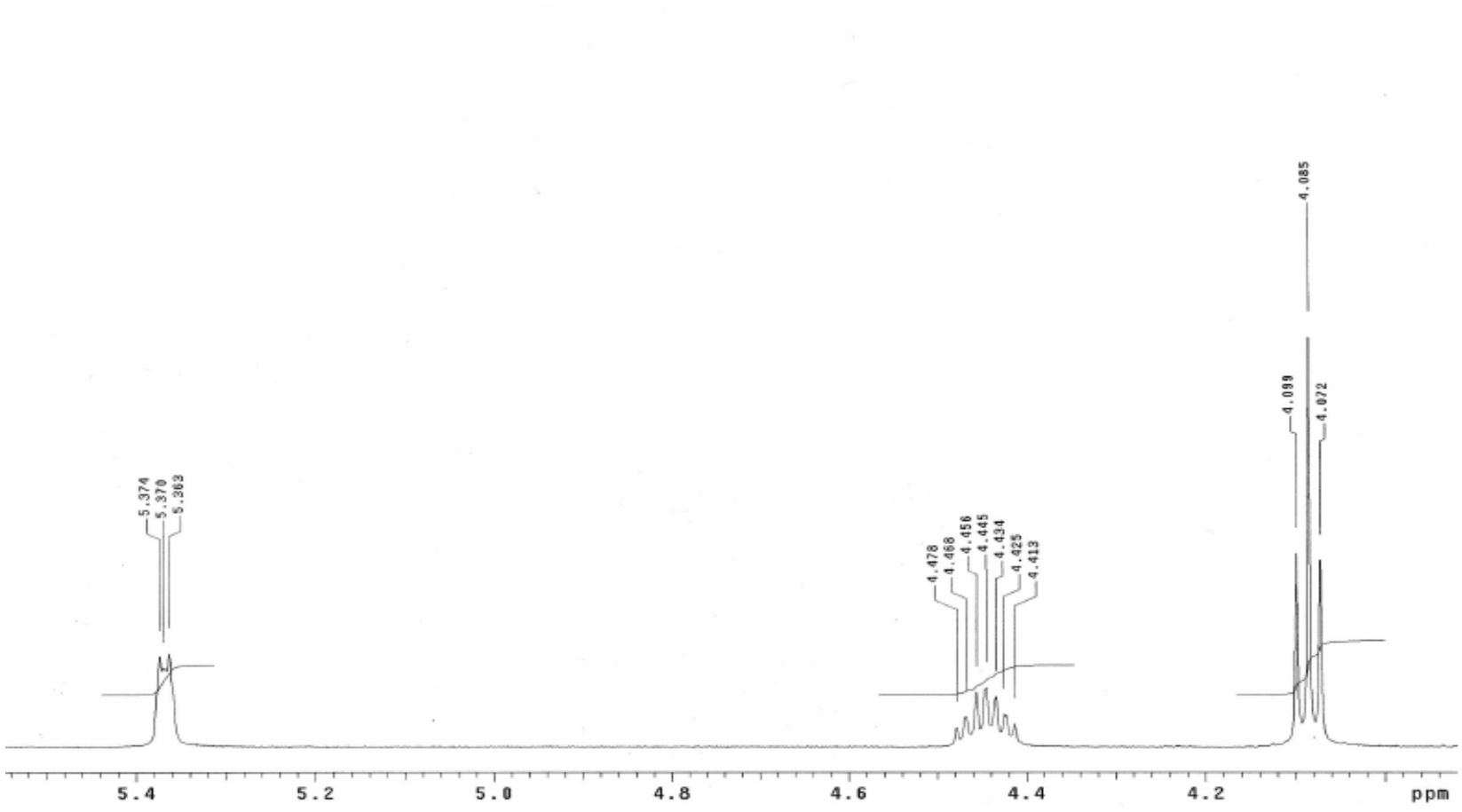

^{1}H-NMR spectra of cholesteryl cetyl carbonate (CCC)

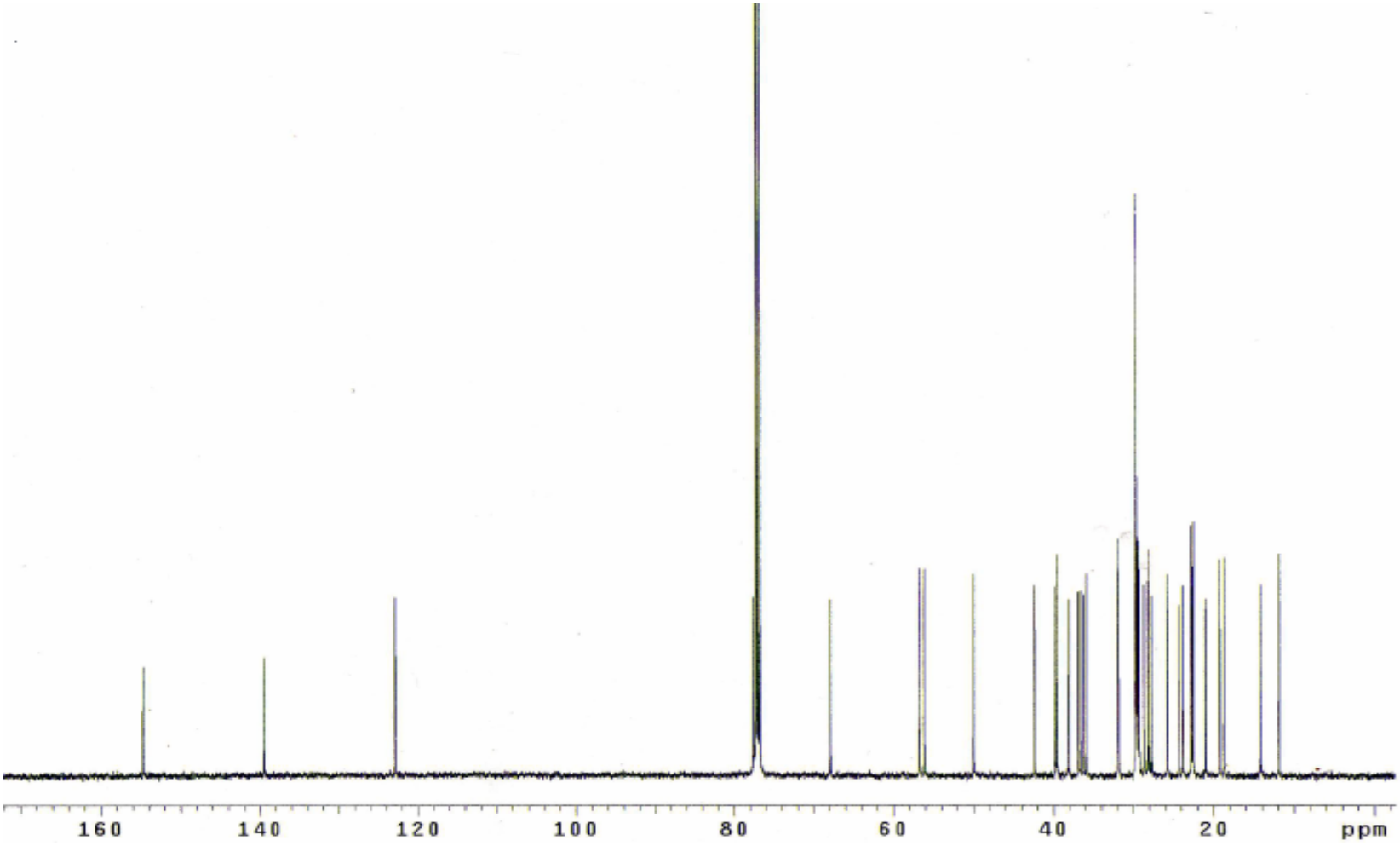

^{13}C-NMR spectra of cholesteryl cetyl carbonate (CCC)

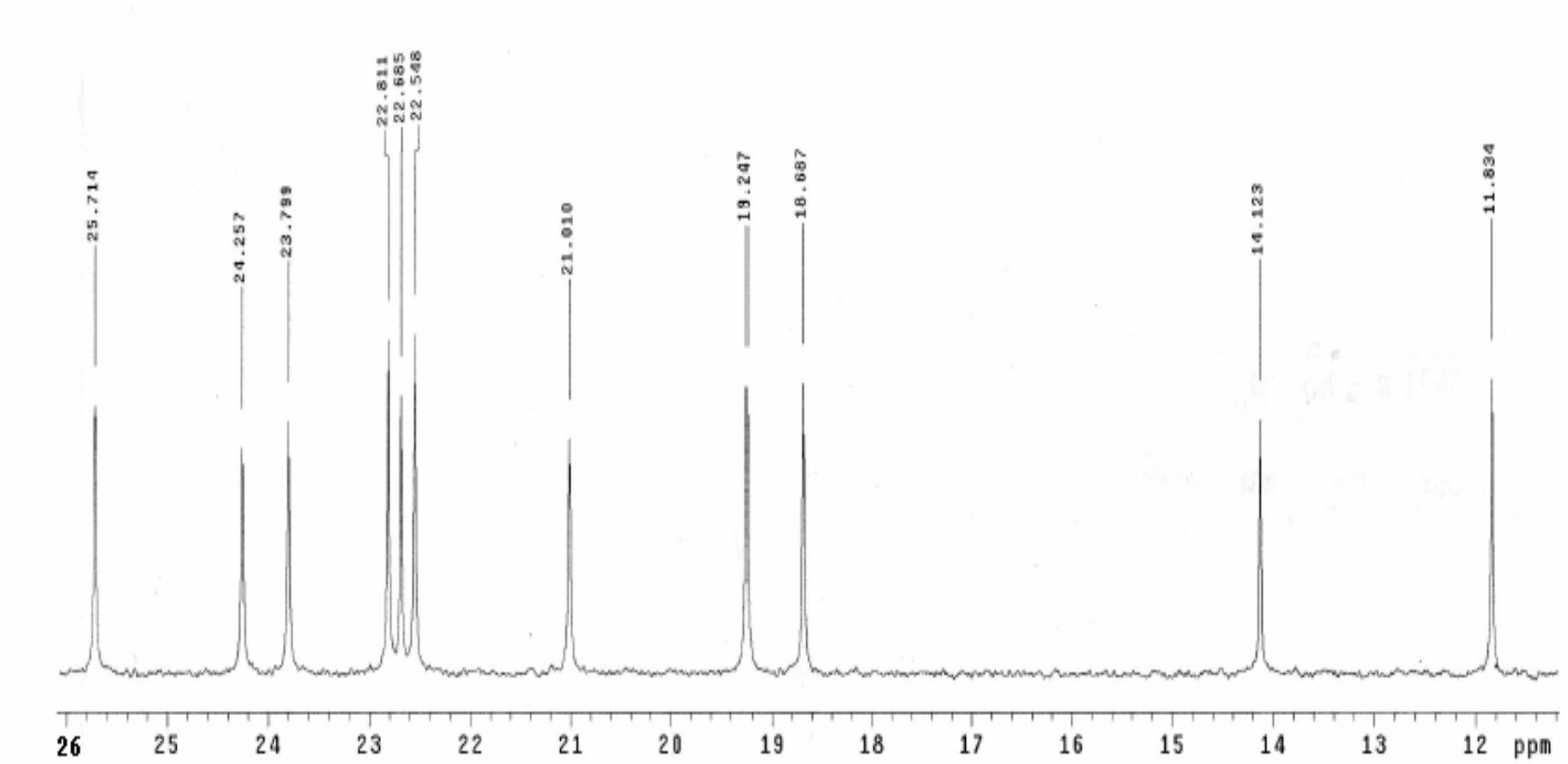

^{13}C-NMR spectra of cholesteryl cetyl carbonate (CCC)

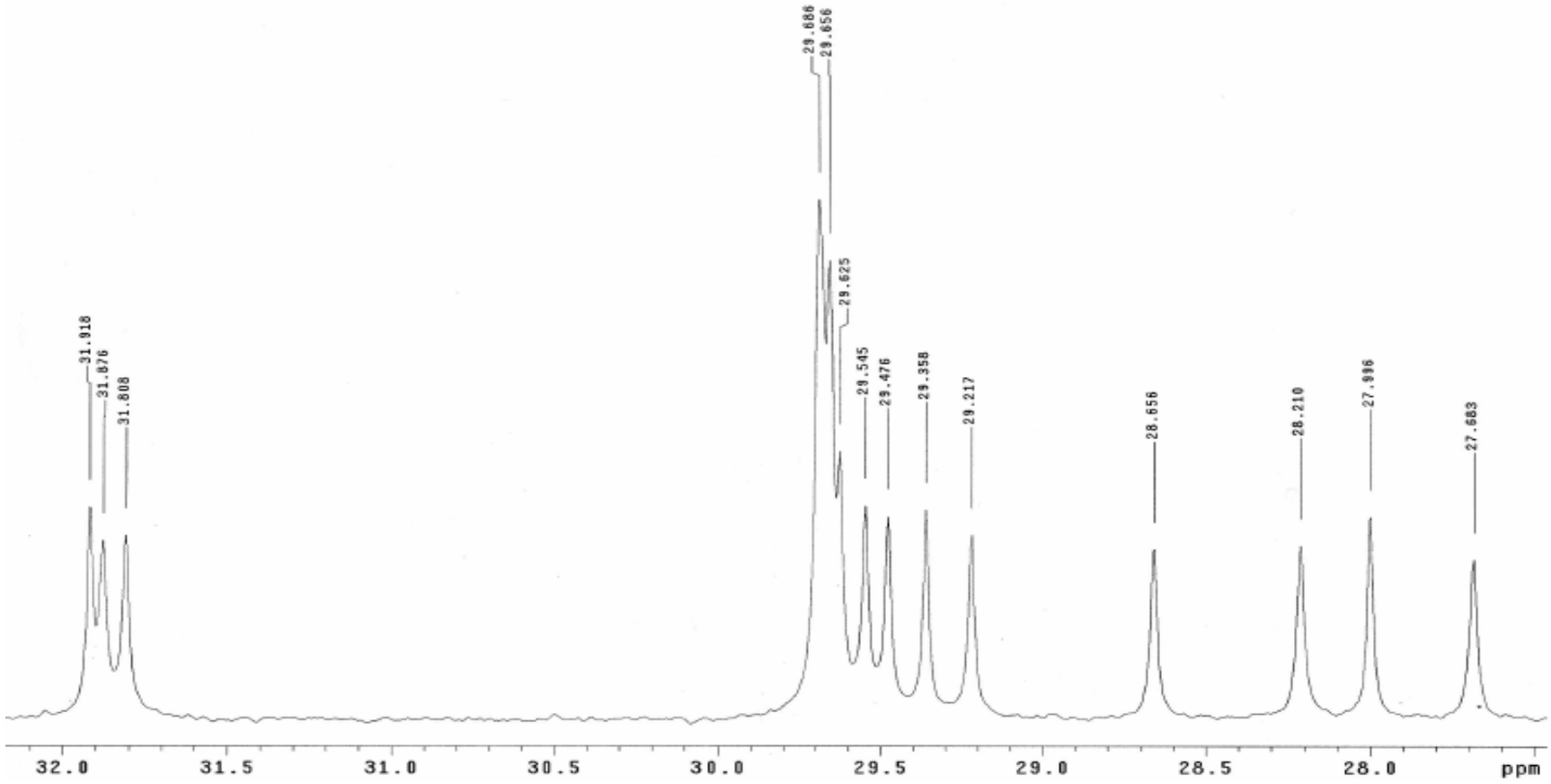

^{13}C-NMR spectra of cholesteryl cetyl carbonate (CCC)

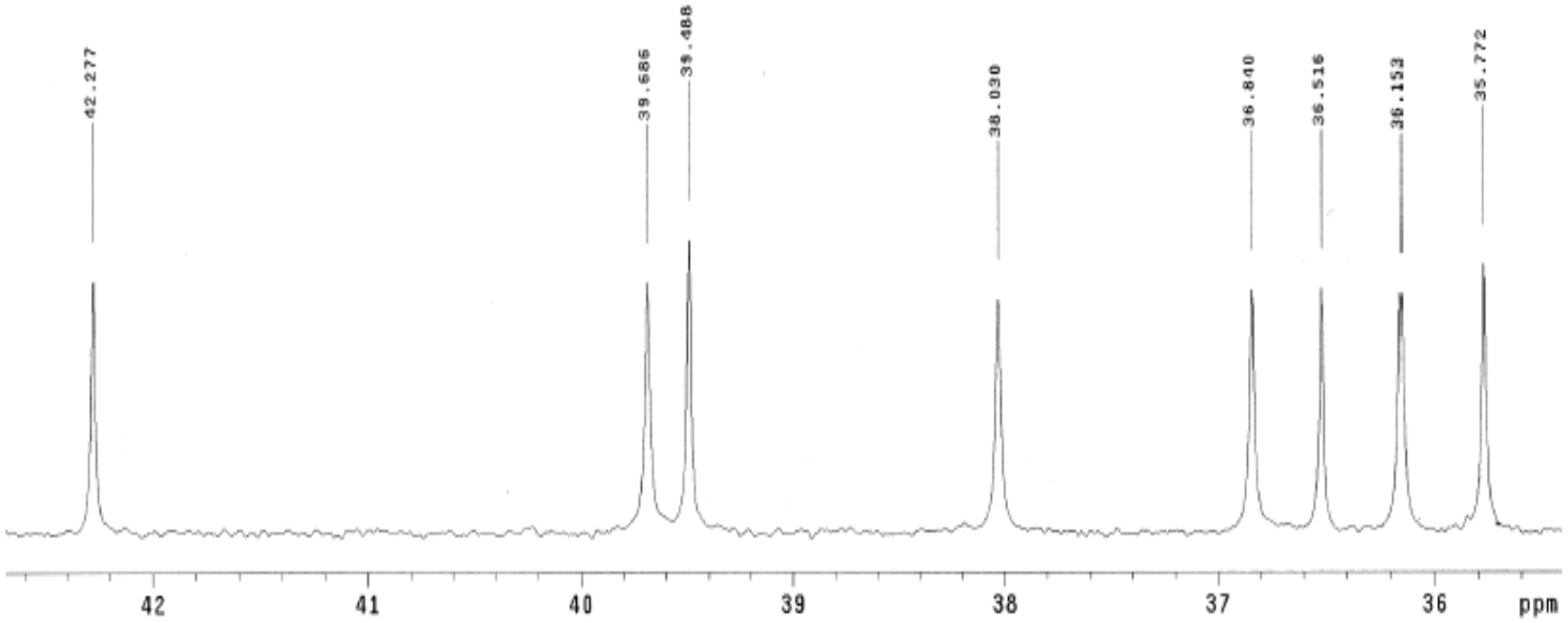

^{13}C-NMR spectra of cholesteryl cetyl carbonate (CCC)

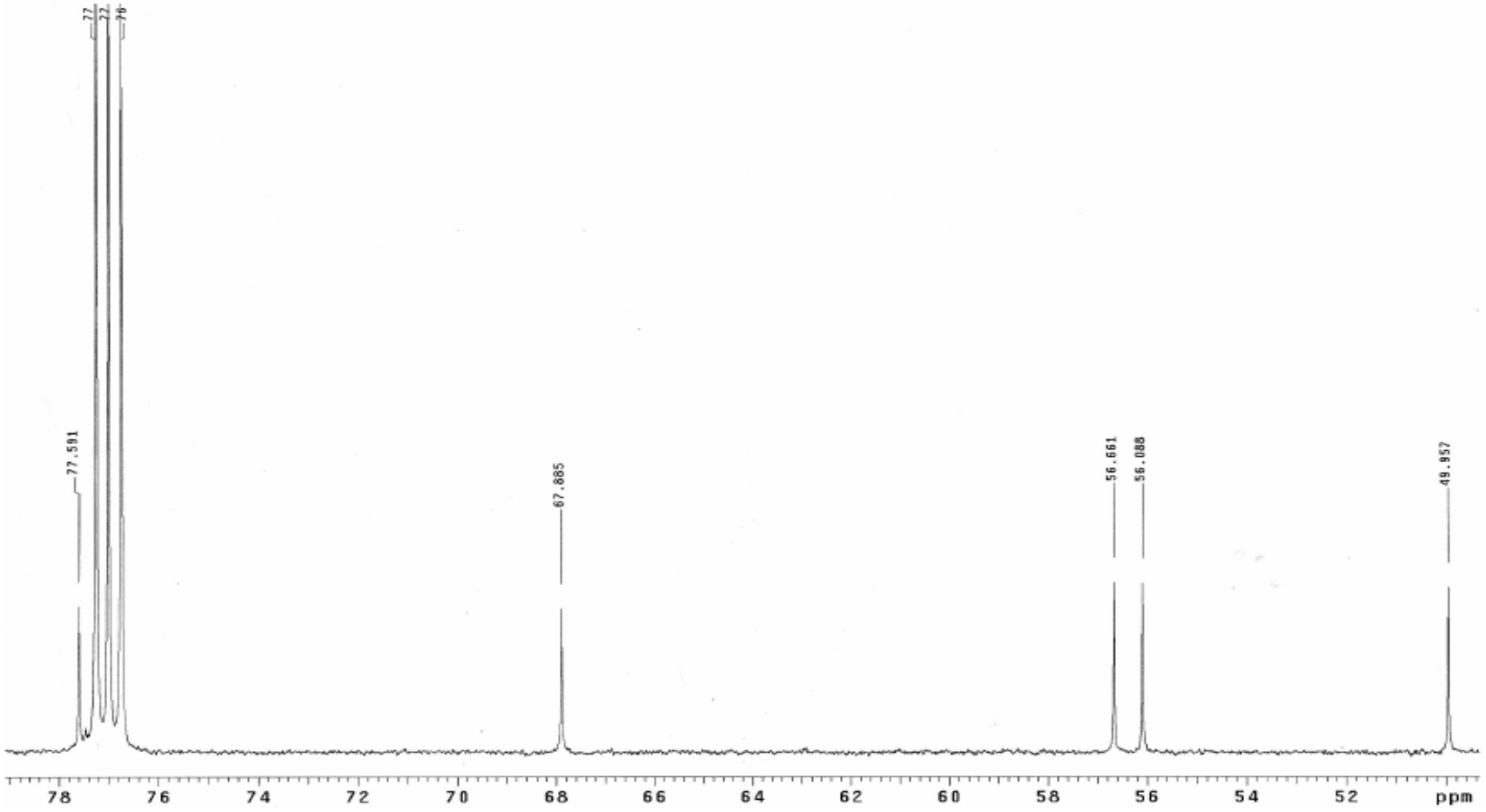

^{13}C-NMR spectra of cholesteryl cetyl carbonate (CCC)

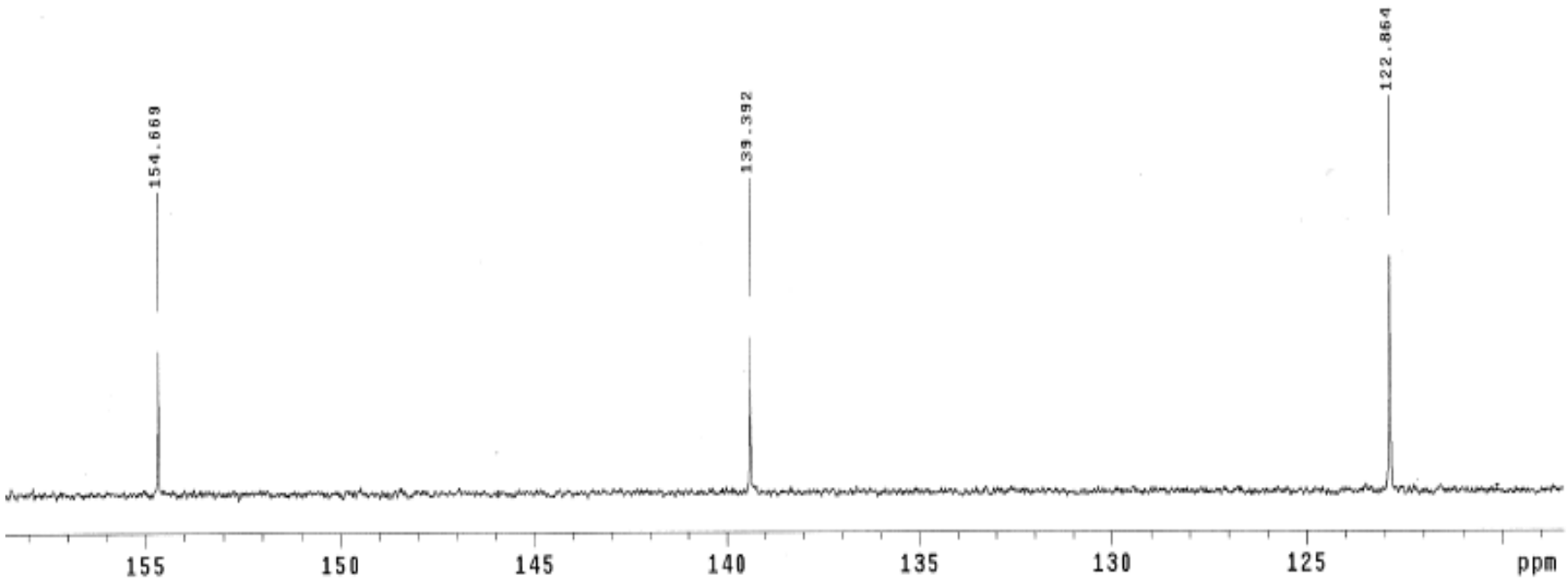

^{13}C-NMR spectra of cholesteryl cetyl carbonate (CCC)

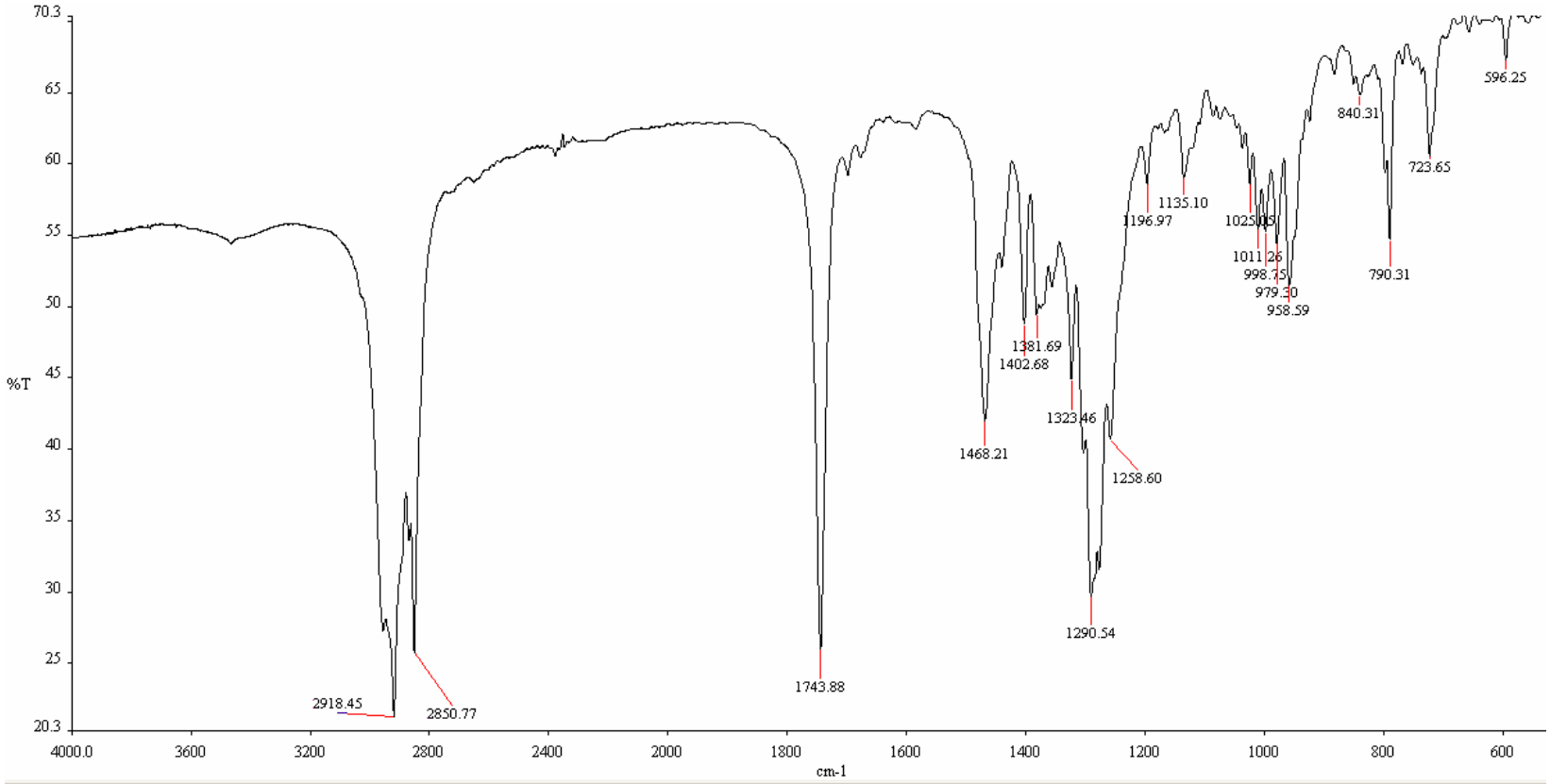

FT-IR spectrum of 1% indomethacin-CCC mixture

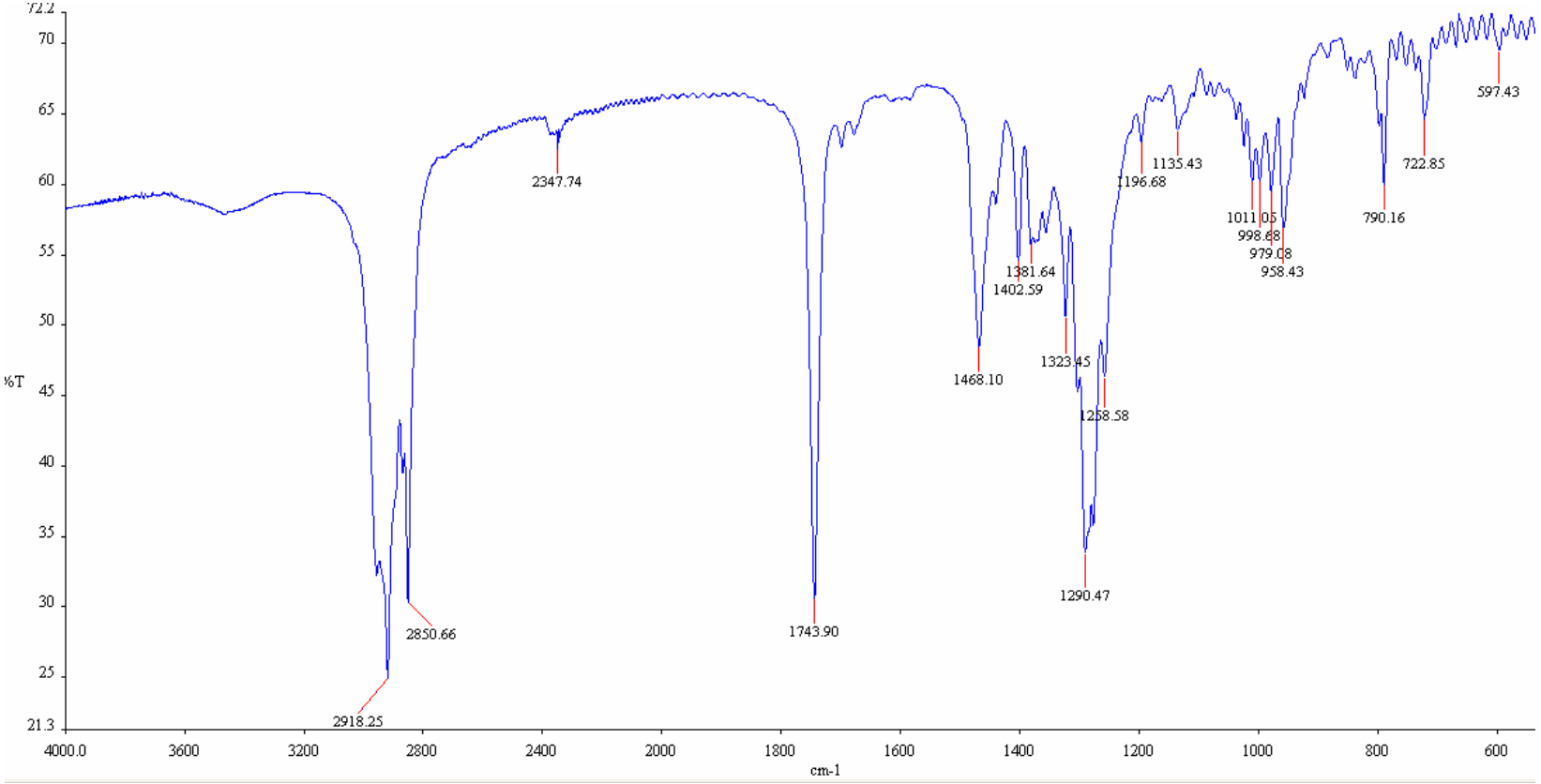

FT-IR spectrum of 2% indomethacin-CCC mixture

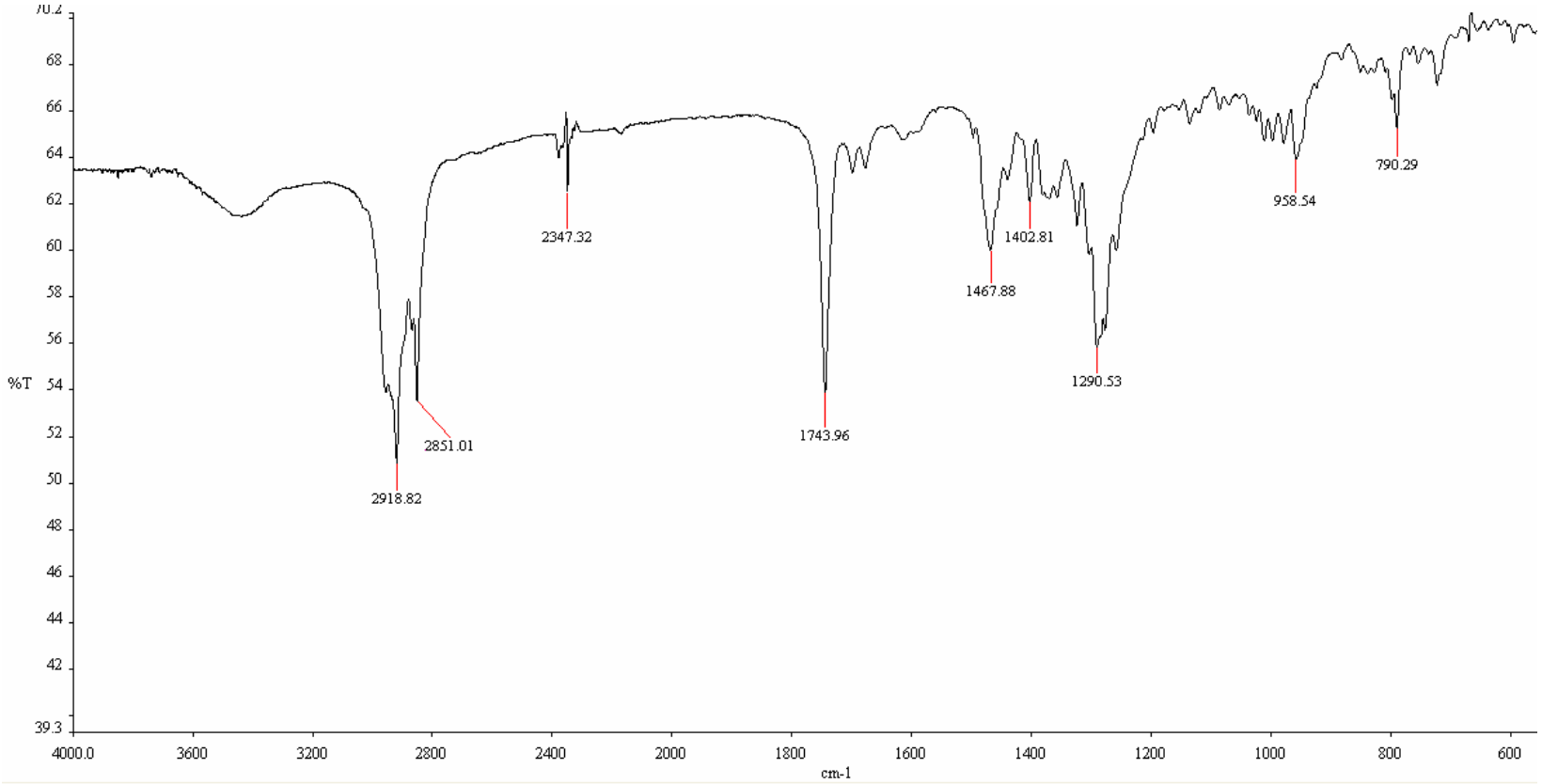

FT-IR spectrum of 5% indomethacin-CCC mixture

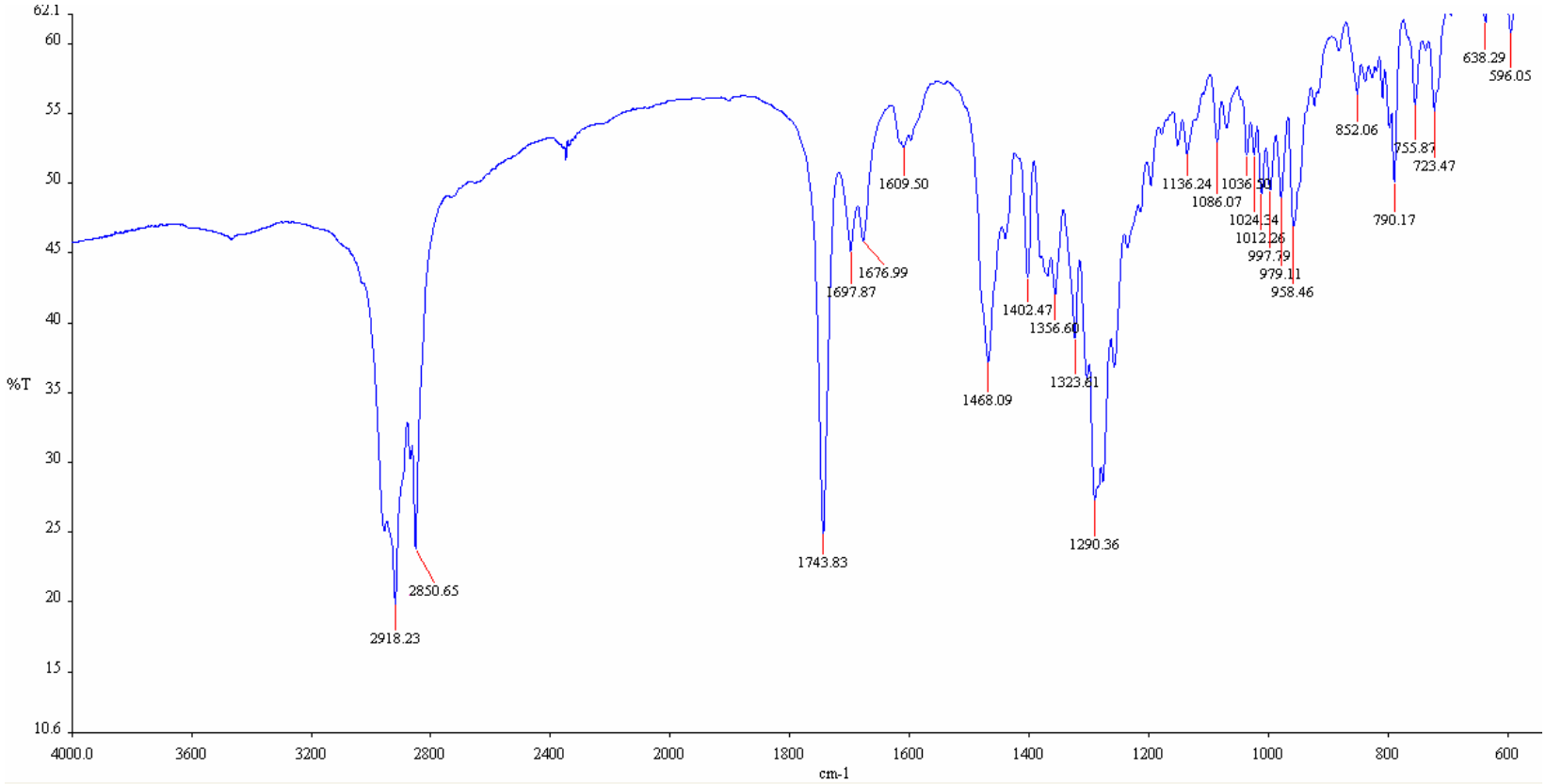

FT-IR spectrum of 10% indomethacin-CCC mixture

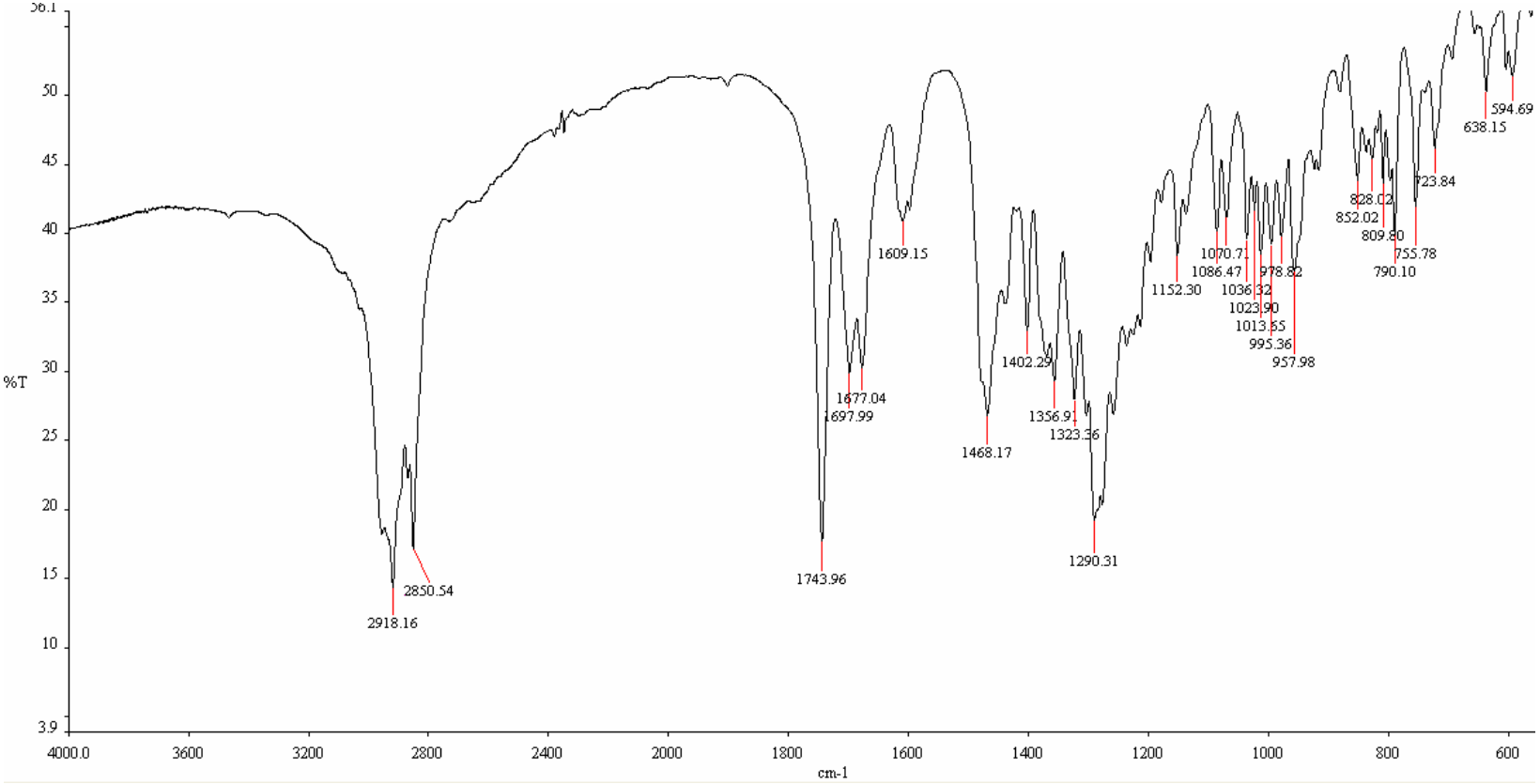

FT-IR spectrum of 20% indomethacin-CCC mixture

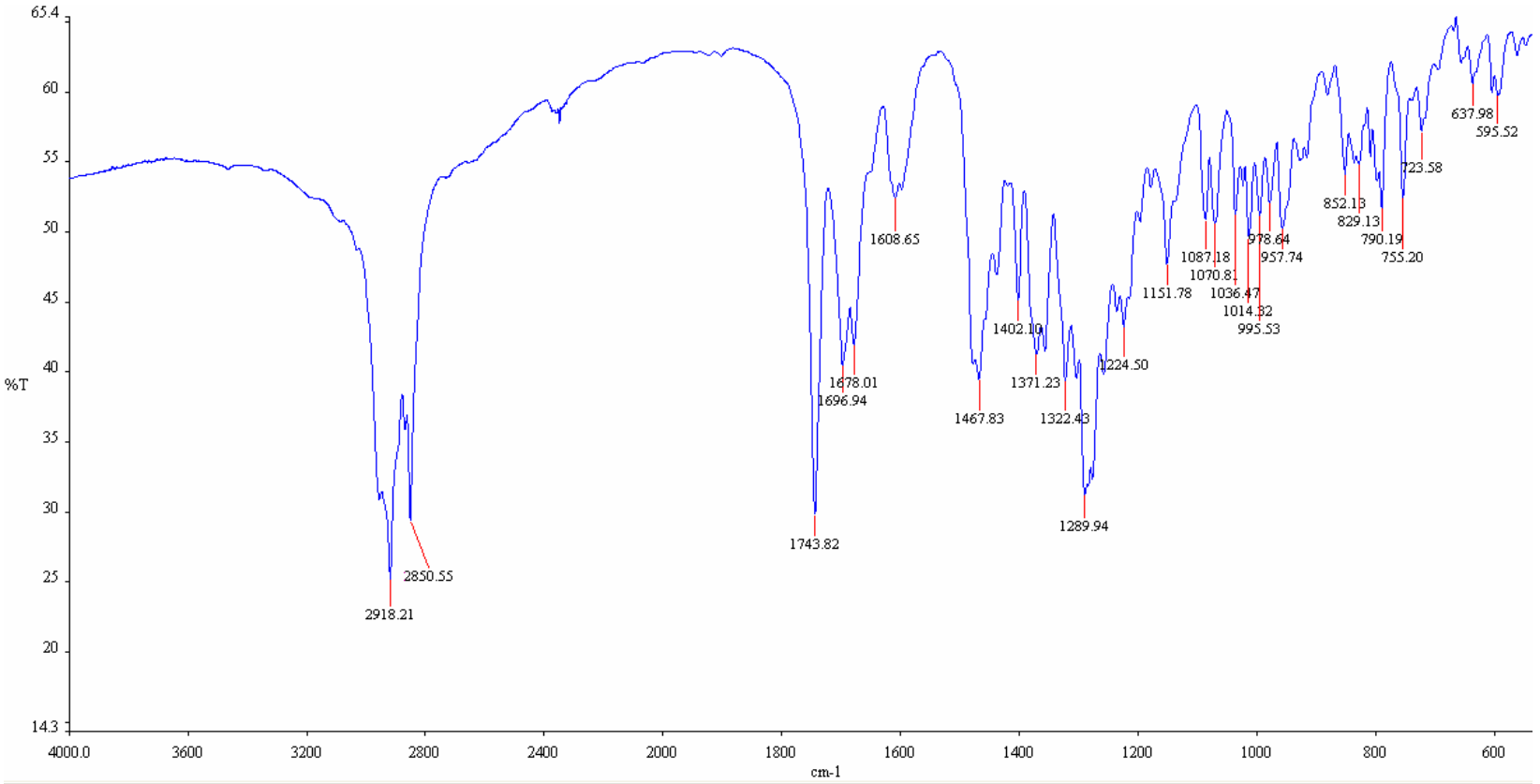

FT-IR spectrum of 30% indomethacin-CCC mixture

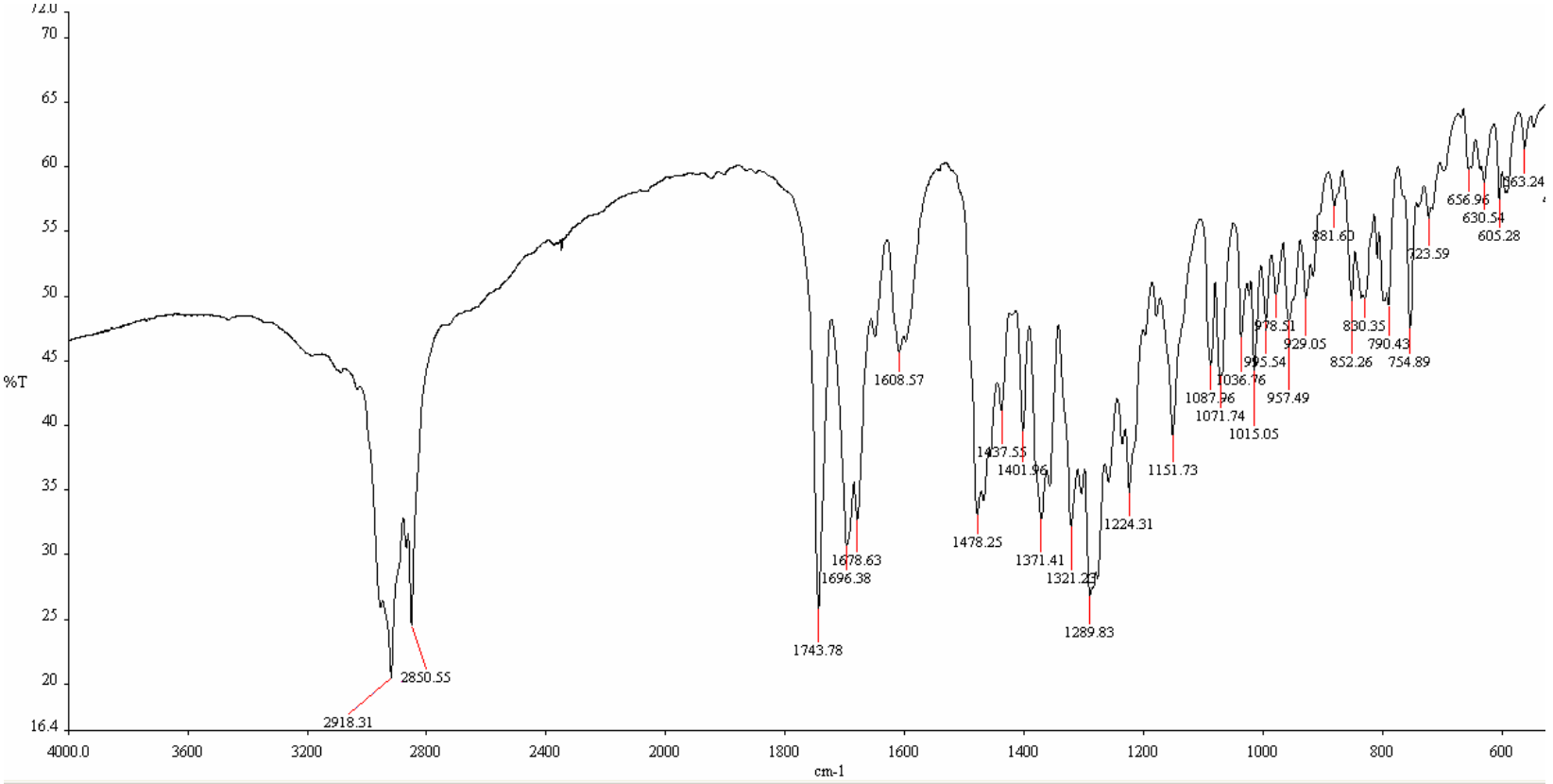

FT-IR spectrum of 40% indomethacin-CCC mixture